The Experimental and Theoretical Study of Fines Migration in Porous Media under Particle-rock Repulsion and Attraction

---

Kaiser Aji

A thesis submitted for the degree of Doctor of Philosophy (PhD)

Australian School of Petroleum

Faculty of Engineering, Computer & Mathematical Sciences

The University of Adelaide

October 2014

Table of Contents

Abstract

This is a PhD thesis by publication. The essence of the research performed has been published in one book chapter, five journal papers and four SPE papers.

The thesis contains laboratory study of deep bed filtration in porous media accounting for particle migration, mobilization and straining for two particular cases: straining-dominant particle capture and filtering under high flow velocities.

Advanced *challenge core flood test* methodology to determine pore throat size distribution *under unfavorable particle retention conditions* is designed and developed in the thesis. It includes significant advance in design of the laboratory set-up if compared with previous version, development of the test procedures to provide the particle-rock repulsion and measure the *post-mortem* retention profile, analysis of accuracy and uncertainties of the experiments.

In more details, the improvements of the laboratory set-up and procedures include sieving of glass beads in the ultrasonic bath with consequent reduction of the sieving time and more reproducible grain size distribution, application of the dual syringe pump system with continuous injection of suspension and pulseless delivery of particles in the porous medium, measurements of the retention profile after the test by cutting up the porous column in 4-6 pieces and dispersing the material in water. The above methods are applicable to continuous as well as to a pulse type particle injection. Latex particle have been injected into packed glass beads or borosilicate filters at different concentrations, velocities, pH, and salinities. However, main varying parameters are size distributions of injected latex particles and compacted glass beads. The tests show that the pore throat size distributions can be recovered from the challenge tests.

Another development of the thesis includes deep bed filtration investigation under *high flow velocities under favorable particle retention conditions*. It includes the design of laboratory set-up, development of the experimental methodology to reveal the hysteretic phenomena of the particle attachment and detachment under high velocities, treatment of the data using the Forchheimer law of high velocity flow in rocks and formulating the modified Forchheimer law under the conditions of formation damage, development of the methodology for estimates of the accuracy and uncertainties of the performed laboratory high-velocity tests.

In more details, high velocity suspension flow in engineered porous medium was studied at various volumetric flow rates and conditions favorable for particle attachment under the occurrence of the phenomena of particle deposition, mobilization, migration and entrainment. The maximum retention function (the critical particle retention concentration) derived is a quadratic function of flow velocity. A strong particle surface attraction as indicated by calculation of DLVO energy potential, translates to almost a quarter of filter surface coverage by the attached particles. The particles can’t be removed by an increase of solution velocity only due to strong particle-matrix attraction. The removal of approximately 17.5 % of the attached particles was achieved only after the reduction of salinity and increase in pH of solution at maximum velocity.

The work includes the development of the Forchheimer model for the case of particle retention, i.e. the advanced formula for inertial coefficient versus retained concentration is proposed. Application of the Forchheimer law to the laboratory data results in the formation damage coefficient dependency of the critical retained concentration and the inverse dimensionless function of velocity. The inertial coefficient showed similar behavior at low velocities, although it remained almost constant at low surface coverage. Partial formation of the external cake on the inlet surface of the filter was observed by a post-experimental examination using an optical microscope and via an abrupt increase in the formation damage and inertial coefficients during particle deposition at lower velocities. The partial cake coverage is the indication of the continuation of deep bed filtration even at high surface coverage which is supported by high filtration coefficient values at lower velocities. Results from the theoretical micro scale model based on the torque balance exerted on attached fine particles agree well with the experimental critical retention concentration data within combined standard uncertainties in the entire range of velocities. It allows proposing the model with modified Forchheimer flow equation and micro scale based maximum retention function for high velocity colloidal flows in porous media.

Statement of Originality

This work contains no material which has been accepted for the award of any other degree or diploma in any university or other tertiary institution and, to the best of my knowledge and belief, contains no material previously published by or written by another person, except where due reference has been made in the text.

I give consent to this copy of my thesis, when deposited in the University Library, being made available for loan and photocopying, subject to the provisions of the Copyright Act 1968.

The author acknowledges that copyright of published works contained within this thesis (as listed below) resides with the copyright holder/s of those works.

I also give permission for the digital version of my thesis to be made available on the web, via the University's digital research repository, the library catalogue, the Australian Digital Theses program (ADTP) and also through web search engines, unless permission has been granted by the university to restrict access for a period of time.

Signed……………………………………..

Date………………………………………..

Acknowledgment

First and foremost I offer my sincerest gratitude to my supervisor, Professor Pavel Bedrikovetsky, who has supported me throughout my thesis with his patience and knowledge whilst allowing me to work in my own way. I am very appreciative of his generosity with his time, advice, and contribution. His guidance helped me in the entire time of researching and writing of this thesis.

Besides my advisor, I would like to thank Dr. Alexander Badalyan and my Co-Supervisor Dr. Themis Carageorgos for her support, reviews, comments, criticisms and advices during my research. They also aided my various laboratorial and experimental works during the development of my research.

My sincere thank also goes to Dr. Zhenjiang You, for helping me with the theoretical part of my research.

In my daily work I have been blessed with a friendly and cheerful group of fellow students at Australian School of Petroleum. Thanks to all for welcoming and helping. I deeply appreciate ASP for providing all the equipments I needed to accomplish my thesis.

Finally, I thank my parents and family members for supporting me throughout all my studies at University. They have always provided unwavering love and encouragement.

Thesis by Publications

Book Chapter

1. **Aji K.**, Badalyan A., Carageorgos T., Zeinijahromi A., Bedrikovetsky P. *High Velocity Colloidal Flow in Porous Media: Experimental study and modeling*, in: Focus on Porous Media Research, Ed. by Zhao C, 2013, Nova Science Publishers, NY.

Peer Reviewed Publications

2. **Aji K.** *Particle deposition and mobilization during deep bed filtration in oil field.* International Journal of Oil, Gas and Coal Technology. Accepted on 31.06. **2013**. (http://www.inderscience.com/info/ingeneral/forthcoming.php?jcode=ijgct)

3. Badalyan A., You Z, **Aji K.**, Bedrikovetsky P., Carageorgos T., Zeinijahromi A. *Size exclusion deep bed filtration: experimental and modelling uncertainties.* Review of Scientific Instruments. V. 85, 015111.**2014**.

4. **Aji K.** *Experimental study of colloidal flow in porous media at high velocities.* Asia-Pacific Journal of Chemical Engineering. DOI: 10.1002/apj.1782.**2013**.

5. **Aji K.**, You Z., Badalyan A. *Transport and straining of suspensions in porous media: experimental and theoretical study*. Thermal Science. **2012**, 16(5), 1444-1448.

6. Badalyan A., Carageorgos T., Bedrikovetsky P., You Z., Zeinijahromi A., **Aji K**. *Critical analysis of uncertainties during particle filtration*. Review of Scientific Instruments, 83, 095106/1-9. **2012.**

SPE (Society of Petroleum Engineering) Papers

7. McLindin C., Saha A., Le K., **Aji K.**, You Z., Badalyan A., Bedrikovetsky P. *Colloidal flow in aquifers during produced water disposal: experimental and mathematical*

modelling. SPE-153502-MS. SPE Middle East Health, Safety, Security, and Environmental Conference, 2-4 April **2012**, Abu Dhabi, UAE. DOI: 10.2118/153502-MS.

8. You Z., **Aji K.**, Badalyan A., Bedrikovetsky P. *Effect of nanoparticle transport and retention in oilfield rocks on the efficiency of different nanotechnologies in oil industry*. SPE-157097-MS. SPE International Oilfield Nanotechnology Conference, 12-14 June **2012**, Noordwijk, The Netherlands. DOI: 10.2118/157097-MS. ISBN: 978-1-61399-206-7.

9. **Aji K.**, You Z., Badalyan A., Bedrikovetsky P. *Study of particle straining effect on produced water management and injectivity enhancement.* SPE-157399-MS. SPE International Production and Operations Conference & Exhibition, 14-16 May **2012**, Doha, Qatar. DOI: 10.2118/157399-MS. ISBN: 978-1-61399-201-2.

10. **Aji K.**, McLindin C., Saha A., Le K., You Z., Badalyan A., Bedrikovetsky P. *Colloidal-suspension flow in rocks: a new mathematical model, laboratory study, IOR.* SPE-152025-MS, The 2012 SPE EOR Conference at Oil and Gas West Asia, 16-18 April 2012, Muscat, Oman. DOI: 10.2118/152025-MS. ISBN: 978-1-61399-199-2.

Statement of Authors’ Contributions

This thesis comprises a portfolio of ten publications that have been published, accepted for publication and/or submitted for publications in accordance with ‘Academic Program Rules and Specifications 2012’. All journals to which the papers have been submitted are indexed in the ‘ERA 2012 Journal List’ database. The research summarized in the papers that constitute this thesis was undertaken within ‘Formation Damage and EOR Research Group’ at Australian School of Petroleum and with other universities and industry collaborators. Hence all the papers presented herein are co-authored and detail statements of relative contributions are endorsed by the co-authors.

Statement of Authorship

Title of Paper	Transport and straining of suspensions in porous media: experimental and theoretical study
Publication Status	● Published, ○ Accepted for Publication, ○ Submitted for Publication, ○ Publication style
Publication Details	Aji K., You Z., Badalyan A. Transport and straining of suspensions in porous media: experimental and theoretical study. Thermal Science. 2012, 16(5), 1444-1448.

Author Contributions

By signing the Statement of Authorship, each author certifies that their stated contribution to the publication is accurate and that permission is granted for the publication to be included in the candidate's thesis.

Name of Principal Author (Candidate)	Kaiser Aji		
Contribution to the Paper	Experimental design and work, data analysis, wrote manuscript		
Signature		Date	08/03/2014

Name of Co-Author	Zhenjiang You		
Contribution to the Paper	Helped model prediction and calculation		
Signature		Date	11/3/14

Name of Co-Author	Alexander Badalyan		
Contribution to the Paper	Supervised experimental set up and work		
Signature		Date	08/03/2014.

Name of Co-Author			
Contribution to the Paper			
Signature		Date	

Statement of Authorship

Title of Paper	Colloidal Flow in Aquifers during Produced Water Disposal: Experimental and Mathematical Modelling
Publication Status	● Published, ○ Accepted for Publication, ○ Submitted for Publication, ○ Publication style
Publication Details	McLindin C., Saha A., Le K., Aji K.,You Z., Badalyan A., Bedrikovetsky P Colloidal Flow in Aquifers during Produced Water Disposal: Experimental and Mathematical Modelling. SPE-153502-MS, The 2012 SPE Middle East Health, Safety, Security, and Environment Conference Held in Abu Dhabi, UAE, 2-4 April 2012, . DOI: 10.2118/153502-MS.

Author Contributions

By signing the Statement of Authorship, each author certifies that their stated contribution to the publication is accurate and that permission is granted for the publication to be included in the candidate's thesis.

Name of Principal Author (Candidate)	Cale McLindin		
Contribution to the Paper	Data assimilation and wrote manuscript		
Signature		Date	23/04/2014

Name of Co-Author	Atanu Saha		
Contribution to the Paper	Helped data analysis and experimental work		
Signature		Date	29/04/2014

Name of Co-Author	Khoi Le		
Contribution to the Paper	Helped experimental work		
Signature		Date	15/04/2014

Name of Co-Author	Kaiser Aji		
Contribution to the Paper	Helped and guided design experimental work, data assimilation and wrote manuscript		
Signature		Date	07/05/2014

Name of Co-Author	Zhenjiang You		
Contribution to the Paper	Helped model prediction, data evaluation wrote manuscript		
Signature		Date	12/5/14

Name of Co-Author	Alexander Badalyan		
Contribution to the Paper	Supervised experimental design and work, data analysis		
Signature		Date	12.05.2014.

Name of Co-Author	Pavel Bedikovetsky		
Contribution to the Paper	Supervised writing of the manuscript		
Signature			12/05/2014

Statement of Authorship

Title of Paper	Effect of Nanoparticle Transportand retention in Oilfield Rocks on The Efficiency of Different Nanotechnologies in Oil Industry
Publication Status	● Published, ○ Accepted for Publication, ○ Submitted for Publication, ○ Publication style
Publication Details	You Z., Aji K., Badalyan A., Bedrikovetsky P. Effect of Nanoparticle Transportand retention in Oilfield Rocks on The Efficiency of Different Nanotechnologies in Oil Industry SPE-157097-MS, The 2012 SPE International Oilfield Nanotechnology Conference held in Nordwijk, The Netherld. 12-14 June 2012, . DOI: 10.2118/157097-MS. ISBN: 978-1-61399-206-7.

Author Contributions

By signing the Statement of Authorship, each author certifies that their stated contribution to the publication is accurate and that permission is granted for the publication to be included in the candidate's thesis.

Name of Principal Author (Candidate)	Zhenjiang You		
Contribution to the Paper	Data assimilation and wrote manuscript		
Signature		Date	12/5/14

Name of Co-Author	Kaiser Aji		
Contribution to the Paper	Helped experimental design, work, data assimilation and writing manuscript		
Signature		Date	07/05/2014

Name of Co-Author	Alexander Badalyan		
Contribution to the Paper	Supervised experimental design and work, data analysis		
Signature		Date	12.05.2014.

Name of Co-Author	Pavel Bedikovetsky		
Contribution to the Paper	Supervised writing of the manuscript		
Signature			12/05/2014

Statement of Authorship

Title of Paper	Study of particle straining effect on produced water management and injectivity enhancement
Publication Status	● Published, ○ Accepted for Publication, ○ Submitted for Publication, ○ Publication style
Publication Details	Aji K., You Z., Badalyan A., Bedrikovetsky P. Study of particle straining effect on produced water management and injectivity enhancement. SPE-157399-MS. SPE International Production and Operations Conference & Exhibition, 14-16 May 2012, Doha, Qatar. DOI: 10.2118/157399-MS. ISBN: 978-1-61399-201-2.

Author Contributions

By signing the Statement of Authorship, each author certifies that their stated contribution to the publication is accurate and that permission is granted for the publication to be included in the candidate's thesis.

Name of Principal Author (Candidate)	Kaiser Aji		
Contribution to the Paper	Experimental design, setup, work and wrote manuscript		
Signature		Date	08/03/2014

Name of Co-Author	Zhenjiang You		
Contribution to the Paper	Helped model prediction, data evaluation wrote manuscrit		
Signature		Date	11/3/14

Name of Co-Author	Alexander Badalyan		
Contribution to the Paper	Supervised experimental design and work, data analysis		
Signature		Date	08/03/2014

Name of Co-Author	Pavel Bedrikovetsky
Contribution to the Paper	Supervised writing of the manuscript
Signature	15/05/2014

Statement of Authorship

Title of Paper	Colloidal-suspension flow in rocks: a new mathematical model, laboratory study, IOR.
Publication Status	● Published, ○ Accepted for Publication, ○ Submitted for Publication, ○ Publication style
Publication Details	Aji K., McLindin C., Saha A., Le K., You Z., Badalyan A., Bedrikovetsky P. Colloidal-suspension flow in rocks: a new mathematical model, laboratory study, IOR. SPE-152025-MS, The 2012 SPE EOR Conference at Oil and Gas West Asia, 16-18 April 2012, Muscat, Oman. DOI: 10.2118/152025-MS. ISBN: 978-1-61399-199-2.

Author Contributions

By signing the Statement of Authorship, each author certifies that their stated contribution to the publication is accurate and that permission is granted for the publication to be included in the candidate's thesis.

Name of Principal Author (Candidate)	Kaiser Aji		
Contribution to the Paper	Experimental design, work, data assimilation and wrote manuscript		
Signature		Date	08/03/2014

Name of Co-Author	Cale McLindin		
Contribution to the Paper	Helped experimental work		
Signature		Date	23/04/2014.

Name of Co-Author	Atanu Saha		
Contribution to the Paper	Helped experimental work		
Signature		Date	29/04/2014

Name of Co-Author	Khoi Le		
Contribution to the Paper	Helped experimental work		
Signature		Date	15/04/2014

Name of Co-Author	Zhenjiang You		
Contribution to the Paper	Helped model prediction, data evaluation wrote manuscript		
Signature		Date	12/5/14

Name of Co-Author	Alexander Badalyan		
Contribution to the Paper	Supervised experimental design and work, data analysis		
Signature		Date	12.05.2014

Name of Co-Author	Pavel Bedikovetsky	
Contribution to the Paper	Supervised writing of the manuscript	
Signature		15/05/2014

Statement of Authorship

Title of Paper	Particle deposition and mobilization during deep bed filtration in oil field
Publication Status	● Published, ○ Accepted for Publication, ○ Submitted for Publication, ○ Publication style
Publication Details	Aji K. Particle deposition and mobilization during deep bed filtration in oil field. International Journal of Oil, Gas and Coal Technology. Accepted on 31.06. 2013. Available online: http://www.insiderscience.com/info/ingeneral/forthcoming.php?jcode=ijgct

Author Contributions

By signing the Statement of Authorship, each author certifies that their stated contribution to the publication is accurate and that permission is granted for the publication to be included in the candidate's thesis.

Name of Principal Author (Candidate)	Kaiser Aji		
Contribution to the Paper	Experimental design and work, data analysis, wrote manuscript		
Signature		Date	09/05/2014

Name of Co-Author			
Contribution to the Paper			
Signature		Date	

Name of Co-Author			
Contribution to the Paper			
Signature		Date	

Name of Co-Author			
Contribution to the Paper			
Signature		Date	

Statement of Authorship

Title of Paper	Experimental study of colloidal flow in porous media at high velocities
Publication Status	● Published, ○ Accepted for Publication, ○ Submitted for Publication, ○ Publication style
Publication Details	Aji K. Experimental study of colloidal flow in porous media at high velocities. Asia-Pacific Journal of Chemical Engineering. Accepted on 20.11.2013.

Author Contributions

By signing the Statement of Authorship, each author certifies that their stated contribution to the publication is accurate and that permission is granted for the publication to be included in the candidate's thesis.

Name of Principal Author (Candidate)	Kaiser Aji		
Contribution to the Paper	Experimental design and work, data analysis, wrote manuscript		
Signature		Date	12/05/2014

Name of Co-Author			
Contribution to the Paper			
Signature		Date	

Name of Co-Author			
Contribution to the Paper			
Signature		Date	

Name of Co-Author			
Contribution to the Paper			
Signature		Date	

Statement of Authorship

Title of Paper	High Velocity Colloidal Flow in Porous Media: Experimental study and modeling
Publication Status	● Published, ○ Accepted for Publication, ○ Submitted for Publication, ○ Publication style
Publication Details	Aji K., Badalyan A., Carageorgos T., Zeinijahromi A., Bedrikovetsky P. High Velocity Colloidal Flow in Porous Media: Experimental study and modeling, in: Focus on Porous Media Research, Ed. by Zhao C, 2013, p 359- 398. Nova Science Publishers, NY.

Author Contributions

By signing the Statement of Authorship, each author certifies that their stated contribution to the publication is accurate and that permission is granted for the publication to be included in the candidate's thesis.

Name of Principal Author (Candidate)	Kaiser Aji		
Contribution to the Paper	Experimental design and work, data analysis, wrote manuscript		
Signature		Date	12/05/2014

Name of Co-Author	Alexander Badalyan		
Contribution to the Paper	Supervised experimental work and manuscript evaluation		
Signature		Date	

Name of Co-Author	Themis Carageorgos		
Contribution to the Paper	Supervised and helped experimental work		
Signature		Date	12/05/14

Name of Co-Author	Abbas Zeinijahromi		
Contribution to the Paper	Helped experimental work and model prediction		
Signature		Date	13/05/14

Name of Co-Author	Pavel Bedrikovetsky		
Contribution to the Paper	Supervised whole of the work		
Signature			15/05/2014

Name of Co-Author			
Contribution to the Paper			
Signature		Date	

Name of Co-Author			
Contribution to the Paper			
Signature		Date	

Statement of Authorship

Title of Paper	Size exclusion deep bed filtration: experimental and modelling uncertainties
Publication Status	● Published, ○ Accepted for Publication, ○ Submitted for Publication, ○ Publication style
Publication Details	Badalyan A., You Z, Aji K., Bedrikovetsky P., Carageorgos T., Zeinijahromi A. Size exclusion deep bed filtration: experimental and modelling uncertainties. Review of Scientific Instruments, 2014. V.85, 015111/1-13.

Author Contributions

By signing the Statement of Authorship, each author certifies that their stated contribution to the publication is accurate and that permission is granted for the publication to be included in the candidate's thesis.

Name of Principal Author (Candidate)	Alexander Badalyan		
Contribution to the Paper	Experimental design and work, data analysis, wrote manuscript		
Signature		Date	12.05.2014.

Name of Co-Author	Zhenjiang You		
Contribution to the Paper	Helped model prediction and calculation		
Signature		Date	12/5/14

Name of Co-Author	Kaiser Aji		
Contribution to the Paper	Experimental set up and work, data analysis		
Signature		Date	09/05/2014

Name of Co-Author	Pavel Bedrikovetsky	
Contribution to the Paper	Supervised of the work	
Signature		5/05/2014

Name of Co-Author	Themis Carageorgos		
Contribution to the Paper	Helped experimental work		
Signature		Date	12/05/14

Name of Co-Author	Abbas Zeinijahromi		
Contribution to the Paper	Helped experimental work and calculation		
Signature		Date	13/05/14

Name of Co-Author			
Contribution to the Paper			
Signature		Date	

Statement of Authorship

Title of Paper	Critical analysis of uncertainties during particle filtration
Publication Status	● Published, ○ Accepted for Publication, ○ Submitted for Publication, ○ Publication style
Publication Details	Badalyan A., Carageorgos T., Bedrikovetsky P., You Z., Zeinijahromi A., Aji K. Critical analysis of uncertainties during particle filtration. Review of Scientific Instruments. 2012, 83, 095106/1-9.

Author Contributions

By signing the Statement of Authorship, each author certifies that their stated contribution to the publication is accurate and that permission is granted for the publication to be included in the candidate's thesis.

Name of Principal Author (Candidate)	Alexander Badalyan		
Contribution to the Paper	Experimental design and work, data analysis, wrote manuscript		
Signature		Date	12.05.2014

Name of Co-Author	Themis Carageorgos		
Contribution to the Paper	Helped experimental work and data evaluation		
Signature		Date	12/05/14

Name of Co-Author	Pavel Bedrikovetsky		
Contribution to the Paper	Supervised writing this manuscript		
Signature			15/05/2014

Name of Co-Author	Zhenjiang You		
Contribution to the Paper	Helped mathematical calculation and model prediction		
Signature		Date	12/5/14

Name of Co-Author	Abbas Zeinijahromi		
Contribution to the Paper	Helped experimental work and data evaluation		
Signature		Date	13/05/14

Name of Co-Author	Kaiser Aji		
Contribution to the Paper	Helped experimental setup and work		
Signature		Date	06/05/2014

Name of Co-Author			
Contribution to the Paper			
Signature		Date	

1. Contextual Statement

In this Section, the main achievements of laboratory studies of deep bed filtration are summarized; the absence of the topics aimed in the thesis in the contemporary literature is stated.

Fines or fine particles (colloids) are small particles that exist in natural porous media. The migration of particles in porous media is a challenging problem for both scientific research and industrial applications, especially in the area of petroleum engineering. During the flow of fluids through a porous medium, fine particles attached to pore surfaces are released under certain sets of condition (Khilar and Fogler, 1998). Fines mobilization in porous media is an important issue as it can lead to drastic changes in the permeability of oil reservoirs (Cerda, 1987). Fines transport and deposition have been considered as significant mechanisms causing formation damage (Mueeke, 1979).

Permeability is an important property of porous media and has been the subject of many studies by engineers and geologists (Mungan, 1965). Many of these studies are concerned with formation damage, i.e., reduction in permeability, resulting from rock contact with fresh water, which is attributed to migration of particles. This reduction in permeability has often been attributed to mobilization, migration, and plugging of fine particles in the rock pore spaces (Gabriel and Inamdar, 1983).

The flow of colloidal suspensions in natural rocks is an important process in many industrial applications ranging from particle filtration to fines migration in oil and gas reservoirs (Ochi and Vernoux, 1998; Moghadasi et al., 2004; Civan, 2007; Ding, 2010). Reservoir formation damage occurs during the invasion of drilling or completion fluid, raw and produced water injection (Nabzar et al., 1996; Pang and Sharma, 1997). Fines migration and retention near to the injection and production wells (Khilar and Fogler, 1998; Civan, 2010; Takahashi and Kovscek, 2010) are also reported to occur. Through reliable modeling of colloidal suspension flow and consequent particle retention in porous media and its permeability reduction, it is possible to reduce the formation damage for the oil and gas industry, or design and plan different improved oil recovery (IOR) technologies where these colloidal particles are used to increase sweep efficiency during waterflooding.

Suspended particles can be captured in porous media by electrostatic attraction, sorption, bridging, diffusion, gravitational segregation etc (Nabzar et al., 1996; Khilar and Fogler, 1998; Torkzaban et al., 2012). Intensity of these particle capture mechanism depends on surface chemistry of particles and porous media, ionic strength of aqueous media, colloid and pore size distributions, chemical heterogeneity of pore space, and concentration of colloids and hydrodynamics of a flowing suspension (Bradford et al., 2011).

There are two distinct mechanisms that lead to the particle capture during filtration: physicochemical and geometrical. The former is controlled by physicochemical characteristics due to hydrodynamic, electrostatic and chemical forces which result in particle attachment and detachment in porous media. The most commonly used approach for physicochemical filtration is the classical colloidal-suspension deep bed filtration theory (Herzig et al., 1970; Payatakes et al., 1974), which contains two governing differential equations: one for particle population balance, and the other for particle capture kinetics. However, the classical theory does not provide accurate predictions of particle propagation and retention when the effect of capture by straining is significant.

Particle straining is a geometrical mechanism. When a particle arrives at a pore throat with a smaller size, the particle is not able to enter this small pore and, thus, it is physically excluded from downstream suspension. Despite seemingly simple straining concept – the particle is captured if its size is smaller than the pore size – this phenomenon is still not well understood and robust models accounting for particle straining mechanism are not available in the literature.

Another aim of this thesis is to observe the process of high velocity particle deposition onto an engineered porous medium with subsequent particle detachment via alteration of fluid velocity, pH and ionic strength of suspension.

Numerous works investigated colloidal transport on micro scale (Payatakes et al., 1974). These includes population balance models (Sharma and Yortsos, 1987; Bedrikovetsky, 2008; Chalk et al., 2012; You et al., 2013), random walk equations (Cortis et al., 2006; Yuan et al., 2010; Yuan et al., 2012; Yuan et al., 2013) and direct pore scale simulation (Bradford et al., 2009). The population balance and random walk models, as well as, the large scale phenomenological models use the detachment rate equation with an empirical kinetics coefficient and do not account for forces, exerting on a single particle.

Asymptotical stabilisation of the retained concentration and permeability with time approaching to infinity is the common feature of mathematical models considering proportionality between particle detachment rate and the following factors affecting particle mobilisation such as drag force, difference between equilibrium and current velocities, difference between the equilibrium and current suspension concentrations (Civan, 2010; Massoudieh and Gynn, 2010). On the contrary, particles show immediate mobilisation as the result of a sharp decrease in ionic strength (Khilar and Fogler, 1998) and abrupt increase in flowrate (Ochi and Vernoux, 1998) which translates to immediate permeability decline.

Mobilisation of a particle retained on the internal filter cake occurs when it is not in the mechanical equilibrium (Bergendahl and Grasso, 2000; Civan, 2007; Bradford et al., 2011). Some models consider mechanical equilibrium of a retained particle through a balance between the drag force and the friction force by introduction of an empirical Coulomb coefficient (Civan, 2007). Other models consider the balance of all moments exerted by forces (Freitas and Sharma 2001; Bradford et al., 2011).

A recently developed deep bed filtration model with a migrating layer of the fine particles attached in the secondary energy minimum (Yuan et al., 2010) also does not consider the forces acting on the retained particles.

The above analysis of contemporary literature shows the lack of experimental studies of size exclusion particle capture under unfavourable attachment. It also shows that experimental studies of high velocity colloidal suspension flows in porous media, which are so important for prediction of well behaviour in petroleum and environmental engineering haven't been performed. The above defines *two main aims* of the thesis: laboratory studies of size exclusion deep bed filtration under the particle-rock repulsion and of filtration under high flow velocities.

In the current thesis, *new experimental methodology for size exclusion deep bed filtration has been developed*, including the significant improvement of the set-up if compared with previous studies, development of laboratory procedures including post-flow retention profile measurements and detailed analysis of uncertainties and accuracy of laboratory measurements. The important co-lateral result is the validation of the stochastic micro-model for deep bed filtration of suspension in porous media and straining under size exclusion capture mechanism. It is validated by laboratory tests on suspension flow in engineered media. Pore size distribution and particle capture mechanisms in porous media are investigated (Papers 2, 3, 5-10).

In the thesis the *formation damage laboratory study of suspension flow under high velocity* is performed, the laboratory test on sequential particle injections at piece-wise increasing velocities is designed, followed by injection of particle-free water at increasing velocity, allows for full characterization of the colloidal flow system with particles attachment and detachment at high velocities. The experimental results with model validation are presented in a later part of the thesis. Forchheimer equation (quadratic law of flow in porous media at high velocities) is fulfilled for porous media with attached particles with high accuracy. The values of the maximum retention function for high velocity flows, as calculated from the torque balance conditions on the pore scale and as obtained from laboratory measurements are in a good agreement. The decrease of absolute permeability during high velocity particle injection fulfils the linear retention concentration dependency of normalised reciprocal to permeability resulting in a common value for formation damage coefficient. The dependency cannot be prolonged for high values of the retained concentration due to formation of external filter cake affecting deep bed filtration. The problem of fines migration towards production well contains strained concentration dependencies for permeability, inertia coefficient, and maximum attached concentration and filtration coefficient. The fines attachment does not occur under the assumption of incompressible flow in the zone of fines lifting, so the filtration coefficient does not enter the system of governing equations. The fines attachment does occur under the assumption of incompressible flow in remote zone of under saturated initial attached fines concentration (Papers 1 and 4).

1.1 Thesis Structure

This is a PhD thesis by publications. Ten papers are included in the thesis, of which one is a book chapter, five papers have been published in peer reviewed journals and four papers have been published by SPE. The PhD student is not the first author in three above mentioned papers. However, due to his significant contribution to the work, these papers are included in this thesis.

Paper	Chapter	Title of the paper	Status
5	Chapter 3	Transport and straining of suspensions in porous media: experimental and theoretical study	Published
7	Chapter 3	Colloid flow in aquifers during produced water disposal: experimental and mathematical modelling	Published
8	Chapter 3	Effect of nanoparticle transport and retention in oilfield rocks on the efficiency of different nanotechnologies in oil industry	Published
9	Chapter 3	Study of particle straining effect on produced water management and injectivity enhancement	Published
10	Chapter 3	Colloidal-suspension flow in rocks: a new mathematical model, laboratory study, IOR	Published
1	Chapter 4	High velocity colloidal flow in porous media: experimental study and modelling	Published
2	Chapter 4	Particle deposition and mobilization during deep bed filtration in oilfield	Accepted
4	Chapter 4	Experimental study of colloidal flow in porous media at high velocities	Published
3	Chapter 5	Size exclusion deep bed filtration: experimental and modelling uncertainties	Published
6	Chapter 5	Critical analysis of uncertainties during particle filtration	Published

The thesis body is formed by five chapters. The *first Chapter* contains the contextual statement that the research aimed by the submitted thesis is not available in the contemporary literature. *Chapter two* presents the detailed literature review on laboratory investigation of deep bed filtration, particularly with straining domination and at high flow velocities, exhibiting the lack of studies on the two above mentioned subjects and formulating the aims of the research presented. Chapters 3, 4 and 5 are novel original chapters of the thesis. The *third Chapter* presents laboratory study of size exclusion dominant deep bed filtration under unfavorable attaching conditions. *Chapter four* contains investigation of deep bed filtration under high flow velocities. The *fifth Chapter* exhibits the analysis of uncertainties and accuracy of the above laboratory study. The main statements of scientific novelty presented in *Chapter six* conclude the thesis.

In Chapter one, the brief summary of the analysis of the contemporary literature show the importance of size exclusion and high velocity deep bed filtration in porous media, from one hand side, and the lack of experimental studies in these areas. It allows formulating two main aims of the thesis, i.e. deep investigation of these areas by laboratory experiments. The main contextual statement in Chapter one is the achieving of the formulated goal of the PhD study.

The second Chapter presents the literature review of experimental and theoretical works performed to investigate suspension transport under net repulsion condition to provide the straining dominant deep bed filtration. The particle-rock repulsion is the main condition for the size exclusion dominant suspension colloidal transport in porous media. The review contains physics and chemical mechanisms of particle capture, the resulting permeability reduction. The analytical models for deep bed filtration of suspension in porous media and straining under size exclusion capture mechanism are analyzed. It is highlighted that there is no any laboratory experimental study of suspended colloidal flow at high velocities.

The third Chapter contains original research on straining dominant particle capture in porous media. The results have been published in papers 2, 5, 7-10. A new laboratory set-up that highly develops previous set-ups on suspended colloidal flows under rock-particle repulsion is designed. DLVO calculations assure electrostatic repulsion between particles and glass beads. The particle-rock repulsion achieved under the laboratory test conditions provides with the domination of particle straining capture. An important novel element of the laboratory methodology is a post-flow analysis of retention profiles by extraction of the core sections into solvent, separation of captured particles and their counting. A new formulation for experimental study methodology in engineered porous media which allows excluding other mechanisms of particle retention except straining was validated by comparison between the laboratory data and mathematical modelling. The presented laboratory study is applied for solution of the important industrial problem of determining pore throat size distribution from challenge testing. The routine challenge method for determining pore throat size distribution has been modified and improved. Several successfully verified tests on calculating the pore throat size distribution for engineered porous columns have been presented in the published papers, indicating the method applicability in the industry.

The fourth Chapter contains high velocity colloidal flow in porous media. Deposition of colloidal particle onto an engineered porous medium (borosilicate filter) has been studied at high suspension velocities at conditions favorable for particle attachment. In this part, experimental work is carried out in condition of particle rock attraction. The size exclusion, as mechanism for particle straining, was absent due to low value of jamming ratio (ratio between particle diameter and mean pore size). The designed experimental test on sequential particle injections at step-wise increasing velocities, followed by injection of particle free water at increasing velocity, used for full characterization of the colloidal flow system with particle attachment and detachment at high velocities. Application of Forchheimer equation to investigate the critical retention concentration and permeability damage in high velocity is presented in this Chapter too. Good match between high velocity colloidal flow and the modified Forchheimer equation is observed, validating the proposed expression. The results must be applied for evaluation of formation damage and skin factor in high rate oil and gas wells.

In chapter five, critical analysis of uncertainties during deep bed filtration has been performed. A detailed uncertainty analysis, associated with carboxyl modified latex particle capture in glass bead formed porous media, enabled verification of the two theoretical models for prediction of particle retention due to size exclusion. In addition, a systematic analysis of experimental and modeling uncertainties associated with permeability measurement during colloidal particle attachment to engineered porous medium is investigated. The results are applicable in wide range of laboratory studies of flow in porous media.

1.2 Relation between Publications and This Thesis

The first aim of the thesis – laboratory study of size exclusion dominated deep bed filtration is presented in Chapter 3 and in publications 5, 7-10.

In the paper "Transport and Straining of Suspensions in Porous Media: Experimental and Theoretical Study", experimental set-up and injection sequence are described. The DLVO calculations of particle-rock electrostatic interactions show that the repulsion takes place under low salinities and high pH applied in the tests. The results from the newly designed experimental work were compared with the data of analytical modelling; finally, the analytical model for size exclusion dominant deep bed filtration was validated.

In more details, the experimental procedures are described in "Colloid Flow in Aquifers during Produced Water Disposal: Experimental and Mathematical Modelling" along with the final conclusions about feasibility of determining the pore size distribution curves from the challenge testing data. Not only good matching of laboratory data was achieved by population balance model, but also good quality prediction of the model with tuned parameters was demonstrated.

The difference between deep bed filtration with particle straining and attachment is discussed in "Effect of Nanoparticle Transport and Retention in Oilfield Rocks on the Efficiency of Different Nanotechnologies in Oil Industry". Here the term "nanoflow" corresponds to porous materials with reference pore size of nano meters. Size exclusion can affect suspension flows only in extremely low permeability formations, like unconventional reservoirs. The paper emphasizes importance of size exclusion even for low values of jamming ratio due to complex forms of pores and particles, where small particle can wedge in front of asperity or thin bund between two grains.

Size exclusion capture of injected fluid can highly affect well injectivity, as investigated in "Study of Particle Straining Effect on Produced Water Management and Injectivity Enhancement". The paper is related to the experimental set-up and laboratorial study for repulsion condition of the background solution (the solution that being mixed with colloids forms the injecting suspension). It contains a simplified geometric model of parallel tubes intercalated by the mixing chambers to form the porous media under consideration. The paper explains a new model for particle straining dominated by particle capture, accounting for the porous space accessibility and fractional flow in the inlet and effluent boundary conditions, as well as in the expression of the particle rate. The laboratory methodology and set-up are applied for verification of the model by matching and predictive modelling.

The application of the designed straining-dominant suspension transport in porous media to validation of the population balance mathematical model is presented in the work "Colloidal-Suspension Flow in Rocks: a New Mathematical Model, Laboratory Study, IOR".

The above papers encompass the newly developed topic of experimental study of straining dominant suspension colloidal flows in porous media, including a set-up with two parallel syringe pumps providing the continuity of suspension injection, laboratory methodology with procedures of sieving using ultra-sonic bath and column cutting with retained particles separation and suspension with the following particle counting. So far, two main applications published are determination of the rock pore throat size distribution from the challenge tests, and validation of the population balance model from the breakthrough and retained concentrations.

The second aim of the thesis – laboratory study of high velocity deep bed filtration is presented in Chapter 4 and Publications 1, 2 and 4.

The paper "Particle Deposition and Mobilization during Deep Bed Filtration in Oilfield" explains the experimental process of high velocity particle deposition onto an engineered porous medium, with subsequent particle detachment via alteration of fluid velocity, pH and ionic strength of suspension. In this paper, the maximum retention concentration function in the engineering porous medium is determined along with formation damage and inertia coefficients, and the modified particle detachment model is validated by the comparison between the experimental data and the model prediction.

Experimental investigation of high velocity colloidal suspension flow for particle retention and formation damage is contained in the next paper "Experimental Study of

Colloidal Flow in Porous Media at High Velocities”. In this paper, experimental set up is described in all details highlighting the new elements, particle attachment and detachment was explained by DLVO theory for electrostatic interactions. The particle deposition at various flow velocities has been introduced into the Forchheimer equation for flow in a porous medium. The data also show a good agreement between the model and the experimental data.

The book Chapter “High Velocity Colloidal Flow in Porous Media: Experimental Study and Modeling” is a combination of the previous two papers which focus on experimental studies of high velocity deep bed filtration. The Chapter has a form of the close theory, with description of physics phenomena, explanation of laboratory procedures, introduction of a new mathematical model and its verification by laboratory study. The paper is concluded by formulating the mathematical model for reliable prediction of wells behavior in oil, gas and aquifer reservoirs during high velocity flow of suspensions. It contains also the critics to the classical filtration theory and formulates the need for modifications. In this paper, the new torque balance model for particle capture in porous media is introduced for high velocities, followed by a laboratory tests for the model validation. The reported experiments in the paper investigate the effect of velocity alternation on particle retention concentration and the consequent formation damage.

The above papers present a hydrodynamic theory for high velocity suspension-colloidal flows in porous media accounting for inertia effects and their interference with the induced formation damage. The theory includes description of physics phenomena of the increase of not only hydraulic resistance but also the inertial resistivity during particle attachment at high velocities, a new methodology of laboratory studies to reveal hysteretic behavior during loading and unloading of the system and validation of the generalized Forchheimer law by laboratory experiments. The method developed can be applied for prediction of formation damage in high rate gas and oil wells in order to choose the optimal rates and wellbore pressures and mitigate the damage.

The above described laboratory tests have been analyzed for uncertainties and accuracy, yielding the increase of the quality of performed measurements. However, the developed methods for the analysis of uncertainties and accuracy can be applied in wide variety of laboratory studies of flow in porous media. Therefore, the results are joined in a separate Chapter 5.

The paper "Size Exclusion Deep Bed Filtration: Experimental and Modeling Uncertainties" analyses in details the uncertainties associated with particle capture due to size exclusion. From our knowledge, this is the first time that the analysis of uncertainties for experimental suspension colloidal flow in rocks has been performed.

In this paper, the uncertainties of experimental results have been analyzed accounting for particle transport, capture and measurements of inlet and effluent concentrations. The general expression for uncertainties in measurements of inlet and effluent concentrations is proposed. Finally, a comparison between normalized suspended particle concentrations, obtained by the related models and respective experimental data, is presented with the explanation of the observed deviations.

The paper "Critical Analysis of Uncertainties during Particle Filtration" aims the systematic analysis of experimental and modeling uncertainties associated with permeability measurements during colloidal particle attachment to an engineered porous medium. Particle attachment during colloidal suspension injection at different velocities was monitored in the experiments. In the paper, the law of propagation of uncertainties was applied for calculation of uncertainties in parameters of Darcy equation, and parameters having the greatest effect on uncertainties in permeability and modeling results were identified. Recommendations for reducing modeling uncertainties were given in the paper.

The results of the fifth Chapter can be used in laboratory studies of any flows in porous media, including petroleum, environmental and chemical engineering applications.

Finally, the above mentioned 10 journal papers and selected SPE papers present a new technology for understanding the mechanism of formation damage during suspension flow in porous media under the condition of particle rock repulsion and attraction.

1.3 References

Bedrikovetsky P., 2008. Upscaling of stochastic micro model for suspension transport in porous media, Transp Porous Med Vol 75, 335–369

Bergendahl, J. and Grasso, D., 2000. Prediction of Colloid Detachment in a Model Porous Media: Hydrodynamics. *J. Chemical Engineering Science* **55** (9): 1523-1532

Bradford, S., H. Kim., B. Haznedaroglu., S. Torkzaban., S. Walker., 2009. "Coupled factors influencing concentration-dependent colloid transport and retention in saturated porous media." Environmental Science and Technology **43**(18): 6996-7002

Bradford, S.A., Torkzaban, S. and Simunek, J., 2011. Modeling Colloid Transport and Retention in Saturated Porous Media under Unfavorable Attachment Conditions. *Water Resour. Res.* **47** (10): W10503

Cerda C.M., 1987. Mobilization of Kaolinite Fines in Porous Media, Colloids and Surfaces Vol 27, 219-241

Chalk, P., N. Gooding., S. Hutten., Z. You., P. Bedrikovetsky., 2012. "Pore size distribution from challenge coreflood testing by colloidal flow." Chemical Engineering Research and Design **90**(1): 63-77

Civan, F., 2007. *Reservoir Formation Damage: Fundamentals, Modeling, Assessment, and Mitigation*. Burlington: Gulf Professional Publishing, Elsevier.

Civan, F., 2010. Non-Isothermal Permeability Impairment by Fines Migration and Deposition in Porous Media Including Dispersive Transport. *Transport in Porous Media* **85** (1): 233-258

Cortis, A., T. Harter., L. Hou., E. Atwill., A. Packman and P. Green., 2006. "Transport of cryptosporidium parvum in porous media: long-term elution experiments and continuous time random walk filtration modeling." Water Resources Research **42**(12): W12S13

Ding, D.Y. 2010. Modelling formation damage for flow simulations at reservoir scale. SPE J 15 (3): 737-750

Freitas, A. and M. Sharma 2001. "Detachment of particles from surfaces: an AFM study." Journal of Colloid and Interface Science **233**(1): 73-82.

Gabriel, G.A and Inamdar, G.R., An Experimental Investigation of Fines Migration in Porous Media. Journal of Society of Petroleum (SPE 12168)., 1983, 1– 12

Herzig, J.P., Leclerc, D.M. and Goff, P.L., 1970. Flow of Suspensions through Porous Media—Application to Deep Filtration. *Industrial and Engineering Chemistry* **62**: 8-35

Khilar, K. and Fogler, H., 1998. *Migrations of Fines in Porous Media*. Dordrecht/London/Boston: Kluwer Academic Publishers.

Massoudieh, A. and T. R. Gynn 2010. Colloid-facilitated contaminant transport in unsaturated porous media. Modelling of Pollutants in Complex Environmental Systems. G. Hanrahan. Glendale, USA, ILM Publications. Vol **II:** 263-292

Moghadasi, J., Müller-Steinhagen, H., Jamialahmadi, M. and Sharif, A. 2004. Theoretical and experimental study of particle movement and deposition in porous media during water injection. J Petrol Sci Eng 43: 163-181

Mueeke,T.W., Formation Fines and Factors Controlling Their Movement in Porous Media. J. Pet. Tec., 1979, Vol 31, 144-150

Mungan, N., 1965. Permeability Reduction through Changes in Ph and Salinity. *Journal of Petroleum Technology* **17** (12): 1449-1453

Nabzar, L., Chauveteau, G. and Roque, C., 1996. A New Model for Formation Damage by Particle Retention. Paper SPE 1283 presented at the SPE Formation Damage Control Symposium, Lafayette, Louisiana, USA, 14-15 February.

Ochi, J. and Vernoux, J.-F., 1998. Permeability Decrease in Sandstone Reservoirs by Fluid Injection: Hydrodynamic and Chemical Effects. *J. of Hydrology* **208** (3): 237-248

Pang, S. and Sharma, M.M. 1997. A model for predicting injectivity decline in water-injection wells. SPE FE 12 (3): 194-201

Payatakes, A.C., R. Rajagopalan and C. Tian., 1974. “Application of Porous Medium Models to the Study of Deep Bed Filtration,” Can. J. Chem. Eng Vol 52, 722-731

Sharma, M. M. and Yortsos, Y. C., c., 1987. Fines migration in porous media, AIChE J Vol 33(13), 1654-1662

Takahashi, S. and Kovscek, A.R., 2010. Wettability Estimation of Low-Permeability, Siliceous Shale Using Surface Forces. *Journal of Petroleum Science and Engineering* **75** (1-2): 33-43

Torkzaban, S., Wan, J., Tokunaga, T.K., Bradford, S.A., 2012. Impacts of bridging complexation on the transport of surface-modified nanoparticles in saturated sand, *Journal of Contaminant Hydrology*, 136-137: 86-95

You, Z., A. Badalyan., and P. Bedrikovetsky., 2013. "Size-exclusion colloidal transport in porous media - stochastic modelling and experimental study." Society of Petroleum Engineers Journal **18**: 1-14

Yuan, H. and Shapiro, A., 2010. A Mathematical Model for Non-Monotonic Deposition Profiles in Deep Bed Filtration Systems. *Chemical Engineering J.* **166** (1): 105-115

Yuan, H., A. Shapiro., Z. You and and A. Badalyan., 2012. "Estimating filtration coefficients for straining from percolation and random walk theories." Chemical Engineering Journal **210**(1 November 2012): 63-73

Yuan, H., Z. You., A. Shapiro., P. Bedrikovetsky., 2013. "Improved population balance model for straining-dominant deep bed filtration using network calculations." Chemical Engineering Journal **226**(15 June 2013): 227-237

2 Literature Review

2.1 Introduction

Fines or fine particles (colloids) are small particles that exist in rocks or are injected together with water into injection wells. The smallest size corresponds to the particles that are just larger than dissolved macromolecules, and the largest size to colloids that resist settling once suspended (Denovio et al., 2004). Colloids in nature include mineral fragments such as clays, microorganisms, mineral precipitates, and debris. These fine particles can be released into flowing fluid due to a variety of hydrologic, geochemical, and microbiological processes (Ryan and Elimelech, 1996).

The migration of particles in porous media is a challenging problem of both scientific and industrial importance especially in the area of petroleum engineering. During the flow of suspension through a porous medium, fine particles attached to pore surfaces are released or detached under certain sets of condition (Khilar and Fogler, 1998). Particle mobilization in porous media is an important issue as it can lead to drastic changes in the permeability of oil reservoirs (Cerda, 1987). The transport of colloidal suspensions in porous media is accompanied by particle capture and consequently permeability impairment. The permeability reduction caused by fine particles capture in reservoirs is known as formation damage in petroleum engineering (Mueeke, 1979; Mays and Hunt, 2005).

In chemical engineering, particle transport is important in several contexts. It occurs in operation of deep bed filters for water treatment and industrial liquids, membrane technologies, and size exclusion chromatography (Mays and Hunt, 2005).

High velocity colloidal suspension, size exclusion dominant colloidal suspension and emulsion transport in porous media with particle capture and consequent permeability decline is essential for numerous environmental, petroleum and chemical technologies. Transport of colloids, suspensions and emulsions also takes place in industrial filtering, size exclusion chromatography, water production by artesian wells, grouting injection to improve soil strength, liquid composite moulding, industrial waste disposal, aquifer remediation, contamination of aquifers by viruses and bacteria, fines migration in low consolidate and high clay content reservoirs and low quality water injection (Mays and Hunt, 2005; Lefevre et al., 2007; Chupin et al., 2007; Kocaefe et al., 2009; Zhou et al., 2009; Gitis et al., 2010; Massoudieh and Gynn, 2010; Noubactep and Care, 2010; Richard and Neretnieks, 2010; Wong and Mettananda, 2010). Near to production and injection wells in petroleum reservoirs and aquifers, flow velocities are 2-3 orders of magnitude higher than in the other parts of the reservoir. Therefore, the bulk of particle mobilization, filtering and attachment occur. In petroleum industry, well injectivity with injection of solid and liquid particles, with fines lifting and straining due to high velocity or water salinity alteration during seawater flooding, re-injection of produced water or disposal of produced water in aquifers is one of the main challenges of oil production by waterflooding of oilfields (Bedrikovetsky et al., 2011; Bedrikovetsky et al., 2012). The problem of oil and gas well productivity with lifting, migration and straining of the reservoir fines is important problem in petroleum industry. Design and behavior prediction of the above mentioned technological processes are based on mathematical modeling. Therefore, creating appropriate model prediction that coincides with experimental results still needs a lot of scientific work.

2.2 Particle Migration in Porous Media

Particle migration is a process involving the release, transport and capture of small particles in a fluid saturated porous media. The definition of fines migration is a very broad phenomenon seen in many different areas, including environmental engineering, chemical engineering and petroleum engineering. For petroleum engineering, the porous medium is usually a petroleum reservoir and small particles are typically considered to be any colloidal particles. Colloidal particles are particles with effective diameters less than 10μm (MacCartthy and Zachara, 1989). These particles maybe made of many different materials such as inorganic, organic, and microbiological compounds but some of the more common materials are clays (Bradford et al., 2002)

In the petroleum industry, particle migration usually has undesirable consequences, such as formation damage and production of fines. Transport of particle suspensions and colloids in porous media is accompanied by particle capture and consequent permeability decline (Shapiro et al, 2007). Particle migration can occur in several different situations. It may occur during primary production from a field, particularly from heavy oil, consolidated in a clay rich reservoir. It may also occur during water flooding because injected water causes the mobilization of fines in the reservoir (Khilar and Fogler, 1998, Civan, 2007). Therefore, to have experimental results with reliable model prediction is essential to do the required water treatment for water injection, to choose the particle size for drilling mud and also to design proper sand screens. Experimental data is also important to be able to predict particle’s behavior, such as attachment and release, and its effects on formation damage while flow of suspension in porous media.

In recent years, fines migration has been recognized as a source of permeability damage and productivity decline in petroleum engineering. Formation damage by particle migration involves mainly two different mechanisms, chemical and physical mechanism.

2.2.1 Chemical Mechanism

Laboratory work in the area of fines migration induced by chemical interactions has showed the rapid and drastic permeability decline resulting from fresh water contact with clay containing formations. Several investigators have described the mechanism of clay particle expansion, dispersion, migration and plugging. Veley (1969) reported that the factors contributing to the binding of clay particles are London-van der Waals forces, recrystallization and chemical alteration, sorption of organic matter from oil, mutual sorption of ions between adjacent unit layers, electrostatic attractions and hydrodynamic drive forces. He demonstrated that opposing these considerations are the factors contributing to clay particle expansion and dispersion such as hydration of exchangeable cations, hydration of particle surface, repulsion of exchangeable cations (double layer theory), desorption or chemical removal of sorbet binding matter, neutralization of positive charges on particle edges, mechanical shear, and thermal (Brownian) motions. He suggested that the diffusion forces are strongly dependent on the concentration of ions in the bulk solution.

Recent research has focused on fines migration in a porous media with respect to different chemical parameters. These parameters include the pH, ionic strength and salinity of the pore fluid. An increase in ionic strength or valence of counter ions has been found to decrease the rate of release of the particles and hence the rate of permeability decline (Khilar and Fogler, 1998). At a higher ionic strength condition, the significant multilayer particle deposition was observed by Kuhnen et al, (2000).

Reduction of permeability is generally caused by decreasing salinity. Valdya and Fogler (1992) clearly showed that the particle release process is started by a combination of low salinity and high pH. The ionic condition of low salinity and high pH appears to be harmful to formation permeability, causing fines migration and drastic damage. An increase in pH has been found to increase the rate of release of particles (Khilar and Fogler, 1998). Permeability reduction due to salinity changes occurs regardless of the type of clay minerals (Mungan, 1965). Chemical perturbations like decreasing ionic strength and increasing pH can increase the mobilization of particles and formation plugging.

2.2.2 Physical Mechanism

Formation damage resulting from physical flow forces, has not been as extensively studied as that caused by chemical interactions. The majority of the work in this area is detailed in the investigations of Gruesbeck and Collins (1982) and Kuhnen et al (2000). In their works, experimental research has been carried out to investigate the release of fine particles or particle entrainment and deposition as a mechanism of permeability reduction. A critical velocity for particle entrainment has been identified. This velocity was determined to be highly dependent upon the properties of the porous medium and the interstitial fluids.

If a particle is initially adsorbed onto the surface of a pore, there are two broad types of forces such as, hydrodynamic and electrostatic force that can act on the particle. Forces that attach a particle to the pore surface are electrostatic forces and, forces that act to remove particle from the pore are hydrodynamic forces. If the forces acting on the particle change and the hydrodynamic forces dominate, this equilibrium may be disrupted and the particle removed from the pore surface into the fluid stream. As the hydrodynamic forces increase with velocity, there should be a critical velocity at which these forces are sufficient to dislodge the particle. A decrease in the forces attaching the particle to the pore surface would decrease the critical velocity required to remove the particle. Therefore, experimental work and modeling of the forces acting on a particle initially attached to a pore surface should be able to predict the critical velocity for a given set of condition. Cerda (1987), Khilar and Fogler (1998) conducted several experimental studies related to hydrodynamically induced release of particles. However, less attention has been paid to particle deposition under the alteration of the velocities.

In this thesis, the profile of high velocity particle deposition onto an engineered porous medium, with particle detachment by the alteration fluid velocity, pH and ionic strength of suspension were observed. The modified particle detachment model for maximum retention concentration was validated (Paper 4). Laboratorial test with colloidal injections at high flow rates were carried out until the stabilized conditions have been reached, and effect of the colloidal retention and permeability damage in porous media have been investigated as paper 5. The mathematical model for reliable prediction of wells behavior in oil, gas and aquifer reservoirs during the high velocity of colloidal suspension with experimental work concluded as paper 1.

2.3 Permeability Reduction due to Size Exclusion

Much of the current knowledge of straining comes from field experiment with traceable colloids, bacteria, viruses, and latex microspheres. A variety of inorganic, organic, and microbiological colloids exist in natural subsurface systems including silicate clays, iron and aluminum oxides, mineral precipitates, humic materials, micro emulsions of nonaqueous phase liquids, viruses and bacteria (Ryan and Elimelech, 1996; Bradford et al., 2002).

Straining is trapping of colloids in pore throats that are too small to allow passage. The critical pore size for straining will depend on the size of the particle and the pore size distribution of the porous media (Bradford et al., 2002). During the well drilling, the main factors that determine formation damage due to particle straining are particle size distribution in the mud (particles in suspension), formation permeability (pore size distribution), concentration of solids in the mud, and mud circulation rate (Suri and Sharma, 2001). Natural porous media typically exhibit a wide range in pore sizes due to variations in grain size, orientation and configuration, and surface roughness. It is possible that straining occurs at both the pore and grain scale (Sakthivadivel, 1969). Herzig et al. (1970) reported that straining is significant when the colloids diameter is greater than 5% of the median grain diameter in porous media. For this reason, most previous studies on colloid transport have neglected straining as a major mechanism for retention (Bradford et al., 2005).

The critical pore size for straining depends on the size of colloid and the pore size distribution of the medium. Many chemical factors (i.e., pH, ionic strength, surface charge, etc.) affect the aggregating behavior of a colloidal particle and the effective pore size distribution (Bradford et al., 2002). These chemical factors (pH, ionic strength, surface charge, and chemical composition) are also known to influence soil structure (disaggregation) and pore size distribution (shrinking and swelling) when soil contains clay and other colloidal materials (Ayers and Westcot, 1989). Several colloidal suspension properties such as surface charge of the colloids, ionic strength of the suspension and type of salt molecules can cause flocculation or dispersion of particles in the suspension and consequently affect the plugging of pore throats. If flocculation does occur, the effective particle size is increased dramatically, therefore increasing the drag force and hence its chance of being dislodged and re-captured on a pore throat. Straining may also be influenced by physical (fluid velocity, colloid concentration, colloid and soil grain size distribution characteristics, and heterogeneity (Bradford at al., 2002).

Experimental observations of colloid transport are not always in agreement with colloid attachment theory (Tufenkji et al., 2004). Colloid attachment theory does not account for straining. Previous colloid transport studies reported in the literature have focused on the quantification of clean bed first order attachment coefficients to describe particle removal in filter beds (Fitzpatrick and Spielman, 1973; Tobiason and O'Melia, 1988). Smaller particles are predicted to be removed more efficiently by diffusive transport and larger particles are predicted to be removed more efficiently by sedimentation and interception.

Recent studies have shown that the importance of straining on colloid transport has been underestimated in the past. Bradford et al. (2002) suggested that straining is an important mechanism of colloid retention for the larger 2.0μm to3.2μm colloids in the various porous media. Straining is also an important mechanism of colloid retention, especially for decreasing median grain size and increasing colloid size. Attachment theory for these larger colloids needs to take into account the role of straining, which involves the interaction between collectors and the particles. An accurate knowledge of the pore size distribution is, therefore, needed for a proper prediction of the retention of colloids. Investigation on the influence of straining on colloid transport in porous media still needs much attention.

In this thesis, experimental results from the laboratory study for validation of the population balance model is improved. The new modification of the size exclusion suspension transport accounting for the pore accessibility and flow fraction in capture kinetics term, in the inlet and outlet conditions of particle mass balance, is discussed (Papers 5-9). New improved model for size exclusion dominated particle capture, which additional takes account of the expression for the particle capture rate with new experimental results are studied (Paper 10).

2.4 Deep Bed Filtration Theory

The classical suspension-colloid filtration theory is the most widespread approach for prediction of particle behaviors in porous formations (Herzig et al., 1970; Bedrikovetsky, 2008). This advection-dispersion model consists of two equations for material balance with a sink term for particle capture and an equation for particle deposition rate (Herzig et al., 1970, Yao et al., 1971). Filtration theories tend to assume that deposition of colloids to the filter media is essentially irreversible. The effect of filter depth on filter performance is described by Iwasaki (1937). The mass balance equation for 1-D flow of an incompressible fluid or suspension is written as (Herzig et al., 1970; Tufenkji, 2007):

$$\frac{\partial c}{\partial t} + U\frac{\partial c}{\partial x} = D\frac{\partial^2 c}{\partial x^2} - \frac{\rho_b}{\phi}\frac{\partial \sigma}{\partial t} \tag{1}$$

Where c is concentration of suspended particles, σ is amount of particle retained in the porous medium, ρ_b is dry bulk density, and U is the fluid velocity. The mobilization and retention of colloidal particles in the classical model is described by first-order kinetics (Bradford et al., 2003; Civan, 2007). The local deposition and capture rate is calculated by:

$$\frac{\partial \sigma}{\partial t} = \lambda c U - k_{\det}\sigma \tag{2}$$

Where k_{det} is usually referred to as the detachment rate constant and λ is filtration coefficient in deep-bed filtration process. The term — is called the filtration rate and explains the particles release and deposition rate. The detachment rate is a function of suspended concentration, flow velocity and also amount of deposited particles (Nabzar et al., 1996; Rousseau et al., 2008).

The process of fine particles detachment has been discussed widely in the literature. However numerous equations have been proposed yet a universal model explaining the particle release does not exist. Kolakowski and Matijevic (1979) have experimentally studied removal of deposited particle. They have used a well-defined system of mono-dispersed spherical particles deposited on glass beads in a packed column to investigate the effect of solution pH on particle removal. The expression for particle detachment rate is given as:

$$\frac{\partial \sigma(x,t)}{\partial t} = k_{\det}\sigma(x,t) \tag{3}$$

Where $\sigma(t)$ is the number of adhered particles and k_{det} is the probability of escape that is determined by the electrical energy barrier. In Kolakowski and Matijevic (1979) model the rate of particle desorption, only depends on interaction potential between particle and porous media and is not affected by the mechanical equilibrium of forces on the deposited particles.

Khilar et al. (1983) showed a first order equation with respect to retained concentration for the particle release rate. However, they mentioned that the initiation and rate of particle removal depend on several variables such as physical and chemical nature of particle attachment, the local brine salt concentration, temperature, and fluid velocity; the model consists of a coefficient for release that is independent of force balance on single particles. The detachment rate expression is given as:

$$
\begin{aligned}
&-\frac{\partial \sigma}{\partial t} = k_{\mathrm{det}}\sigma \\
&C_{salt} < CSC :\ k_{\mathrm{det}} = 0 \\
&C_{salt} > CSC :\ k_{\mathrm{det}} = k_{\mathrm{det}}
\end{aligned}
\tag{4}
$$

Where σ concentration of attached particles on pore wall and k_{det} is so called release coefficient and is equal to zero for salt concentration higher than the critical salt concentration.

An empirical law for the rate of particle detachment is also presented by Schechter (1992):

$$
\begin{aligned}
&\frac{\partial \sigma}{\partial t} = -k_{\mathrm{det}}\sigma\left(U - U_{crt}\right)H\left(U - U_{crt}\right)\sigma + \beta c \\
&H\left(U - U_{crt}\right) = \begin{cases} 1 & U > U_{crt} \\ 0 & U \le U_{crt} \end{cases}
\end{aligned}
\tag{5}
$$

The model includes Heaviside function that causes the particle removal to stop, if the fluid velocity U is less than the critical velocity U_{crt}. He mentioned that the equation for release rate (Eq. 3) is purely empirical and there is no experimental evidence confirming that using this particular equation is more beneficial than any other plausible forms (Schechter, 1992).

New deep bed filtration model by Yuan and Shapiro (2011a) introduces a surface associated phase migration. They have defined a migrating layer of the particles associated with the pore walls via secondary energy minimum, to model particle capture and release which is not function of force balance on attached particles.

Apart from the equations mentioned above, several other detachment rate equations have also been presented in Khilar and Fogler (1998). Despite the known physical dependency of particle detachment to forces acting on particles, there is no theory for calculating the detachment coefficients. The major shared aspect of all release rate equations is their threshold characteristic. That means, the particle release happens beyond a critical value of specific parameters (Khilar and Fogler, 1998) and is assumed to be proportional to the difference between current condition such as velocity, salinity, pH, and temperature, and their critical value (Gruesbeck and Collins, 1982; Bedrikovetsky et al., 2011). The detachment coefficients are also empirical constants and could be determined by models tuning using experimental results (Schechter, 1992; Tufenkji, 2007).

Another shortcoming of the Classical Filtration Theory is the prediction of an asymptotic response to the flow condition change. Lever and Dawe (1984) investigated the effect of brine salinity on a sandstone core. They have observed an abrupt change in permeability due to brine salinity change. Likewise, Mungan (1965) has reported an instant permeability response to a change to injected water pH. Numerous experimental studies also show that fines release occurs instantly under brine chemistry or injection velocity alternation (Gruesbeck and Collins, 1982; Khilar et al., 1983; Sharma et al., 1992; Miranda and Underdown, 1993; Ochi and Vernoux, 1998; Ju et al., 2007). Various experimental studies have reported an abrupt core response to a flow condition change too (salinity, pH, flow rate.), while the classical filtration theory, with the kinetics of particle detachment; predicts an asymptotical stabilization of the retention concentration and permeability (Bedrikovetsky et al., 2011; Yuan and Shapiro, 2011b).

2.5 Methodology of Experimental Study

In this Section, we present some laboratory works targeting suspension flow in porous media under the particle-rock repulsion and discuss how pore throat size distribution can be determined from those tests.

2.5.1 Experimental Study under the Particle-Rock Repulsion during Suspension Flow

In order to examine the attachment and straining of colloids moving through a single layer of glass beads, the micro model housings are designed to support the observation under an optical microscope (Chalk et al., 2012). The housings are milled out of polyvinyl chloride (PVC) plastic and are designed in such a way that two glass slides are held in place to contain the porous media in a single layer. The deionised ultrapure MilliQ water (resistivity of 18.2 MOhm×cm at 25 °C) after degassing in vacuum at pressure $\approx 10^{-2}$ Pa is used for the preparation of a colloidal suspension. The salinity, acidity and alkalinity of the prepared suspensions are adjusted with the addition of NaCl(aq), HCl(aq) and NaOH(aq), respectively.

The effect of colloidal suspension salinity on the particle retention is investigated under three different NaCl(aq) concentrations (0 mM, 10 mM and 100 mM) at constant acidity/alkalinity. A proportional increase in particle attachment with salinity is observed throughout these experiments, as shown in Fig. 1(a), where the images of colloid particles are small bright “points” while the images of glass beads are semi-transparent large circles. So, the images in Figure 1a allow concluding that the higher is the brine ionic strength the stronger is the particle attachment. Simultaneously, the particle-rock interaction force was calculated for three salinity values using DLVO theory (Khilar and Fogler, 1998). Three plots of the force vs the particle-surface separation distance show that the increase in retention is due to an increased depth of the secondary minimum and a reduced energy barrier to the primary minimum (Tufenkji and Elimelech 2004, 2005). The same results were obtained by Kuznar and Elimelech (2007).

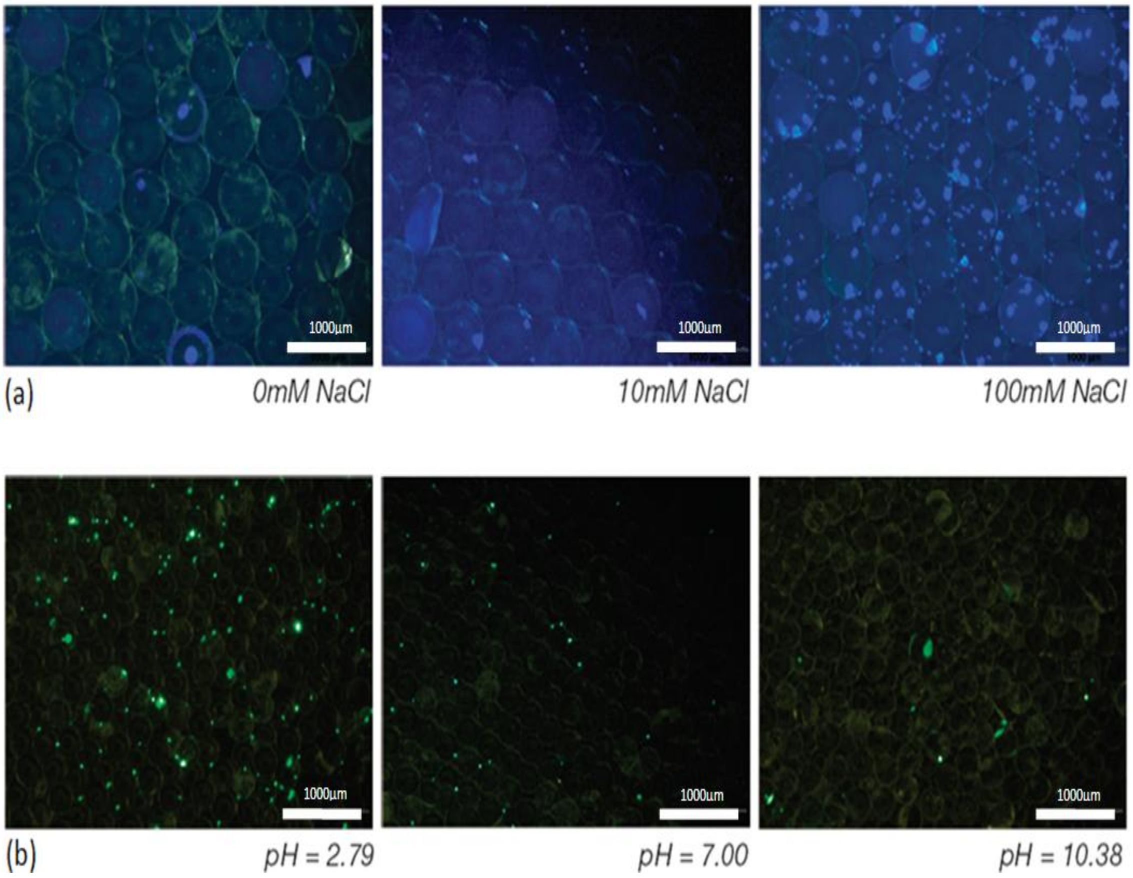

Figure 1. Images of particles strained in porous media: (a) different salinities (blue bright points are attached colloids) and (b) different pH levels (green bright points are attached colloids).

Colloidal particle retention by glass beads is investigated using suspensions with five different pH levels (2.79, 4.26, 7, 8.48 and 10.38) at constant salinity. The monotonic decrease in attachment is found to occur with increased alkalinity. The colloid retention in the unit is comparatively low in all alkaline resident solutions, as shown in Fig. 1(b). The high particle retention in acidic conditions is probably due to the reduction in the strength of the electrical charge on the surface of the glass beads and the colloidal particles. Figure 1b shows that the higher is the pH the weaker is the electrostatic particle-grain attachment. Those conclusions indicate that net repulsion exists between the porous media and the colloidal particles, and that size exclusion is the dominant capture mechanism.

2.5.2 Determining the Pore Throat Size Distribution

Presently there are two commonly used methods in the industry for the determination of pore size distribution. There are mercury porosimetry and challenge testing. Mercury porosimetry is used extensively for the characterization of porous materials. It is one of the most simple and rapid methods available to give a basic representation of a porous media (Brakel et al., 1981). The method provides information about pore size distribution, the total volume or porosity, the skeletal and apparent density and specific area of a sample. The disadvantages of the method include: it underestimates concentration of thin pores because high pressures must be applied in order to force the non-wetting fluid into thin pores; it can be destructive under high pressure hence not applicable for deformable and fragile porous materials; it is environmental unfriendly because of mercury. The challenge testing method, which was recently significantly improved, utilizes the injection of particle suspension into porous media (Purchas and Sutherland 2002; Rideal 2006, 2009). The method is based on calculation of the particle capture probability in a single sieve and cannot be applied for deep bed filtration. Yet, usually the reservoir rock sample sizes vary as 0.5-10 cm; a thin slice can be submitted to flow only for highly consolidated cores. To the best of our knowledge, there is no available in the literature method to determine the overall pore size distribution of core plugs from particle size distribution in the injected and produced suspensions. Therefore, the pore size distribution determined from the experimental data using solution of the inverse problem, and also the Monte Carlo simulation will be used to predict the pore throat size distribution based on the Descartes' theorem. A method is proposed by which the pore throat size distribution will be determined using particle suspension core flood tests through engineered porous media when only straining effects are present. The method involves a suspension flow of particles with a known size distribution through porous media and measuring the inlet, breakthrough and stabilized outlet particle concentrations throughout the test. For these requirements, the new designed challenge core flood test is developed and continuously improved based on previous work (Chalk et al., 2012).

The above critical analysis of the past and current laboratory investigation of suspended colloidal transport in porous media allows concluding the importance of experimental study under high flow velocities and under straining capture and unavailability of this research in the contemporary literature.

2.6 References

Ayers, R.S., and Westcot, D.W., 1989. Water Quality for Agriculture. FAO Irrig, And Drain, Pap., 29, Rev 1, U.N. *Food and Agric. Organ.*, Rome

Bedrikovetsky, P., 2008. Upscaling of Stochastic Micro Model for Suspension Transport in Porous Media. *Transport in Porous Media* **75** (3): 335-369

Bedrikovetsky, P., Siqueira, F., Furtado, C. and Souza, A., 2011. Modified Particle Detachment Model for Colloidal Transport in Porous Media. *Transport in Porous Media* **86** (2): 353-383

Bedrikovetsky, P., A. Zeinijahromi., F. Siqueira., C. Furtado and A. Souza., 2012. "Particle detachment under velocity alternation during suspension transport in porous media." *Transport in Porous Media* **91**(173-197)

Bradford, S.A., Yates, S.R., Bettahar, M., Simunek, J. 2002. Physical factors affecting the transport and fate of colloids in saturated porous media. *Water Resour. Res.* Vol 38 (12), 1327

Bradford, S., Simunek, J., Bettahar, M., van Genuchten, M. and Yates, S., 2003. Modeling Colloid Attachment, Straining, and Exclusion in Saturated Porous Media. *J. Environ. Sci. Technol* **37** (10): 2242-2250

Bradford, S.A., Simunek, J., Bettahar, M., Tadassa, Y.F., 2005. Straining of Colloids at Textural Interfaces, *Water Resour. Res.* Vol 41, 1-17

Brakel, J.V., Modry, S. & Svata, M. 1981. Mercury Porosimetry: State of the Art. *Powder Technology*, Vol 29 , 1-12

Cerda C.M., 1987. Mobilization of Kaolinite Fines in Porous Media, *Colloids and Surfaces* Vol 27, 219-241

Chalk, P., N. Gooding, S. Hutten., Z. You., P. Bedrikovetsky., 2012. "Pore size distribution from challenge coreflood testing by colloidal flow." Chemical Engineering Research and Design **90**(1): 63-77

Chupin, O., N. Saiyouri and P. Hicher., 2007. "The effects of filtration on the injection of cement-based grouts in sand columns." *Transport in Porous Media* **72**(2): 227-240

Civan, F., 2007. *Reservoir Formation Damage: Fundamentals, Modeling, Assessment, and Mitigation*. Burlington: Gulf Professional Publishing, Elsevier.

DeNovio, N.M., Saiers, J.E. and Ryan, J.N., 2004. Colloid Movement in Unsaturated Porous Media Recent Advances and Future Directions. *Vadose Zone Journal* **3** (2): 338-351

Fitzpatrick, J.A., and Spielman, L.A.,1973. Filtration of Equeous Latex Suspensions Through Beds of Glass Spheres, J. *Colloid Interface Sci*. Vol 43, 350-369

Gitis, V., Rubinstein, I., Livshits, M. and Ziskind, G., 2010. Deep-Bed Filtration Model with Multistage Deposition Kinetics. *Chemical Engineering Journal* **163** (1-2): 78-85

Gruesbeck, C. and Collins, R.E., 1982. Entrainment and Deposition of Fine Particles in Porous Media. *SPE Journal* **22** (6): 847-856

Herzig, J.P., Leclerc, D.M. and Goff, P.L., 1970. Flow of Suspensions through Porous Media—Application to Deep Filtration. *Industrial and Engineering Chemistry* **62**: 8-35

Iwasaki, T., J.,1937. *Amer. Water Works Ass.* **29** (1591-1597)

Ju, B., Fan, T., Wang, X. and Qiu, X., 2007. A New Simulation Framework for Predicting the Onset and Effects of Fines Mobilization. *Transport in Porous Media* **68** (2): 265-283.

Khilar, K.C., Fogler, H.S. and Ahluwalia, J.S., 1983. Sandstone Water Sensitivity: Existence of a Critical Rate of Salinity Decrease for Particle Capture. *Chemical Engineering Science* **38** (5): 789-800

Khilar, K. and Fogler, H., 1998. *Migrations of Fines in Porous Media*. Dordrecht/London/Boston: Kluwer Academic Publishers.

Kuhnen, F., Barmettler, K., Bhattacharjee, S., Elimelech, M. and Kretzschmar, R., 2000. Transport of Iron Oxide Colloids in Packed Quartz Sand Media: Monolayer and Multilayer Deposition, *Journal of Colloid and Interface Science.* Vol 231, 32–41

Kolakowski, J.E. and Matijevic, E., 1979. Particle Adhesion and Removal in Model Systems. Part 1.-Monodispersed Chromium Hydroxide on Glass. *Journal of the Chemical Society, Faraday Transactions 1: Physical Chemistry in Condensed Phases* **75**: 65-78

Kocaefe, D., T. R. Bui and P. Waite., 2009. "2D transient filtration model for aluminum." *Journal of Applied Mathematical Modelling* **33**(11): 4013-4030

Kuznar, Z.A. and Elimelech, M. 2007. Direct microscopic observation of particle deposition in porous media: role of the secondary energy minimum, *Colloid Surf. Physicochem. Eng. Aspect*, Vol. 294, Nos. 1-3, 156-162.

Lefevre, D., S. Comas-Cardona., C. Binetruy., 2007. "Modelling the flow of particle-filled resin through a fibrous preform in liquid composite moulding technologies." Composites Part A *Applied Science and Manufacturing* **38**(10): 2154-2163

Lever, A. and Dawe, R., 1984. Water-Sensitivity and Migration of Fines in the Hopeman Sandstone. *Journal of Petroleum Geology* **7** (1): 97-107

MacCarthy, J.F., and J.M. Zachara. 1989. Subsurface transport of contaminants, *Environ. Sci. Technol,* Vol 23, 496-502

Massoudieh, A. and Ginn, T.R., 2010. Colloid-Facilitated Contaminant Transport in Unsaturated Porous Media. In *Modelling of Pollutants in Complex Environmental Systems*, ed. G. Hanrahan, Chap. 8, 263. Hertfordshire, Glensdale: ILM Publications.

Mays, D.C. and Hunt, J.R., 2005. Hydrodynamic Aspects of Particle Clogging in Porous Media. *Environmental science & technology* **39** (2): 577-584

Miranda, R.M. and Underdown, D.R., 1993. Laboratory Measurement of Critical Rate: A Novel Approach for Quantifying Fines Migration Problems. Paper SPE 25432 presented at the SPE Production Operations Symposium, Oklahoma City, Oklahoma,USA, 21-23 March.

Muecke, T.W., 1979. Formation Fines and Factors Controlling Their Movement in Porous Media. *Journal of Petroleum Technology* **31** (2): 144-150

Mungan, N., 1965. Permeability Reduction through Changes in Ph and Salinity. *Journal of Petroleum Technology* **17** (12): 1449-1453

Nabzar, L., Chauveteau, G. and Roque, C., 1996. A New Model for Formation Damage by Particle Retention. Paper SPE 1283 presented at the SPE Formation Damage Control Symposium, Lafayette, Louisiana, USA, 14-15 February.

Noubactep, C. and S. Care 2010. "Dimensioning metallic iron beds for efficient contaminant removal" *Chemical Engineering Journal* **163**: 454-460

Ochi, J. and Vernoux, J.-F., 1998. Permeability Decrease in Sandstone Reservoirs by Fluid Injection: Hydrodynamic and Chemical Effects. *J. of Hydrology* **208** (3): 237-248

Purchas D.B., Sutherland K., 2002. Handbook of Filter Media (2nd ed.). *Elsevier Advanced Technology*, Oxford

Richards, T. and I. Neretnieks 2010. "Filtering of clay colloids in bentonite detritus material." *Chemical Engineering and Technology* **33**: 1303-1310

Rideal, G., 2006. Analysis and monitoring: how to improve precision pore size measurement, *Filtr. Separat.* Vol 43: 28-29

Rideal, G., 2009. The filtration society: the importance of testing and standards, *Filtr. Separat.* Vol 46: 28-30

Rousseau, D., Latifa, H. and Nabzar, L., 2008. Injectivity Decline from Produced-Water Reinjection: New Insights on in-Depth Particle-Deposition Mechanisms. *SPE Prod & Oper* **23** (4): 525-531

Ryan, J.N. and Elimelech, M., 1996. Colloid Mobilization and Transport in Groundwater. *Colloids and Surfaces A: Physicochemical and Engineering Aspects* **107**: 1-56

Sakthivadivel, R., 1969. Clogging of a granular porous medium by Sediment, Rep. HEL 15-7

Schechter, R.S., 1992. *Oil Well Stimulation*. TX: Richardson, Society of Petroleum Engineers.

Shapiro A.A., Bedrikovetsky P.G., Santos A., Medvedev O.O. 2007. A Stochastic Model for Filtration of Particulate Suspensions with Incomplete Pore Plugging, *Journal of Transport in Porous Media.*Vol 67, (1), p.135-164

Sharma, M.M., Chamoun, H., Sarma, D.S.H.S.R. and Schechter, R.S., 1992. Factors Controlling the Hydrodynamic Detachment of Particles from Surfaces. *Journal of Colloid and Interface Science* **149** (1): 121-134

Suri, A. and Sharma, M.M., 2001. Stratigies for Sizing Particles in Drilling and Completion Fluids, SPE 68964, 1-14

Tobiason, J.E., and O'Melia, C.R., 1988. Physicochemical Aspects of Particle Removal in Depth Filtration. J.Am, *Water Works Assoc*. Vol 80: 54-61

Tufenkji, N., and M. Elimelech., 2004. Deviation from Classical Colloid Filtration Theory in the Presence of Repulsive DLVO Interactions, *Langmuir*, Vol 20:10818–10828

Tufenkji, N. and Elimelech, M., 2005. Breakdown of Colloid Filtration Theory: Role of the Secondary Energy Minimum and Surface Charge Heterogeneities. *Langmuir* **21** (3): 841-852

Tufenkji, N., 2007. Colloid and Microbe Migration in Granular Environments: A Discussion of Modelling Methods. In *Colloidal Transport in Porous Media*, ed. F.H. Frimmel, F. von der Kammer and F.-C. Flemming, Chap. 5, 119-142. Berlin: Springer-Verlag.

Valdya, R.N. and Fogler, H.S., 1992. Fines Migration and Formation Damage: Influence of pH and ion exchange, SPE, 325-330

Veley, C.D, 1969. Howhydrolyzable Metal Ion React with Clays to Control Formation Water Sensitivity. *Journal of Petroleum Tech*, 1111-1118

Wong, R. and Mettananda, D., 2010. Permeability Reduction in Qishn Sandstone Specimens Due to Particle Suspension Injection. *Transport in Porous Media* **81** (1): 105-122

Yao, K.-M., Habibian, M.T. and O'Melia, C.R., 1971. Water and Waste Water Filtration. Concepts and Applications. *Environmental science & technology* **5** (11): 1105-1112

Yuan, H. and Shapiro, A.A., 2011a. A Mathematical Model for Non-Monotonic Deposition Profiles in Deep Bed Filtration Systems. *Chemical Engineering Journal* **166** (1): 105-115

Yuan, H. and Shapiro, A.A., 2011b. Induced Migration of Fines During Waterflooding in Communicating Layer-Cake Reservoirs. *Journal of Petroleum Science and Engineering* **78** (3–4): 618-626

Zhou, J., X. Zheng., M. Flury and G. Lin., 2009. "Permeability changes during remediation of an aquifer affected by sea-water intrusion: a laboratory column study." *Journal of Hydrology* **376**(3-4): 557-566.

3 Particle Transport in Porous Media under Particle–Rock Repulsion: Experimental and Theoretical Study

3.1 Transport and Straining of Suspension in Porous Media: Experimental and Theoretical Study

Aji K., You Z., Badalyan A.

Thermal Science, 2012, 16(5), 1444-1448.

TRANSPORT AND STRAINING OF SUSPENSIONS IN POROUS MEDIA: EXPERIMENTAL AND THEORETICAL STUDY

by

Kaiser AJI, Zhenjiang YOU*, and Alexander BADALYAN
Australian School of Petroleum, The University of Adelaide, Adelaide, Australia

Short paper
DOI: 10.2298/TSCI1205344A

An analytical model for deep bed filtration of suspension in porous media and straining under size exclusion capture mechanism is developed and validated by laboratory tests on suspension flow in engineered media. The fraction of swept particles is introduced in the inlet boundary condition. The model is successfully matched with the results from column experiments, predicting the suspended particle concentrations at the outlet.

Key words: *colloidal suspension, porous media, straining*

Introduction

Colloidal transport is a complex and industrially important process, attracting a great deal of interest for years [1-7]. Flow of colloidal suspensions in natural rocks occurs in many industrial applications ranging from particle filtration to fines migration in oil and gas reservoirs [1]. Through reliable modeling of suspension flow and consequent particle retention in rocks, it is possible to reduce the formation damage in oil and gas wells, to design and plan different oil recovery technologies where the colloidal particles are used to increase sweep efficiency during waterflooding.

Suspended particles can be captured in porous media by electrostatic attraction, sorption, bridging, diffusion, gravitational segregation, *etc.* [3]. In the current work, only the size exclusion (straining) capture, where a particle is retained by a smaller pore only, is considered.

The large scale deep bed filtration is described by governing equations of mass balance and capture kinetics for two unknowns – suspended and retained concentrations. These equations can be obtained by exact averaging of mono-size suspension transport in stochastic porous media [8].

Despite the importance of size exclusion population balance in many industrial applications, the validation of population balance models with particle straining, to the best of our knowledge, is not available in the literature. In the present work, we provide new experimental results from the laboratory study on colloidal transport in engineered porous media, aiming at the validation of the population balance model. The new modification of the size exclusion suspension transport accounting for the pore accessibility and flow fraction in the capture kinetics term, in the inlet and outlet conditions of particle mass balance, is discussed.

---

* Corresponding author; e-mail: zhenjiang.you@adelaide.edu.au

Good agreement between the experimental results and model prediction validates the mathematical model.

Stochastic micro model for particle size exclusion

Net repulsion condition between particles and rock matrix indicates that the size exclusion is the only particle capture mechanism. The pore space geometry is represented by the bundle of parallel capillary intercalated by the mixing chambers. Derivations of the equations for suspension transport in porous media can be found in [8, 9]. The particle population balance equation is written as:

$$\frac{\partial}{\partial t}\left[\phi_a(H,r_s)C(r_s,x,t)+\Sigma(r_s,x,t)\right]+U\frac{\partial}{\partial x}\left[C(r_s,x,t)f_a(H,r_s)\right]=0 \tag{1}$$

where the accessible porosity ϕ_a and accessible flow fraction f_a are functional of pore concentration distribution H and particle size r_s, C and Σ – concentration distributions for suspended and retained particles, respectively. The total flux U is independent of the coordinate x due to the incompressibility of particulate suspension. The particle capture rate is proportional to the advective particle flux:

$$\frac{\partial\Sigma(r_s,x,t)}{\partial t}=\frac{1}{l}UC(r_s,x,t)f_a(H,r_s)f_{ns}(H,r_s) \tag{2}$$

where f_{ns} is the flux fraction via smaller pores. The plugging rate of the pores is derived under the assumption that one particle plugs one pore:

$$\frac{\partial H(r_p,x,t)}{\partial t}=-\frac{k_1(r_p)}{k}UH(r_p,x,t)\int_{r_p}^{\infty}C(r_s,x,t)f_a(H,r_s)\,\mathrm{d}r_s \tag{3}$$

Introduction of inaccessible porosity and accessible fractional flow is analogous to two-phase flow in porous media [10, 11], inaccessible large pores corresponding to ganglia of non-wetting phase [12]. Equations (1)-(3) are similar to the system of two-phase multicomponent flow in porous media [1, 10].

The initial conditions $t = 0$: $C(r_s, x, t) = 0$, $H(r_p, x, t) = H_0(r_p)$, are applied to the clean bed without suspension where $H_0(r_p)$ is the initial pore size distribution of the medium. The suspension flux with the injected concentration entering larger pores is equal to that being transported through accessible pore space, which results in the following boundary condition at the inlet:

$$x=0:\ C^0(r_s,t)\left[f_a(H,r_s)+f_{nl}(H,r_s)\right]U=C(r_s,0,t)f_a(H,r_s)U \tag{4}$$

Let us formulate boundary conditions at the core inlet. The particles approaching smaller pores can be either swept by the tangent flux component parallel to the core edge and finally enter the larger pores, or stay captured in deep larger throats of the thin pores. The particles approaching smaller pores are more likely to be redirected into larger pores for the clean cut inlet core surface. In the case of rough inlet surface, the particles approaching smaller pores are more likely to remain in the deep entrances into small pores. If α is the fraction of swept particles, $C^0(r_s, t)[1 - f_{ns}(H, r_s) + \alpha f_{ns}(H, r_s)]U$ is the carrier water flux carrying particles into larger pores. The entering particles are transported via porous medium by the accessible flux f_aU. The continuity of the particle flux at the outlet yields the following boundary condition: $x = 0$: $C^0(r_s, t)[1 - f_{ns}(H, r_s) + \alpha f_{ns}(H, r_s)]U = C(r_s, 0, t) f_a(H, r_s)U$. Further in the text, the case $\alpha = 0$ is assumed, *i. e.* the suspension flux with the injected concentration entering larger pores is equal to that being transported through accessible pore space, which results in the boundary condition at the inlet (4). On the other side, the particle suspension at the outlet is diluted in the overall water flux after passing the core outlet, corresponding to the pre-outlet condition:

$$x = L: \; C(r_s, L, t) f_a(r_s)U = C^L(r_s, t)U \tag{5}$$

Particularly, for the case of low retention filtration, time variation of the pore size distribution during the straining can be ignored. The steady state suspension concentration profile is obtained:

$$C(r_s, x) = \frac{C^0(r_s)[f_a(r_s) + f_{nl}(r_s)]}{f_a(r_s)} \exp\left[-f_{ns}(r_s)\frac{x}{l}\right] \tag{6}$$

Laboratory study on suspension transport through engineered porous media

The glass beads are sieved using stainless steel sieves, before being packed in column at wet conditions with a theoretical porosity of 39.6%. Colloidal suspension is then delivered through packed column at constant rate by dual-pump/syringe system. Concentrations of injected and collected suspensions $C^0(r_{si})$ and $C^L(r_{si})$ are measured by the particle counter (fig. 1).

(a) bead sieving (b) column packing (c) suspension injection (d) particle counting

Figure 1. Schematic for laboratory set-up on size exclusion suspension transport in porous media

During the experiment, $C^0(r_{si})$ and $C^L(r_{si})$, are measured for each test (here, $i = 1, 2, ..., n$). The "n" tests result in the system of "n" transcendental equations for three unknowns – mean pore radius $<r_p>$, standard deviation σ_0 and dimensionless inter-chamber distance l. The least squares method is applied to minimize the total quadratic deviation between the experimental data and those predicted by the analytical model (6):

$$R = \min_{<r_p>, \sigma_0, l/L} \sum_{i=1}^{n} \left\{ [f_a(r_{si}) + f_{nl}(r_{si})] \exp\left[-f_{ns}(r_{si})\frac{L}{l}\right] - \frac{C^L(r_{si})}{C^0(r_{si})} \right\}^2 \tag{7}$$

For a porous medium PM1 with glass beads size range of 20~31.5 μm, the optimized mean pore size $<r_p> = 3.58$ μm, the standard deviation $\sigma_0 = 1.82$ μm, and the inter-chamber distance l = 0.55 mm. For a porous medium PM2 with glass beads size ranging from 31.5 to 45 μm, $<r_p>$ = 5.11 μm, σ_0 = 2.42 μm, and l = 0.15 mm. The results of data treatment are shown in fig. 2. The six star points from laboratory test data for PM1, fig. 2(a) and five test data points for PM2, fig. 2(b) match well with the curve predicted by the model (6). The dashed curves in figs. 2(a) and 2(b) are from the classical model [6], which does not account for the concentration increase at the inlet (4), dilution effect at the outlet (5) and accessible flux in the capture rate expression (2). The deviation between the two models can be expected for intermediate sized particles.

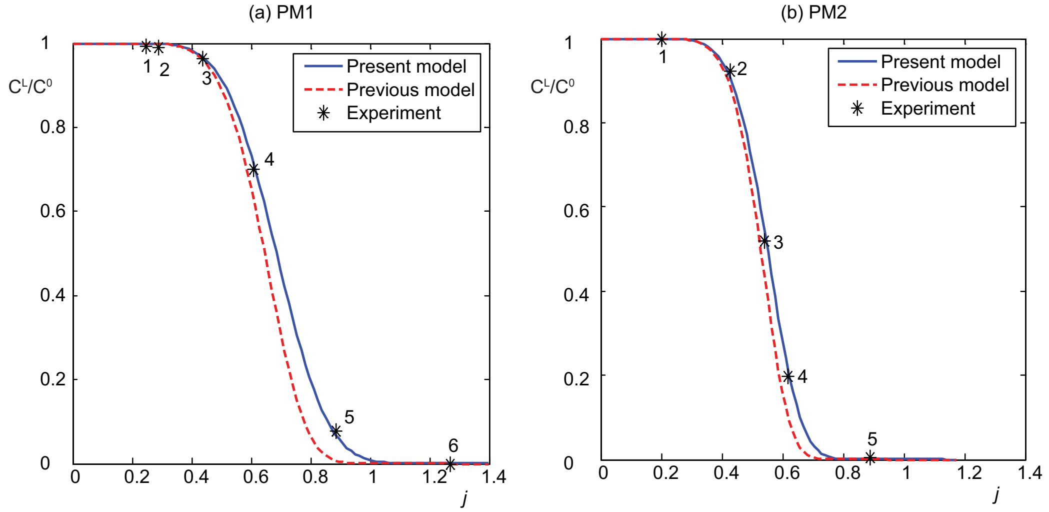

Figure 2. Normalized breakthrough concentrations *vs.* jamming ratio

Conclusions

A stochastic micro model is presented to describe suspension transport under size exclusion particle capture mechanism. The model accounts for the increase of particle concentration at the inlet due to the injected flux entrance only into accessible fraction of large pores, for the decrease of particle concentration at the outlet due to dissolution of the particle suspension carried by the accessible water flux in the overall water flux outside the porous media, and for the retention rate proportional to the accessible suspension flux. The fraction of swept particles introduced in the inlet boundary condition accounts for the redirection of particles into larger pores. The data from two laboratory tests have been successfully matched by the proposed model.

Acknowledgment

Financial supports from the Australian Research Council (ARC) Discovery Project 1094299, ARC Linkage Project 100100613 and Santos Pty Ltd are gratefully acknowledged.

References

[1] Bedrikovetsky, P. G., Mathematical Theory of Oil & Gas Recovery (With applications to ex-USSR oil & gas condensate fields), Kluwer, London, 1993

[2] Bradford, S. A., Torkzaban, S., Wiegmann, A., Pore-Scale Simulations to Determine the Applied Hydrodynamic Torque and Colloid Immobilization, *Vadose Zone Journal, 10* (2011), 1, pp. 252-261
[3] Torkzaban, S., *et al.*, Impacts of Bridging Complexation on the Transport of Surface-modified Nanoparticles in Saturated Sand, *Journal of Contaminant Hydrology, 136-137* (2012), Aug., pp. 86-95
[4] Yu, M., Lin, J. Z., Chan, T. L., Effect of Precursor Loading on Non-Spherical TiO_2 Nanoparticle Synthesis in a Diffusion Flame Reactor, *Chem. Eng. Sci, 63* (2008), 9, pp. 2317-2329
[5] Yu, M., Lin, J. Z., Taylor-Expansion Moment Method for Agglomerate Coagulation due to Brownian Motion in the Entire Size Regime, *Journal of Aerosol Science, 40* (2009), 6, pp. 549-562
[6] Yu, M., Lin, J. Z., Chan, T. L., Numerical Simulation of Nanoparticle Synthesis in Diffusion Flame Reactor, *Powder Technology, 181* (2008), 1, pp. 9-20
[7] Yu, M., Lin, J. Z., Chan, T. L., A New Moment Method for Solving the Coagulation Equation for Particles in Brownian Motion, *Aerosol Science and Technology, 42* (2008), 9, pp. 705-713
[8] Bedrikovetsky, P., Upscaling of Stochastic Micro Model for Suspension Transport in Porous Media, *Transport in Porous Media, 75* (2008), 3, pp. 335-369
[9] Chalk, P., *et al.*, Pore Size Distribution from Challenge Coreflood Testing by Colloidal Flow, *Chemical Engineering Research and Design, 90* (2012), 1, pp. 63-77
[10] Barenblatt, G. I., Entov, V. M., Rizhik, V. M., Theory of Fluid Flows through Natural Rocks, Kluwer, London, 1987
[11] Ilina, T., *et al.*, A Pseudo Two-Phase Model for Colloid Facilitated Transport in Porous Media, *Transport in Porous Media, 71* (2008), 3, pp. 311-329
[12] Bedrikovetsky, P. G., WAG Displacements of Oil-Condensates Accounting for Hydrocarbon Ganglia, *Transport in Porous Media, 52* (2003), 2, pp. 229-266

Paper submitted: August 1, 2012
Paper revised: September 7, 2012
Paper accepted: September 12, 2012

3.2 Colloidal Flow in Aquifers during Produced Water Disposal: Experimental and Mathematical Modelling

McLindin C., Saha A., Le K., **Aji K.**, You Z., Badalyan A., Bedrikovetsky P

SPE-153502-MS. DOI: 10.2118/153502-MS.

McLindin, C., Saha, A., Le, K., Aji, K., You, Z., Badalyan, A. & Bedrikovetsky, P. (2012) Colloidal flow in aquifers during produced water disposal: experimental and mathematical modelling. *Presented at the SPE Middle East Health, Safety, Security and Environment Conference, Abu Dhabi, UAE, 2-4 April 2012*

3.3 Effect of Nanoparticle Transport and Retention in Oilfield Rocks on the Efficiency of Different Nanotechnologies in Oil Industry

You Z., **Aji K.**, Badalyan A., Bedrikovetsky P

SPE-157097-MS. DOI: 10.2118/157097-MS. ISBN: 978-1-61399-206-7.

You, Z., Aji, K., Badalyan, A. & Bedrikovetsky, P. (2012) Effect of nanoparticle transport and retention in oilfield rocks on the efficiency of different nanotechnologies in oil industry. *Presented at the SPE International Oilfield Nanotechnology Conference, The Netherlands, 12-14 June, 2012*

3.4 Study of Particle Straining Effect on Produced Water Management and Injectivity Enhancement

Aji K., You Z., Badalyan A., Bedrikovetsky P.

SPE-157399-MS. DOI: 10.2118/157399-MS. ISBN: 978-1-61399-201-2.

Aji, K., You, Z., Badalyan, A. & Bedrikovetsky, P. (2012) Study of particle straining effect on produced water management and injectivity enhancement.
Presented at the SPE International Production and Operations Conference and Exhibition, Doha Qatar, 14-16 May, 2012

3.5 Colloidal-Suspension Flow in Rocks: A New Mathematical Model, Laboratory Study, IOR

Aji K., McLindin C., Saha A., Le K., You Z., Badalyan A., Bedrikovetsky P.

SPE-152025-MS, DOI: 10.2118/152025-MS. ISBN: 978-1-61399-199-2.

Aji, K., McLindin, C., Saha, A., Le, K., You, Z., Badalyan, A. & Bedrikovetsky, P. (2012) Colloidal-suspension flow in rocks: a new mathematical model, laboratory study, IOR.
Presented at the SPE EOR Conference at Oil and Gas West Asia, Muscat, Oman, 16-18 April, 2012

4 Particle Transport in Porous Media under Particle-Rock Attraction: Experimental and Theoretical Study

4.1 Particle Deposition and Mobilization during Deep Bed Filtration in Oilfields

Aji Kaiser

International Journal of Oil, Gas and Coal Technology, Accepted on 21/06/2013

Available online:

(http://www.inderscience.com/info/ingeneral/forthcoming.php?jcode=ijgct)

Aji, K. (2013) Particle deposition and mobilisation during deep bed filtration in oilfields. *International Journal of Oil, Gas and Coal Technology, v. 8(3), pp. 262-274*

4.2 Experimental Study of Colloidal Flow in Porous Media at High Velocities

Aji Kaiser

Asia-Pacific Journal of Chemical Engineering, Accepted on 20/11/2013. DOI: 10.1002, apj.1782

Aji, K. (2013) Experimental study of colloidal flow in porous media at high velocities.
Asia-Pacific Journal of Chemical Engineering, v. 9(4), pp. 535-542

4.3 High Velocity Colloidal Flow in Porous Media: Experimental Study and Modeling

Aji K., Badalyan A., Carageorgos T., Zeinijahromi A., Bedrikovetsky

Accepted by Book Chapter

Focus on Porous media Research, Ed. by Zhao C, 2013, Nova Science Publishers,NY.

Aji, K., Badalyan, A., Carageorgos, T., Zeinijahromi, A. & Bedrikovetsky, P. (2013) High velocity colloidal flow in porous media: experimental study and modelling.
In: Focus on Porous Media Research, Nova Science Publishers, New York

NOTE:
This publication is included on pages 140-178 in the print copy of the thesis held in the University of Adelaide Library.

5 Critical Analysis of Uncertainties during the Deep Bed Filtration

5.1 Size Exclusion Deep Bed Filtration: Experimental and Modeling Uncertainties

Badalyan A., You Z, **Aji K.**, Bedrikovetsky P., Carageorgos T., Zeinijahromi A.

Review of Scientific Instruments, 2014, V. 85, 015111/1-13

REVIEW OF SCIENTIFIC INSTRUMENTS **85**, 015111 (2014)

Size exclusion deep bed filtration: Experimental and modelling uncertainties

Alexander Badalyan,[a] Zhenjiang You, Kaiser Aji, Pavel Bedrikovetsky,
Themis Carageorgos, and Abbas Zeinijahromi
Australian School of Petroleum, University of Adelaide, Adelaide, South Australia 5005, Australia

(Received 23 July 2013; accepted 17 December 2013; published online 16 January 2014)

A detailed uncertainty analysis associated with carboxyl-modified latex particle capture in glass bead-formed porous media enabled verification of the two theoretical stochastic models for prediction of particle retention due to size exclusion. At the beginning of this analysis it is established that size exclusion is a dominant particle capture mechanism in the present study: calculated significant repulsive Derjaguin-Landau-Verwey-Overbeek potential between latex particles and glass beads is an indication of their mutual repulsion, thus, fulfilling the necessary condition for size exclusion. Applying linear uncertainty propagation method in the form of truncated Taylor's series expansion, combined standard uncertainties (CSUs) in normalised suspended particle concentrations are calculated using CSUs in experimentally determined parameters such as: an inlet volumetric flowrate of suspension, particle number in suspensions, particle concentrations in inlet and outlet streams, particle and pore throat size distributions. Weathering of glass beads in high alkaline solutions does not appreciably change particle size distribution, and, therefore, is not considered as an additional contributor to the weighted mean particle radius and corresponded weighted mean standard deviation. Weighted mean particle radius and LogNormal mean pore throat radius are characterised by the highest CSUs among all experimental parameters translating to high CSU in the jamming ratio factor (dimensionless particle size). Normalised suspended particle concentrations calculated via two theoretical models are characterised by higher CSUs than those for experimental data. The model accounting the fraction of inaccessible flow as a function of latex particle radius excellently predicts normalised suspended particle concentrations for the whole range of jamming ratios. The presented uncertainty analysis can be also used for comparison of intra- and inter-laboratory particle size exclusion data. © *2014 AIP Publishing LLC*. [http://dx.doi.org/10.1063/1.4861096]

I. INTRODUCTION

Retention of suspended particles flowing through porous media results in decrease in its permeability and translates to the reduced oil and gas well productivity and injectivity,[1] quick depletion of aquifers in geothermal fields due to clay migration,[2,3] etc. Such particle capture, according to Herzig *et al.*,[4] occurs via two mechanisms: particle separation at the entrance of a porous media through an external cake formation called mechanical filtration[5,6] and particle deposition inside a porous matrix. Formation of an external cake on the injection well surface is responsible for well injectivity decline.[7] The second mechanism of particle retention is called deep bed filtration, and it has implications during transport of suspended particles in oilfields, injection of produced water in aquifers, transport of contaminants in ground water reservoirs, filtration in wastewater treatment, etc.

Deep bed filtration during suspended transport in porous media is characterised by various micro-sized particle capture mechanisms occurred separately or in combination: straining,[6] size exclusion of large particles in smaller pores,[6] particle bridging at pore entrance,[5,8] internal cake formation,[5,8] sedimentation/segregation of particles due to gravity, diffusion of particles into pores with dead ends, and particle attachment to a porous matrix via London-van der Waals attractive forces.[5,6] Field or experimental conditions such as particle and pore size distributions, salinity and pH of suspension, surface chemistry and irregularities of particles and porous matrix, particle concentration, particle density, suspension velocity, etc. determine the dominance of one or several particle retention mechanisms over others.

Among the above particle capture mechanisms, particle size exclusion is responsible for formation damage when the following conditions are satisfied: particle dimensions exceed pore throat size, there is a weak or no attraction between particles and porous media, low particle concentration excludes competition between particles to pass through a pore throat and thus excludes the formation of bridges.

Appropriate selection of surface chemistry of suspended particles and a porous medium, particle concentration, alkalinity and ionic strength of suspension makes particle size exclusion mechanism dominant compared to other particle retention processes which at such conditions are considered negligible.[9–13] Although being an important particle retention mechanism, size exclusion deep bed filtration as a dominant particle capture mechanism has not been given a due attention in the literature;[6] previous studies mostly dealt with particle diffusion, attachment and sedimentation. Poor

---

[a] Author to whom correspondence should be addressed. Electronic mail: alexander.badalyan@adelaide.edu.au

0034-6748/2014/85(1)/015111/13/$30.00

agreement between experimental data and theoretical results during "polystyrene latex-glass beads" repulsion observed in various studies[14–16] was attributed, according to Ryan and Elimelech,[9] to surface charge heterogeneity and surface irregularities of particles and collectors. Quantification of these discrepancies would have been possible if the experimental and modelling uncertainties were available.

According to Yuan and Sin,[17] uncertainty analysis of filtration models can be done by the two commonly used methods, namely, Monte-Carlo simulations (MCS) or linear uncertainty propagation (LUP). The major drawbacks of the MCS method for uncertainty analysis are as follows: significant computational time[18] due to the fact that the accuracy of this method is a square root function of runs; and its inability to clearly identify the contribution of each parameter's uncertainty to the combined standard uncertainty (CSU) of the final result in analytical form.[19] On the contrary, when experimental uncertainties of model parameters are known, computational efficiency,[20] simplicity,[18] and representation of the CSU in analytical form are the advantages of LUP analysis. Additionally, unlike MCS method,[21] a more conservative LUP method does not underestimate model's uncertainty.[22] Another uncertainty propagation method such as sensitivity analysis also tends to deliver underestimated model's uncertainties when the number of input parameters changing "at a time" is limited to one or two thus not covering all their possible combinations.[23]

Tien[24] reported that the accuracy of 10% in particle concentration translates to a maximum uncertainty of ≈27% in initial collection efficiency of a filter. In an attempt to quantify uncertainty in their breakthrough concentration data, Deshpande and Shonnard[25] performed experiments in triplicate and used standard deviation as a measure of experimental uncertainty. Although sometimes repeatability can to some extent reflect the accuracy of measurements, in most cases experimental uncertainty is the most appropriate indicator of the experimental data accuracy. Authors estimated uncertainty in experimental breakthrough data calculated from the model as $<\pm 6\%$. Al-Abduwani *et al.*[26] used computer tomography for the determination of suspended particle concentration during filtration though granular media. They evaluated sensitivity of their experimental method to various particles concentrations; also, they calculated uncertainties in initial particle concentration and filtration coefficient. Using these uncertainty parameters, the authors concluded the poorness of their first model for prediction of filtration coefficient. Thus, the efficiency of the particle retention model was verified via instrument-related sensitivity data. Mays and Hunt[27] using Monte-Carlo simulations estimated uncertainty in the clogging parameter for several data sets. However, in these simulations they ignored experimental uncertainty in particle concentration data, which leads to underestimation of CSU in the simulated results. As a result, they were not able to conclude how well the clogging model agrees with the experimental data.

Various theoretical models[28–32] have been developed for prediction of particle capture due to size exclusion. These models were verified through comparison with the respective experimental data. However, such approach is incomplete and should be enhanced by the analysis of uncertainties in experimental data and modelling results achievable by the propagation of experimental uncertainties through modelling formulae. During model development, model parameters having direct physical meaning are usually preferred over empirical coefficients with indirect physical meaning. Sometimes, these parameters are the products of other experimental parameters with their own uncertainties. In this case, these model parameters may be characterised by a significantly higher uncertainty, than that for an empirical coefficient, translating to an unexpected high CSU in a modelling result. To circumvent such outcome, a detailed uncertainty analysis for each model parameter should accompany model development.

In the previous publications,[33–35] a methodology for the evaluation of the CSU in experimental data considered not only the contribution of the uncertainties in the measured experimental parameters, but also those arisen from the application of various models. Similar approach for the evaluation of CSU inherent to particle size exclusion experiment is necessary. Such detailed analysis of uncertainties for this type of experiments is done for the first time to the best of our knowledge.

In this paper, the uncertainties associated with particle capture due to size exclusion during deep bed filtration are analysed in details. Initially, appropriate measurements of electrophoretic mobilities of suspended particles and calculations of their outer surface potentials, zeta potentials of a porous medium and total potential of interaction between them were performed ensuring the existence of total repulsion between particles and a porous medium, leading to particle capture due to only size exclusion. This is followed by the discussion of the first category of uncertainties regarded as experimental which arise from the application of appropriate instruments. We demonstrate how these uncertainties propagate to normalised suspended particle concentrations in the two theoretical stochastic models developed in the previous papers[36,37] and used for correlation between breakthrough concentrations and fractions of accessible and inaccessible flows in size exclusion experiments. We identified the experimental and derived parameters having the highest uncertainties and showed how they affect the modelled uncertainties. Finally, a comparison between normalised suspended particle concentrations obtained by the two models and the respective experimental data is presented with the explanation of the observed deviations. Recommendations from NIST[38] and EURACHEM[39] uncertainty guidelines were used in this paper.

II. MATERIALS

A. Glass beads

Spherical soda-lime glass beads of AH-type (Ballotini Bead, Potters Industries Pty. Ltd., Australia) packed in a plastic flow-through column were used as an engineered porous medium in size exclusion experiments. Their chemical composition as reported by the manufacturer is presented in Table I.

Procedure outlined in Chalk *et al.*[13] and aimed ensuring experimental conditions favourable for repulsion between

TABLE I. Chemical composition of glass beads.

Compound	SiO_2	Na_2O	CaO	MgO	Fe_2O_3	Al_2O_3
% (w/w)	73.1	15.0	7.0	4.2	0.4	0.3

latex particles and porous matrix was used for glass beads preparation. Negative net surface charge of glass beads was achieved by adjusting alkalinity of flushing deionised high-purity MilliQ water (EMD Millipore, former Millipore Corporation, electrical resistivity of 18.2 MΩ cm at 25 °C) and suspensions at $\mathrm{pH} > 10$. At such conditions, metal oxides presented on the surface of glass beads have negative charge,[40] resulting in the net total repulsion with carboxyl latex suspended particles (see Sec. IV C). Therefore, size exclusion is adopted as the only mechanism of suspended particle capture inside a glass beads-formed porous medium. Quantitatively, suspended particle-glass bead interaction is discussed in Sec. IV C using Derjaguin-Landau-Verwey-Overbeek (DLVO) theory.[41,42]

B. Latex particles

Spherical latex particles modified by surface carboxyl groups (Polysciences, Inc., Warrington, PA, USA) were used for the preparation of suspensions. In alkaline solutions with $\mathrm{pH} > 10$, carboxyl surface groups undergo deprotonation, thus, creating a net negative charge on the surface of suspended particles.[43] At high pH-values and low salinity suspended carboxyl modified latex particles are prevented from aggregation[44] and from attachment to the surface of also negatively charged engineered porous medium (packed glass beads), leading to a suspended particle capture due to size exclusion. Previous studies with carboxyl latex particles flowing through a single layer of glass beads have shown no particle straining due to electrostatic attraction from surface metal oxides.[12,13,40]

Deionised high-purity MilliQ water was used for preparation of suspensions with $\mathrm{pH} > 10$ (by adding 0.1 M NaOH). In the present study, suspended particle concentrations varied between 0.5 and 2.0 ppm – such low values result in the reduction of particle competition to pass through a pore throat and in the absence of bridging.

III. EXPERIMENTAL

A. Experimental setup for size exclusion studies

Polyvinylchloride (PVC) flowthrough column *1* was used for size exclusion experiments (see Fig. 1). Column packing with clean glass beads *2* was carried out inside an ultrasonic bath filled with MilliQ water for several reasons: to avoid air ingress inside the packed column, which affects particle capture, and to get a more homogeneous packing, which improves experimental data reproducibility. Reduction of inlet and outlet dead-volumes differs the present column from that used in the previous study.[13]

The following improvements of the experimental setup and procedure aimed to improve the quality and reliability of experimental data compared to the previous experimental setup.[13] Alkaline (pH ≈ 10) suspension *3* at 25 ± 0.5 °C was pumped through the PVC column using a pulseless NE-100 dual-pump/syringe system *4* (New Era Pump Systems, Inc., Farmingdale, NY, USA) equipped with two 60 ml plastic syringes *5*. Combination of one-way valves *6–9* allowed uninterrupted pumping of suspension with a volumetric flowrate of 2 ml/min (5×10^{-5} m/s linear velocity) through a glass beads-packed column separated by manual valves 10 and 11. Mass of effluent samples in collecting beakers *12* were measured by the precision balance *13* (KERN EW 420-3NM, Inscale Ltd., Bucks, UK) and were used for calculation of pore volumes injected (PVI) using values for suspension density (which without an appreciable error was adopted as equal to water density).[36] Inlet (C^0) and outlet (C^L) particle concentrations were measured by a portable particle counter PAMAS S4031 GO (PAMAS GmbH, Salzuflen, Germany; later in the text referred as PAMAS) *14* and data transmitted to a personal computer *15*. Thus, the time-dependent relationship of the normalised outlet suspension concentration was established.

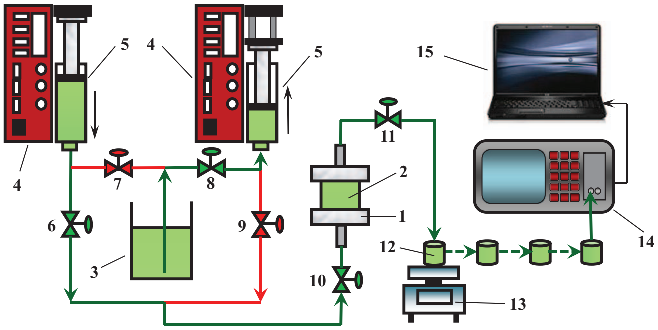

FIG. 1. Schematic of particle size exclusion setup: 1 – column; 2 – glass beads; 3 – latex particle-based suspension vessel; 4 – syringe pump; 5 – syringes; 6–9 – one-way valves; 10, 11 – valves; 12 – collection beaker for effluent suspension; 13 – analytical balance; 14 – PAMAS particle counter; 15 – personal computer.

B. Particle size distribution measurements

1. *Glass beads*

According to the manufacturer, radii of beads, r_b, vary from 15 to 62.5 μm (see Table II). The beads were sieved to the desired radius range of 20–31.5 μm using stainless steel test sieves (Pro-lab Scientific, Australia) certified to AS 1152-93/BS 410-86/ISO 3310. Mastersizer 2000 particle size analyser (Malvern Instruments Limited, Worcestershire, United Kingdom) was used to determine size distributions of supplied and sieved beads, which were later used for the evaluation of mean pore size.

2. *Latex particles*

Latex particles of 5 different sizes were used in present studies (see Table III). Concentrations of these particles in inlet and outlet suspensions, and particle size distribution were measured by PAMAS.

TABLE II. Combined results for supplied and sieved glass beads – from Mastersizer 2000 and Monte-Carlo simulations.

r_b^{min} (μm)	r_b^{max} (μm)	$r_{b,mean}^{LogNorm}$ (μm)	$\pm\sigma\left(r_b^{LogNorm}\right)$ (μm)	Comments
15.0	62.5	35.814	9.558	Supplied beads
20.0	31.5	28.761	7.589	Sieved beads
20.0	31.5	28.707	7.535	Sieved beads[a]
20.0	31.5	28.640	7.518	Sieved beads, 24 h at pH ≈ 10[a]
r_p^{min} (μm)	r_p^{max} (μm)	$r_{p,mean}^{LogNorm}$ (μm)	$\pm\sigma\left(r_p^{LogNorm}\right)$ (μm)	Comments
$-\infty$	$+\infty$	4.274	0.673	Pore
$-\infty$	$+\infty$	4.272	0.655	Pore[a]
$-\infty$	$+\infty$	4.258	0.668	Pore, 24 h at pH ≈ 10

[a] Used in glass beads corrosion experiments.

C. pH, electrophoretic mobilities and zeta-potential measurements

Mettler Toledo pH meter (model FE20, Mettler-Toledo AG, Analytical, Schwerzenbach, GERMANY) was used for pH measurements of suspensions with latex and glass beads, and solutions. This pH-meter has two-point calibration with ±0.01 pH error limit (accuracy). Two buffer solutions with pH 7.00 ± 0.02 and 10.01 ± 0.05 (HACH LANGE GmbH, Dűsseldorf, GERMANY) were used for calibration of pH meter prior to each pH measurement.

Since maximum duration of each size-exclusion experiment was approximately 10 h, therefore, it was very important to ensure that suspended latex particle-glass bead interaction inside the column corresponds to the repulsion condition for the duration of each experiment. For this reason, we measured variation of pH of the effluent suspensions during experiments.

Preliminary results on electrophoretic mobilities measurements showed that suspended latex particles concentration of 2 ppm (maximum concentration used in size exclusion experiments) was insufficient for reproducible electrophoretic mobility data. Therefore, by trial and error, the concentration of suspended particles was adjusted at 50 ppm.

In order to reduce the effect of particle sedimentation and obtain reproducible zeta-potential data for glass beads, the latter were crushed using mortar and pestle, and the obtained powder was sedimented in MilliQ water for 10 min in 100 ml measuring glass cylinder. Size of particles in 50 ml supernatant varied in the range from 0.8 to 2.5 μm. Concentration of these particles for zeta potential measurements was equal to 0.5% w/w.

Zetasizer Nano ZS (Malvern Instruments Ltd., Worcestershire, UNITED KINGDOM) was used for measurements of electrophoretic mobilities of latex particles and glass beads, which were used for calculation of the outer surface potentials for latex particles and zeta potentials for glass beads according to Ohshima's electrophoretic theory for "soft" particles[45,46] and modified Henry expression,[47] respectively. Zetasizer Nano ZS was verified against zeta potential transfer standard with accuracy of −50 mV ± 5 mV.

D. Metrological characteristics of instrumentation

The primary sources of equipment-associated uncertainties used for calculation of CSUs in modelling parameters are metrological characteristics of instrumentation reported by the respective manufacturers (see Table IV). Accuracy of the analytical balance was used for calculation of uncertainties in "pore volumes injected." Performance of NE-1000 dual-syringe pump was checked over the period of experiment (10 h): masses of MilliQ water delivered by these pumps were measured by KERN analytical balance, and calculated standard deviation of 10 mass measurements was equal to 0.8%, agreeing with reported pump accuracy (see Table IV). Density of water needed for the evaluation of water volumes was adopted from Wagner *et al.*[48] In all tests, the standard deviation in water volumes was <±1%. The reported accuracy for Mastersizer 2000 was adopted as the experimental uncertainty for glass bead size distribution measurements.

TABLE III. Latex particle characteristics.

Polysciences Inc.		PAMAS S4031 GO				
$r_{c,\,mean}$ (μm)	$\pm\sigma(r_c)$ (μm)	$r_{c,wm}$ (μm)	$\pm\sigma_{wm}(r_c)$ (μm)	$\pm\sigma_N$ (particles)	$\pm\delta_N$ (%)	% of particles
0.886	0.023	0.816	0.083	11 690	1.55	91.5
1.032	0.034	1.149	0.316	6828	0.83	91.7
1.568	0.037	1.543	0.270	1641	0.59	91.7
2.179[a]	0.057[a]	2.061[a]	0.335[a]	2026[a]	0.46[a]	94.2[a]
3.168	0.183	3.069	0.182	727	0.83	90.8

[a] Used as an example for calculations.

TABLE IV. Metrological characteristics of instrumentation.

Instrument	Measuring range	Accuracy
KERN EW 420-3NM	0–420 g	0.005 g
NE-100 dual-syringe pump	29.13 μl/h–2120 ml/h	1.0%
Mastersizer 2000	0.02–2000 μm	1.0%

Experimental uncertainties for particles number in inlet and outlet suspensions from the packed column were determined using accuracy of PAMAS. This accuracy was determined via repeatability measurements of particles number for 5 different-sized latex particles. For each particle size we carried out 10 consecutive measurements. The weighted mean values for particle radii, $r_{c_i,wm}$, and corresponded weighted mean standard deviations, $\sigma_{wm}(r_{c_i})$, are more representative than the respective mean values, since the PAMAS delivers data for particle number over a narrow particle size distribution range. These values were calculated by processing $r_{c_i} = f(N_i)$-data, where N_i is the number of particles for $''i''$ range of particle radii measured by the PAMAS. Numbers of particles used in these calculations were between 90.8% and 94.2% of the total number of particles delivered by PAMAS, $\pm\delta_N$. Thus obtained data are reported in Table III and, according to NIST Guidelines,[38] are adopted as precisions for particle number, $\pm\sigma_{N_i}$, and radii, $\sigma_{wm}(r_{c_i})$.

IV. RESULTS

A. pH, electrophoretic mobilities and zeta-potential

Variation of pH of effluent latex-based suspensions during size exclusion studies never dropped below 10.16. This is a sure sign of consistent experimental conditions.

Although MilliQ deionised water was used for the preparation of suspension, it is not appropriate to consider this medium as the so-called "salt-free" due to the presence of H^+ and OH^- in MilliQ water.[49] According to Merck Millipore,[50] concentration of sodium and chlorine ions in MilliQ water is 0.22 and 1 ppt (ng/l), respectively. This, together with the amount of NaOH added to MilliQ water to adjust pH > 10 translates to a maximum molar concentration of sodium ions as $C_{Na^+} = 1.248 \times 10^{-4}$ M and ionic strength of $I = 6.24 \times 10^{-5}$ M. Taking into account the radius of latex microspheres as $r_c = 2.061$ μm, we arrive at $\kappa r_c = 53.43$, where $\kappa = 2.592 \times 10^{7}$ m^{-1} is the Debye-Hückel (D-H) reciprocal length for a symmetrical monovalent electrolyte (NaCl), according to Elimelech *et al.*[51]

For the evaluation of zeta-potential from experimental electrophoretic mobility data the Smoluchowski ($\kappa r_c \gg 1$ and electrolyte concentration should be $>10^{-3}$ M) and Hückel ($\kappa r_c \ll 1$ and non-aqueous solutions) equations are widely used in literature. However, for the present experimental conditions for latex microspheres ($\kappa r_c = 53.43$ and ionic strength $I = 6.24 \times 10^{-5}$ M), according to Elimelech *et al.*,[51] both of these equations are not suitable, since calculated ζ-potential values do not accurately represent actual surface potentials of carboxyl coated latex microspheres. Another reason for non-applicability of the above zeta-potential models is that when latex microspheres are coated by a polyelectrolyte layer (carboxyl-modified in the present study), they are treated as the so-called "soft" particles since ions from an electrolyte solution can penetrate into the surface layer of carboxyl coating.[45,46]

To overcome limitations of Smoluchowski and Hückel models, several formulas were proposed by Ohshima[45,46] for electrophoretic mobilities of "soft" particles:

$$\mu = \frac{\varepsilon_r \varepsilon_0}{\eta} \frac{\dfrac{\psi_0}{\kappa_m} + \dfrac{\psi_{DON}}{\lambda}}{\dfrac{1}{\kappa_m} + \dfrac{1}{\lambda}} + \frac{\rho_{fix}}{\eta \lambda^2}, \tag{1}$$

$$\psi_0 = \frac{kT}{ze}\left(ln\left[\frac{\rho_{fix}}{2zen^{\infty}} + \left\{\left(\frac{\rho_{fix}}{2zen^{\infty}}\right)^2 + 1\right\}^{1/2}\right] + \frac{2zen^{\infty}}{\rho_{fix}}\left[1 - \left\{\left(\frac{\rho_{fix}}{2zen^{\infty}}\right)^2 + 1\right\}^{1/2}\right]\right), \tag{2}$$

$$\psi_{DON} = \frac{kT}{ze} ln\left[\frac{\rho_{fix}}{2zen^{\infty}} + \left\{\left(\frac{\rho_{fix}}{2zen^{\infty}}\right)^2 + 1\right\}^{1/2}\right], \quad \text{and} \tag{3}$$

$$\kappa_m = \kappa\left[1 + \left(\frac{\rho_{fix}}{2zen^{\infty}}\right)^2\right]^{1/4}, \tag{4}$$

where μ is electrophoretic mobility, $\frac{m^2}{V \times s}$; ε_r is relative permittivity of aqueous solutions of NaCl at 25 °C and various ionic strengths, adopted from Buchner *et al.*;[52] $\varepsilon_0 = 8.854 \times 10^{-12}$ is dielectric permittivity of vacuum; $\eta = 8.9002 \times 10^{-4}$ Pa s is dynamic viscosity of water;[53] ψ_0 and ψ_{DON} are the outer surface and the Donnan potentials, respectively, V; κ_m is the Debye-Hückel parameter for the polyelectrolyte layer with fixed charges contribution,[46] m^{-1}; $\frac{1}{\lambda}$ is electrophoretic "softness" of latex particle, m; $\rho_{fix} = ZeN$ is fixed charge density of for the polyelectrolyte layer, $\frac{C}{m^3}$; $Z = 1$ is the valence of the symmetrical functional groups; $e = 1.602 \times 10^{-19}$ C is the elementary electric charge; and N is the number concentration of the dissociated carboxyl functional groups, m^{-3}; k is Stefan-Boltzmann constant, $\frac{J}{K}$; $T = 298.15 \pm 0.1$ K is absolute temperature of suspension; z is valence of a symmetrical electrolyte solution; and n^{∞} is bulk concentration of the electrolyte, m^{-3}.

Equation (1) can be re-written in the following form:

$$\begin{aligned} \mu &= \frac{\varepsilon_r \varepsilon_0}{\eta} \frac{\dfrac{\psi_0}{\kappa_m}}{\dfrac{1}{\kappa_m} + \dfrac{1}{\lambda}} + \frac{\varepsilon_r \varepsilon_0}{\eta} \frac{\dfrac{\psi_{DON}}{\lambda}}{\dfrac{1}{\kappa_m} + \dfrac{1}{\lambda}} + \frac{\rho_{fix}}{\eta \lambda^2} \\ &= \frac{\varepsilon_r \varepsilon_0}{\eta} \frac{\psi_0 \lambda}{\kappa_m + \lambda} + \frac{\varepsilon_r \varepsilon_0}{\eta} \frac{\psi_{DON} \kappa_m}{\kappa_m + \lambda} + \frac{\rho_{fix}}{\eta \lambda^2} \\ &= \mu^0 + \mu^{DON} + \mu^{\infty}. \end{aligned} \tag{5}$$

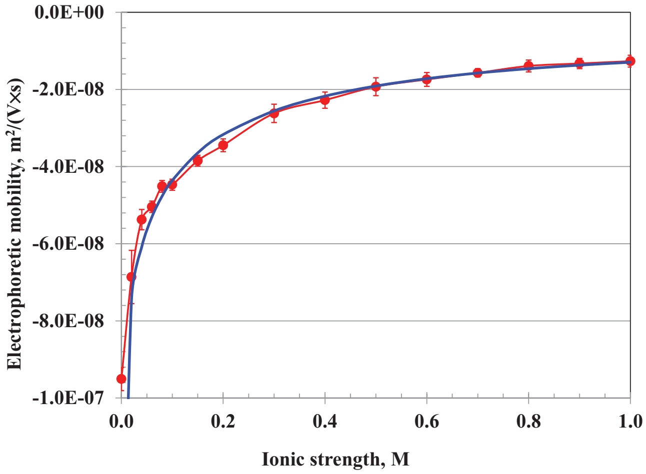

FIG. 2. Variation of electrophoretic mobility for latex particles as a function of ionic strength of NaCl solution: red ●, experimental data; dark blue ——, according to (1).

Increase of electrolyte concentration, $n^{\infty} \rightarrow \infty$, results in shrinkage of the diffuse layer with $\kappa \rightarrow \infty$ (and, consequently, $\kappa_m \rightarrow \infty$). At this limit, $\psi_0 \rightarrow 0$ and $\psi_{DON} \rightarrow 0$ as follows from Eqs. (2) and (3), leaving $\mu^0 \rightarrow 0$ and $\mu^{DON} \rightarrow 0$, respectively. As the result, $\mu^{\infty} = \frac{\rho_{fix}}{\eta\lambda^2}$, meaning vanishing of all potentials.[46]

Limiting non-zero value of μ^{∞} with two unknown parameters, ρ_{fix} and λ, corresponds to the experimental condition with maximum electrolyte concentration. At high ionic strengths of solutions, electrophoretic mobility of rigid particles tends to zero. When residual electrophoretic mobility values are observed at high ionic strength of an electrolyte one is dealing with "soft" particles.[40] Electrophoretic mobilities of latex microspheres were measured at ionic strengths of NaCl solutions varying from 0.000125 to 1 M (see Fig. 2) and were reproducible within their experimental uncertainties (the highest deviation was 12.3%, which can be regarded as satisfactory). Electrophoretic mobilities measurements at higher ionic strengths 2, 3, 4, and 5 M NaCl were very difficult to perform due to strong polarisation of electrodes of the measuring cell[54] and agglomeration of suspended particles.[11] This led to a significant spread of experimental electrophoretic mobility data at high ionic strengths of electrolyte solution, although every effort was made to improve data repeatability such as: ultrasonification of sample prior to measurements and reduction of time interval after sample ultrasonification and measurement down to 5 s (stabilisation of sample time). Electrophoretic mobility of $\mu^{\infty} = (-1.268 \pm 0.156) \times 10^{-8}$ $m^2/(V\ s)$ corresponding to 1.0 M NaCl salinity was adopted as a residual electrophoretic mobility of carboxyl-modified latex microspheres.

According to Ohshima *et al.*,[55] the first approximation of the pair ρ_{fix} and λ can be obtained by fitting $\frac{\rho_{fix}}{\eta\lambda^2}$ to the electrophoretic mobility value corresponded to maximum electrolyte concentration, μ^{∞}. However, the authors did not specify which iteration algorithm was employed to fit electrophoretic mobility data at lower ionic strength resulting in the final values of ρ_{fix} and λ. de Kerchove and Elimelech[56] applied the Levenberg-Marquardt method to $\mu = f(I)$-data for the determination of ρ_{fix} and λ in the range of ionic strengths from 1 to 300 mM KCl.

In the present study, a weighted nonlinear least squares method[57] with the two adjusting parameters ρ_{fix} and λ was used. Since each experimental value of electrophoretic mobility for latex particles, μ_i, has its own standard deviation, σ_i (which is adopted as experimental uncertainty), respective weight functions, $w_i = \frac{1}{\sigma_i^2}$, were calculated for electrophoretic mobility data. Values of μ_i^{calc} were calculated according to Eq. (5) using ρ_{fix} and λ data for similar carboxyl microspheres adopted from Kuznar and Elimelech[40] as the initial input data. Then, the following values of $(\mu^{calc} - \mu^{exper})^2$ and $w_i(\mu^{calc} - \mu^{exper})^2$ were calculated. Minimising $\sum_{i=1}^{i=16} [w_i(\mu^{calc} - \mu^{exper})^2]$ via iteration procedure using Solver in the Microsoft Excel™ resulted in the final values of the particle charge density $\rho_{fix} = -1064$ mM and electrophoretic "softness" $\frac{1}{\lambda} = 0.242$ nm.

Using Eqs. (2) and (3), the following potentials were calculated: $\psi_0 = -206.8$ mV and $\psi_{DON} = -232.5$ mV. Application of Smoluchowski model to electrophoretic mobility data significantly overestimates surface potential of carboxyl-modified latex particles, resulting in $\psi_0^{Smol.} = (-96.32 \pm 5.25)$ mV.

Application of corrections for the electrophoretic retardation and relaxation effects for glass beads according to Abramson[58] gives the following value for the Henry correction factor $f_1(\kappa r_c) = 1.440$. Using experimental electrophoretic mobility data for glass beads and Henry expression:[47]

$$\zeta_b = \frac{3U_E\mu}{2\varepsilon f_1(\kappa r_c)}, \tag{6}$$

where U_E is electrophoretic mobility of particle of interest, mV; μ – fluid dynamic viscosity, Pa s; and ε – permittivity of MilliQ water; we obtained the following zeta-potential value: $\zeta_{beads} = (-51.99 \pm 3.15)$ mV.

B. Particle size distribution

1. Glass beads particle and pore size distribution

Results of size distributions for supplied and sieved beads are presented in Table II. Sieved glass beads were used for the preparation of packed bed, through which suspended latex particles were pumped. To use experimental data for calculations, pore size distribution of a porous medium in a packed column is needed. Previous experiments for bed packing with glass beads have shown that the most probable bead packing type is rhombohedral with 39.6% porosity.[13] In such a packing, two dimensional cross-section gives a pore throat formed by three circles with the forth one (circular pore throat) inscribed between them. The radius of the forth circle can be determined by the Descartes theorem.[59] Using this theorem and @RISK analysis software with Monte-Carlo simulations for Excel (Palisade Corporation, Ithaka, NY, USA) pore throat size distribution was determined, r_p, with LogNormal distribution giving the best fit to the experimental data. Results of Monte-Carlo simulations (100 000 iterations) are given in

Table II. Standard deviation was adopted as an uncertainty in the evaluation of pore radius.[60]

2. Latex particle size distribution

Although the manufacturer supplied latex microspheres with values of their mean diameter and standard deviation, in order to keep internal consistency in calculations of latex microsphere concentrations and jamming ratios we used our experimental data obtained using PAMAS particle counter/sizer as described in Secs. III B 2 and III D. Suspended particle size distribution used as the example for uncertainty calculations (see footnote for Table III) together with weighted mean radii and standard deviations for the studied latex particles are presented in Table III.

C. Total interaction potential between latex particles and glass beads

In the present study, the major mechanism of particle capture is size exclusion, meaning that particle attachment and bridging are negligible. Particle-bead interaction[41,42] is determined by attractive long-range London-van der Waals, and short-range repulsive electrical double layer and Born forces contributing to the total particle-surface potential energy, V_{tot}, as follows:

$$V_{tot} = V_{LW} + V_{EDL} + V_B, \tag{7}$$

where V_{LW}, V_{EDL}, and V_B are London-van der Waals, electrostatic double layer, and Born potential energies, respectively, k_BT. Introduction of a short-range Born repulsion force from the Lennard-Jones "m-n" potential into Eq. (7), according to Elimelech *et al.*,[51] accounts for overlapping of electron clouds when atoms find themselves in the close vicinity from each other.

Since the ratio between mean glass bead radius and weighted mean latex particle radius is equal to $\frac{r_{b,mean}^{LogNorm}}{r_{c,wm}} = 14.4$ (see Table II), the formula proposed by Gregory[61] was used for calculation of sphere-plate retarded London-van der Waals potential:

$$V_{LW} = -\frac{A_{123} r_{c,wm}}{6h}\left[1 - \frac{5.32h}{\lambda} ln\left(1 + \frac{\lambda}{5.32h}\right)\right], \tag{8}$$

where $A_{123} = 1.028 \times 10^{-20}$ J is Hamaker constant for a system latex-water-glass calculated in the present study according to Ref. 43; $\lambda = 100$ nm is the characteristic wavelength of the interaction according to Ref. 61; and h is particle-surface (sphere-plate) separation distance, $h \ll r_c$, m.

Value of $\kappa r_c = 53.43 \gg 1$ indicates that the double-layer thickness is significantly smaller than the particle size, therefore, electrostatic double-layer potential can be calculated according to Gregory:[62]

$$V_{EDL} = \frac{128\pi r_{c,wm} r_{b,mean}^{LogNorm} n_\infty k_B T}{\left(r_{c,wm} + r_{b,mean}^{LogNorm}\right)\kappa^2} \gamma_1 \gamma_2 e^{-\kappa h}, \tag{9}$$

where $n_\infty = 6.022 \times 10^{25}$ number/m^3 is bulk number density of ions; $k_B = 1.381 \times 10^{-23}$ J/K is Boltzmann constant; T is absolute temperature of the system, K; $\gamma_1 = \tanh(\frac{ze\psi_c}{4kT})$ and $\gamma_1 = \tanh(\frac{ze\zeta_b}{4kT})$ are reduced surface potentials for latex particles and glass beads;[51] $\psi_c = \psi_0$ and ζ_b are surface and zeta potentials for latex microspheres and glass beads, respectively, V; in this equation mean LogNorm bead radius approaches infinity for a sphere-plate system.

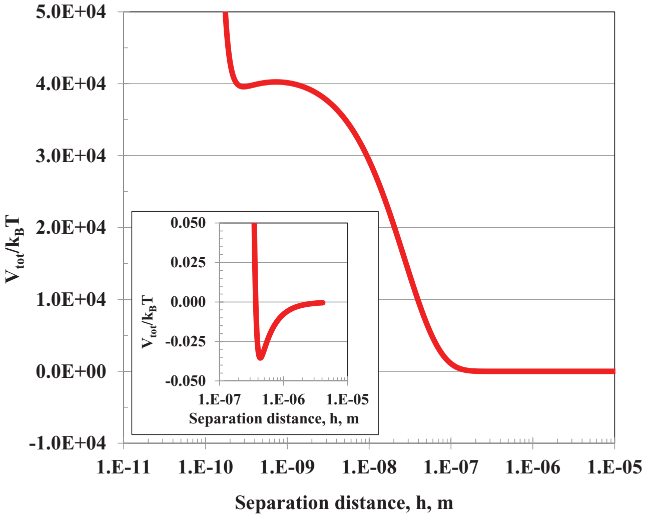

FIG. 3. Total interaction potential between latex microspheres and glass beads.

Short-range Born repulsion potential between latex microspheres and glass beads was evaluated according to Ruckenstein and Prieve:[63]

$$V_B = \frac{A_{123}\sigma^6}{7560}\left[\frac{8r_{c,wm} + h}{(2r_{c,wm} + h)^7} + \frac{6r_{c,wm} - h}{h^7}\right], \tag{10}$$

where $\sigma_c = 0.5$ nm is collision diameter and $n = 12$ is Lennard-Jones parameter.

Calculation of the total potential of interaction between latex microspheres and glass beads revealed a high repulsion energy barrier of 40 244 k_BT observed on the "total interaction potential/particle-wall distance"-curve at 0.733 nm as shown in Fig. 3. A presence of a negligible secondary energy minimum with depth of −0.035 k_BT was observed at ≈436 nm. It means that at all separation distances, electric-double-layer and Born repulsive forces dominate over attractive LW forces, and, therefore, experimental conditions are favourable for particle-wall repulsion. It can be concluded that particle retention mechanism in the present study is size exclusion particle capture.

V. SOURCES OF UNCERTAINTIES AND THEIR CONTRIBUTIONS

Linear uncertainty propagation method is used for calculation of CSUs for latex particle concentrations in the form of the first-order Taylor series approximation:[38]

$$u_c^2(y) = \sum_{i=1}^{N}\left(\frac{\partial f}{\partial x_i}\right)^2 u^2(x_i) + 2\sum_{i=1}^{N-1}\sum_{j=i+1}^{N}\frac{\partial f}{\partial x_i}\frac{\partial f}{\partial x_j}u(x_i, x_j), \tag{11}$$

where $u_c(y)$ is CSU for a function; $u(x_i)$ is CSU for the parameter i; and N is the number of parameters. In the present uncertainty analysis, input parameters are independent and uncorrelated; therefore, the truncated form of Eq. (11) is used for the evaluation of combined uncertainties[64,65]

$$u_c(y) = \sqrt{\sum_{i=1}^{N} \left[\left(\frac{\partial f}{\partial x_i} \right) u(x_i) \right]^2}. \tag{12}$$

A. Weathering of glass beads in alkaline suspensions

Alkaline nature of flowing suspension may affect the size of glass beads. As was reported earlier by Jeong *et al.*,[66] soda-lime glass undergoes weathering (corrosion) in solutions with pH-values as high as 10 at 20 to 90 °C due to dissolution of silica from silica-oxygen (Si–O) bonds. As the result, radii of glass beads are reduced with the duration of exposure to high-pH solutions. Such dissolution causes the change in initial particle size distribution and, consequently, in pore size distribution of a porous medium. We determined the effect of weathering on glass bead radii used in the present studies at the following conditions: pH ≈ 10 and 20 °C. According to Jeong *et al.*,[66] silica dissolution rate at pH = 9.81 and 20 °C is equal to $\approx 6 \times 10^{-2}$ g/(m^2 day). Taking into account that the maximum duration of an experiment is ≈24 h, the reduction of glass bead radii varied from 0.04% to 0.19% for bead radii from 31.5 to 20 μm, respectively (see Table II).

Using Mastersizer 2000, we measured particle size distribution for glass beads (sieving range for r_b varied from 20 to 31.5 μm) soaked and stirred for 24 h in MilliQ water with pH ≈ 10 at 20 °C and compared with those prepared according to the procedure outlined in Sec. II A of the present paper. According to Table II, the agreement between the obtained $r_{b,mean}^{LogNorm}$-values is 0.23%, which can be regarded as satisfactory, taking into account that the reproducibility of beads sieving procedure is 0.19%. Such reduction in $r_{b,mean}^{LogNorm}$-values due to weathering translates to the differences in respective $r_{p,mean}^{LogNorm}$-values of 0.33%. Overall, $r_{p,mean}^{LogNorm}$ results for washed glass beads and for those soaked in alkaline MilliQ water solution agree within respective standard deviations, $\sigma(r_p^{LogNorm})$.

B. Latex particle concentrations and jamming ratios

Concentrations of latex particles in inlet and effluent streams were determined by PAMAS and expressed in "particles/ml," rather than in "ppm" or "vol/vol." Parameters C^0 and C^L correspond to those from Eq. (12) in the following form: $y = C$, $x_1 = C^0$, and $x_2 = C^L$, thus contributing to CSU in normalised outlet suspended concentration according to the following expression:

$$u_c(C) = u_c\left(\frac{C^L}{C^0}\right) = \sqrt{\left[\frac{\partial C}{\partial C^L}u(C^L)\right]^2 + \left[\frac{\partial C}{\partial C^0}u(C^0)\right]^2}$$
$$= \sqrt{\left[\frac{1}{C^0}u(C^L)\right]^2 + \left[-\frac{C^L}{(C^0)^2}u(C^0)\right]^2}. \tag{13}$$

As an example, CSU in normalised concentration was calculated for suspended particles with $r_{c,wm} = 2.061 \pm 0.335$ μm (see Table III) flowing through glass beads with $r_b = 20.0 \div 31.5$ μm (see Table I). Respective CSUs are given in Table V, and after using (13) they translate to a normalised concentration $C = 0.701 \pm 0.001$. Similar approach was applied to latex particles with different radii (see Table III).

The "jamming ratio" (with a physical meaning of a "dimensionless particle size") as one of the parameters in the stochastic model for size exclusion experiments is determined as the ratio between weighted mean latex particle radius and mean LogNormal pore radius obtained by Monte-Carlo simulations (see Sec. IV B and Tables II and III):

$$j = \frac{r_{c,wm}}{r_{p,mean}^{LogNorm}}. \tag{14}$$

Using Eq. (12), CSU in jamming ratio is determined as follows:

$$u_c(j) = u_c\left(\frac{r_{c,wm}}{r_{p,mean}^{LogNorm}}\right) = \sqrt{\left[\frac{\partial j}{\partial r_{c,wm}}u(r_{c,wm})\right]^2 + \left[\frac{\partial j}{\partial r_{p,mean}^{LogNorm}}u\left(r_{p,mean}^{LogNorm}\right)\right]^2}$$
$$= \sqrt{\left[\frac{1}{r_{r_{p,mean}^{LogNorm}}}\sigma_{wm}(r_{c,wm})\right]^2 + \left[-\frac{r_{c,wm}}{\left(r_{p,mean}^{LogNorm}\right)^2}\sigma\left(r_{p,mean}^{LogNorm}\right)\right]^2}. \tag{15}$$

In Eq. (15), we substituted CSU of weighted mean latex particle radius and CSU of mean LogNormal pore radius by their weighted mean standard deviation and standard deviation, respectively. For the above example, the value for the jamming ratio of $j = 0.482 \pm 0.114$ was obtained. Therefore, the jamming ratio can be determined with a relatively high

TABLE V. Summary of experimental uncertainty analysis results.

Parameter	Units	CSU	RCSU
L	m	5.00×10^{-6}	8.44×10^{-5}
$N_{particle}^{MASTERSIZER\ 2000}$	particles	N/A	1.00×10^{-2}
$d_{particle}^{MASTERSIZER\ 2000}$	m	2.06×10^{-8}	1.00×10^{-2}
$N_{particle}^{PAMAS}$	particles	4624	2.38×10^{-2}
$d_{particle}^{PAMAS}$	m	8.52×10^{-8}	4.13×10^{-2}
$Q_{syringe}$	m^3/s	3.33×10^{-10}	1.0×10^{-2}
C^0	particles/ml	4.258×10^4	0.0046
C^L	particles/ml	2.983×10^4	0.0046
C	N/A	4.558×10^{-3}	0.0065
$r_{c,wm}$	m	3.77×10^{-7}	0.19
$r_{p,mean}^{LogNorm}$	m	6.73×10^{-7}	0.16
j	N/A	0.116	0.246
Corrosion of glass	m	1×10^{-9}	7×10^{-4}
Int-25-1	m/s	0.0325	1.66×10^{-4}
Int-25/26-2	m/s	0.0610	1.58×10^{-4}
Int-26-1	m/s	3.3000	0.251
$f_a(r_c)$	N/A	1.16×10^{-4}	2.29×10^{-4}
$f_{ns}(r_c)$	N/A	8.54×10^{-3}	2.51×10^{-1}
l	m	6.73×10^{-7}	1.03×10^{-3}
$u_c(C_{model})$, Eq. (27)	N/A	3.40×10^{-3}	7.92×10^{-3}
$u_c(C_{model})$, Eq. (28)	N/A	3.43×10^{-2}	4.97×10^{-2}

uncertainty of 24.3% which can be reduced to 15.5%, if values of particle radius and their standard deviations were adopted after the manufacturer (see Table III). However, since we are dealing with a population of particles of different radii (rather than with a population of particles of the same radius), for a more rigorous approach, one should use a weighted mean value for the particle radius and its weighted mean standard deviation, which would provide higher uncertainty value for the jamming ratio. Such approach is also correct, since suspended particle concentrations were determined by PAMAS giving results in particle number distribution over the range of latex particle radii resulting in a more representative weighted mean value for the particle radius, appropriate for the present experimental conditions.

VI. UNCERTAINTIES FOR TWO STOCHASTIC PARTICLE SIZE EXCLUSION MODELS

Information about uncertainties in experimental data and uncertainties in modelling results provide full information for model evaluation. Some model variables are experimental parameters with their experimental uncertainties; other model variables are derived from experimental parameters via empirical or theoretical formulas. Therefore, the law of propagation of uncertainties (12) should be applied to the respective modelling equations to calculate uncertainties in modelling results.

Correlation between breakthrough concentration and fraction of accessible and inaccessible flows in size exclusion experiments can be predicted by the two stochastic micromodels developed in Refs. 36 and 37:

$$\frac{C^L(r_c)}{C^0(r_c)} = \exp\left(-\frac{f_{ns}(r_c)\,L}{f_a(r_c)\,l}\right), \quad \text{and} \tag{16}$$

$$\frac{C^L(r_c)}{C^0(r_c)} = \{1 - f_{ns}(r_c)\}\exp\left(-f_{ns}(r_c)\,\frac{L}{l}\right), \tag{17}$$

where $f_a(r_c)$ is the fraction of accessible flow as a function of suspended particle radius; $f_{ns}(r_c)$ is the fraction of inaccessible flow as a function of suspended particle radius; L is the length of the column of the porous medium, m; l is the interval between chambers where suspended particles are mixed and redistributed; a porous medium is represented by a bundle of a parallel capillaries alternated by chambers, m; and $\frac{l}{L}$ is dimensionless correlation length.

Propagation of experimental uncertainties in the two micromodels described by Eqs. (16) and (17) was evaluated as follows. Initially, we evaluate uncertainties in the parameters of these equations, namely, $u(f_a(r_c))$, $u(L)$, $u(f_{ns}(r_c))$ and $u(l)$. As follows from Table V, $u(L) = 5.00 \times 10^{-6}$ m. Due to the small value of the interval between mixing chambers, the parameter l, without a significant error, can be approximated by the value of the mean LogNormal bead diameter, $d_{b,mean}^{LogNorm}$, and, then, $u(l)$ is equal to the weighted mean standard deviation, $u(l) = u(r_{b,mean}^{LogNorm}) = \sigma(r_{b,mean}^{LogNorm})$.

The following approach was used to evaluate $u(f_a(r_c))$ and $u(f_{ns}(r_c))$. As reported in the paper,[36] fractions of accessible and inaccessible flows can be determined as follows:

$$f_a(r_c) = \frac{U_a}{U} = \frac{\int_{r_c}^{\infty} k_1(r_p)\gamma(j)\,H(r_p,x,t)dr_p}{\int_0^{\infty} k_1(r_p)H(r_p,x,t)dr_p}, \quad \text{and} \tag{18}$$

$$f_{ns}(r_c) = \frac{U_{ns}}{U} = \frac{\int_0^{r_c} k_1(r_p)H(r_p,x,t)dr_p}{\int_0^{\infty} k_1(r_p)H(r_p,x,t)dr_p}, \tag{19}$$

where U, U_a, and U_{ns} are linear velocities of the total, accessible, and inaccessible fluxes, respectively, m/s; $k_1(r_p)$ is the conductance through a single pore of a triangular cross-section; and $\gamma(j)$ is the flux reduction factor; $H(r_p, x, t)$ is the concentration of pores with sizes between r_p and $r_p + dr_p$ at a certain distance x from the inlet of the column and time t, m^{-3}. These parameters are determined as follows:

$$k_1(r_p) = \frac{9\sqrt{3}}{20}r_p^4, \quad \text{and} \tag{20}$$

$$\gamma_i(j) = \begin{cases} (1-j)^2\left(1 + 2j - \frac{1}{3}j^2 - \frac{4}{9}j^3\right), & j < 1 \\ 0, & j > 1 \end{cases}. \tag{21}$$

In uncertainty calculations, we consider only the case, when $j < 1$. Substituting Eqs. (20) and (21) into (16) and (17), yields:

$$f_a(r_c) = \frac{\int_{r_c}^{\infty} (r_p)^4 \left(1 - \frac{r_c}{r_p}\right)^2 \left(1 + 2\frac{r_c}{r_p} - \frac{1(r_c)^2}{{}^3(r_p)^2} - \frac{4(r_c)^3}{{}^9(r_p)^3}\right) H(r_p, x, t)dr_p}{\int_0^{\infty} (r_p)^4 H(r_p, x, t)dr_p}, \quad \text{and} \tag{22}$$

$$f_{ns}(r_c) = \frac{\int_0^{r_c} (r_p)^4 H(r_p, x, t)dr_p}{\int_0^{\infty} (r_p)^4 H(r_p, x, t)dr_p}. \tag{23}$$

Parameter $H(r_p, x, t)$ can be approximated by the Log-Normal curve of pore size distribution for the certain porous medium (in this case we use beads with radii 20–31.5 μm) obtained from Monte-Carlo simulations in the form:

$$H(r_p, \mu, \sigma) = \frac{1}{r_p\sigma\sqrt{2\pi}} e^{-\frac{(lnr_p-\mu)^2}{2\sigma^2}}, \tag{24}$$

where $r_p > 0$, $\mu = r_{p,\,mean} = 4.274$ μm, and $\sigma = 0.673$ μm are mean and standard deviation, respectively, of the natural logarithm of the pore radius obtained using Monte-Carlo simulations of the glass bead radii distribution and the Descartes formula (see Table II).

According to Eqs. (22) and (23), integral limits in nominators vary from r_s to ∞. Latex particles with $r_{c,wm} = 2.061 \pm 0.335$ μm (see Table III) have their radii distributed from 1.726 to 2.396 μm which correspond to $\approx$ 94.2% of the total number of latex particles detected by PAMAS. This range almost coincide with $\pm 2\sigma_{wm}(r_c)$ or 95% confidence interval. Thus, the integral limits for nominators of Eqs. (22) and (23) are chosen as follows: 1.391 and 2.731 μm (95% confidence interval), for the lower and upper limits, respectively. Similarly, as the lower and upper limits for the integral in the denominator of Eqs. (22) and (23) we choose $r_{p,mean}^{LogNorm} \pm 2\sigma(r_p^{LogNorm})$ corresponding to 95% confidence interval, i.e., 2.928 and 5.620 μm, respectively. With these assumptions, Eqs. (22) and (23) look as follows:

$$f_a(r_c) = \frac{\int_{r_c}^{\infty} (r_p)^4 \left(1 - \frac{r_c}{r_p}\right)^2 \left(1 + 2\frac{r_c}{r_p} - \frac{1(r_c)^2}{{}^3(r_p)^2} - \frac{4(r_c)^3}{{}^9(r_p)^3}\right) \frac{1}{r_p\sigma\sqrt{2\pi}} e^{-\frac{(lnr_p-\mu)^2}{2\sigma^2}} dr_p}{\int_0^{\infty} (r_p)^4 \frac{1}{r_p\sigma\sqrt{2\pi}} e^{-\frac{(lnr_p-\mu)^2}{2\sigma^2}} dr_p}, \quad \text{and} \tag{25}$$

$$f_{ns}(r_c) = \frac{\int_0^{r_c} (r_p)^4 \frac{1}{r_p\sigma\sqrt{2\pi}} e^{-\frac{(lnr_p-\mu)^2}{2\sigma^2}} dr_p}{\int_0^{\infty} (r_p)^4 \frac{1}{r_p\sigma\sqrt{2\pi}} e^{-\frac{(lnr_p-\mu)^2}{2\sigma^2}} dr_p}. \tag{26}$$

In order to get an accurate approximation for all integrals from Eqs. (25) and (26), fractions of accessible and inaccessible flows can be evaluated by numerical integration using composite Simpson's rule in the form of the quadrature algorithm.[67]

Parameters x_1 and x_2 (lower and upper limits of integrals) are not fixed numbers, since latex particles are distributed over their radii. The correct choice of these integration limits has significant effect on the values of these integrals, and consequently, on the values of $f_a(r_c)$ and $f_{ns}(r_c)$ and their CSUs.

We used the following approach in numerical integration of the above integrals. The lower limit for the integral in the nominator of formula (25), referred as Int-25-1, was chosen as $r_{c,min} = r_{c,wm} = 2.061$ μm, consistent with all previous calculations. The upper limit for Int-25-1 was chosen using consecutive iterations by changing values for r_c from 2.061 μm to the value which delivers two consecutive numbers for this integral differing by no more than 0.01% resulting in $r_{c,\,max} = 8.861$ μm; applying these lower and upper limits we calculated the value of Int-25-1 to be equal to 195.698 m/s.

Similar approach was used for the evaluation of integrals in denominators of formulas (25) and (26), called Int-25/26-2. Using the lower and upper limits for Int-25/26-2 as $r_{p,\,min} = 0.010$ μm and $r_{p,\,max} = 8.699$ μm, respectively, the value of the integral was equal to 386.396 m/s with the precision of 0.01%. The lower integration limit for the integral in the denominator of formula (26), called Int-26-1, was chosen as $r_{p,\,min} = 0.020$ μm, and the upper limit was chosen as $r_{p,max} = r_{c,wm} + 4\sigma_{wm}(r_c) = 3.401$ μm to count for more than 99.9% of latex particle sizes used in the experiment; thus, the value of Int-26-1 was equal to 13.1577 m/s. The above approach delivered the following values for parameters in stochastic models: $f_a(r_c) = 0.3982$ and $f_{ns}(r_c) = 0.0334$.

For the evaluation of uncertainties in these integrals the following approach was applied. Precision of 0.01% cannot be used as a value for the combined uncertainty for

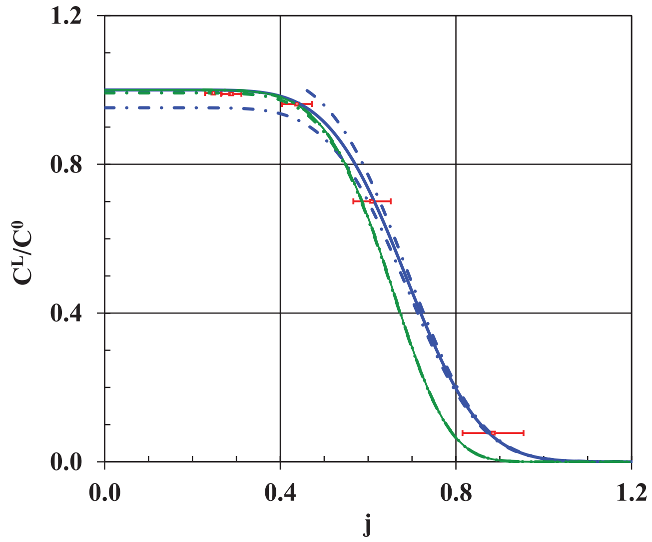

FIG. 4. Suspended normalised concentration vs jamming ratio for the two stochastic models (16) and (17): red •, experimental data; dark green ——, model (16); dark green – – –, lower and upper limit for model (16); dark blue ——, model (17); dark blue – – –, lower and upper limits for model (17).

Int-25-1, since latex particles are distributed over various size ranges; otherwise this uncertainty will be significantly underestimated. In order to overcome this problem, values of Int-25-1 were calculated for the two lower integration limits, such as $r_{c,min_1} = r_{c,wm} - 2\sigma_{wm}\,(r_c) = 1.391$ μm and $r_{c,min_2} = r_{c,wm} + 2\sigma_{wm}(r_c) = 2.731$ μm, and the difference between them was adopted as the combined uncertainty of Int-25-1 (see Table V).

Similarly, precision of 0.01% does not reflect the actual value of uncertainty in Int-25/26-2. Initially, we attempted to evaluate uncertainty in Int-25/26-2 as for Int-25-1 with the one difference that this integral is calculated for the two values of the mean of the natural logarithm of the pore radius: $\mu - 2\sigma(r_p^{LogNorm}) = 1.1275$ and $\mu + 2\sigma(r_p^{LogNorm}) = 1.7531$. The difference between thus calculated integrals was thought to be adopted as an uncertainty for Int-25/26-2. However, this difference is enormously sensitive to variations of μ: value of Int-25/26-2 is equal to the area under pore size distribution curve which varies significantly for the above two values of the mean of the natural logarithm of the pore radius, 1.1275 and 1.7531. The difference between thus calculated integrals does not reflect the actual value of its uncertainty. Therefore, this approach cannot be considered as appropriate. A better way to evaluate this integral for the two values of the upper limits is as follows: $r_{p,max_1} = r_{p,max} - 2\sigma_{wm}(r_c) = 8.029$ μm, $r_{p,max_2} = r_{p,max} + 2\sigma_{wm}(r_c) = 9.369$ μm, and the difference between two integral values, equal to 0.032%, adopt as the uncertainty for Int-25/26-2. For the evaluation of Int-25-1 we used $r_{c,min} = r_{c,wm} = 2.061 \pm 0.335$ μm similarly to Int-26-1; the obtained value for uncertainty for Int-26-1 is 3.3000 m/s, which is significantly higher than that for Int-25-1.

Thus determined uncertainties in the integrals from Eqs. (25) and (26) were used for the evaluation of $u(f_a(r_c))$ and $u(f_{ns}(r_c))$ – see Table V. Having determined values of the parameters in the Eqs. (16) and (17) and their CSUs, we can now evaluate how these uncertainties propagate to $u_c(C_{model}) = u_c(\frac{C^L(r_s)}{C^0(r_s)})$, using Eq. (12) and properties of derivatives of an exponential function and that of a product of two functions. Equation (12) when applied to Eqs. (16) and (17) translates them into the following equations, respectively:

$$u_c\,(C_{model}) = e^{-\frac{f_{ns}(r_c)L}{f_a(r_c)l}} \sqrt{\begin{array}{l} \left[\left(-\dfrac{L}{f_a(r_c)l}\right) u\,\{f_{ns}(r_c)\}\right]^2 + \left[\left(-\dfrac{f_{ns}(r_c)}{f_a(r_c)l}\right) u(L)\right]^2 \\ + \left[\left(-\dfrac{f_{ns}(r_c)L}{\{f_a(r_c)\}^2\,l}\right) u\,\{f_a(r_c)\}\right]^2 + \left[\left(-\dfrac{f_{ns}(r_c)L}{f_a(r_c)l^2}\right) u(L)\right]^2 \end{array}}, \quad \text{and} \tag{27}$$

$$u_c\,(C_{model}) = e^{-\frac{f_{ns}(r_c)L}{l}} \sqrt{\begin{array}{l} \left[\left((f_{ns}(r_c)-1)\dfrac{L}{l}-1\right) u\{f_{ns}(r_c)\}\right]^2 + \left[(f_{ns}(r_c)-1)\dfrac{f_{ns}(r_c)}{l}u(L)\right]^2 \\ + \left[(1-f_{ns}(r_c))\left(-\dfrac{f_{ns}(r_c)L}{l^2}\right)u(l)\right]^2 \end{array}}. \tag{28}$$

Using uncertainty $u_c(C_{model})$ from Table V, graphs for experimental data and stochastic models results obtained from Eqs. (16) and (17) were plotted in Fig. 4. As follows from this figure, model (16) having lower CSU (with its boundary indicated by the "green" dotted line) delivers the following results for $\frac{C^L(r_c)}{C^0(r_c)} = f(j)$: agreement between modelling results and experimental data is within combined respective CSUs at lower values of jamming ratios, however, at higher jamming ratios agreement is not good. Although characterised by a higher CSU (with its boundary indicated by the "blue" dotted line), Eq. (17) delivers more accurate results in the entire jamming ratio range: agreement between experimental data and modelling results is within the CSU of experimental data. This uncertainty analysis clearly shows superiority of the model (17) over (16).

The presented uncertainty analysis can be used not only for the evaluation of the validity of theoretical models used for deep bed filtration, but also for comparison of intra- and inter-laboratory data.

VII. CONCLUSIONS

Two theoretical stochastic models for prediction of carboxyl-modified latex particles capture due to size exclusion were compared and verified using a detailed analysis of experimental and modelling uncertainties. Calculation of modelling uncertainties was carried out using the law of propagation of experimental uncertainties through the modelling formulas.

Surface potentials for carboxyl-modified latex particles were calculated using Ohshima theory for "soft" particles due to the presence of the residual electrophoretic mobility at high values of ionic strength of electrolyte. Application of the Smoluchowski model to electrophoretic mobility data significantly overestimates surface potentials for latex particles.

Size exclusion particle capture is characterised by repulsive electric-double-layer and Born forces which dominate at all separation distances between latex particles and a porous media, and consequently, by a very high repulsive DLVO energy barrier and a shallow secondary energy minimum.

Weighted mean radius and weighted mean standard deviation better than respective mean values represent size of latex particles due to their distribution over various sizes. High alkalinity of suspensions does not have appreciable weathering effect on the diameter of glass beads resulting in stability of the jamming ratio factor used as a modelling parameter. However, as the result of particle and pore-throat size distributions, jamming ratio factor is characterised by the highest combined standard uncertainty among all experimental and modelling parameters.

Normalised suspended particle concentrations calculated via two theoretical models are characterised by higher CSUs than those for experimental data. The model accounting the fraction of inaccessible flow as a function of latex particle radius excellently agrees with experimental normalised suspended particle concentrations in the entire range of jamming ratios.

Overall, the proposed methodology makes a valuable contribution towards better understanding of the correlation between experimental parameters and modelled results, determining the ways of reduction of respective uncertainties, validating the proposed models during size exclusion experiments and provides criteria for estimation of reproducibility of intra- and inter-laboratory experimental data.

ACKNOWLEDGMENTS

Authors thank Institute of Minerals and Energy Resources (IMER) of the University of Adelaide for financial support. Financial support from the Australian Research Council (ARC) Discovery Project 1094299 and Santos Pty. Ltd. is gratefully acknowledged.

[1] K. C. Khilar and H. S. Fogler, *Migration of Fines in Porous Media* (Kluwer Academic Publishers, Dordrecht, 1998).

[2] J. L. Bergosh, R. B. Wiggins, and D. O. Ennis, *Mechanisms of formation damage in matrix-permeability geothermal wells.* Contactor Report for Sandia National Laboratories. Sandia National Laboratories, Albuquerque, New Mexico, 87185, USA. 74 pp, (1981). Available at: http://0-www.osti.gov.iii-server.ualr.edu/geothermal/servlets/purl/5350144-YeZvsW/native/5350144.pdf.

[3] A. A. Tchistiakov, in *Proceedings of World Geothermal Congress 2000, Kyushu, Tohoku, Japan* (International Geothermal Association, Bohum, Germany, 2000), pp. 3087–3095.

[4] J. P. Herzig, D. M. Leclerc, and P. Le Goff, Ind. Eng. Chem. **62**(5), 8–35 (1970).

[5] L. Nabzar, G. Chauveteau, and C. Roque, "A new model for formation damage by particle retention," in *SPE Formation Damage Control Conference, Lafayette, Louisiana, USA* (Society of Petroleum Engineers, Inc., Richardson, Texas, USA, 1996), SPE-31119-MS, 16 pp. Available at: http://www.onepetro.org/mslib/servlet/onepetropreview?id=00031119.

[6] S. A. Bradford, J. Simunek, M. Bettahar, M. T. van Genuchten, and S. R. Yates, Water Resour. Res. **42**, W12S15/11–W12S15/16, doi:10.1029/2005WR004791 (2006).

[7] R. G. Guedes, F. Al-Abduwani, P. Bedrikovetsky, and P. K. Currie, Soc. Pet. Eng. J. **14**(September), 477–487, doi:10.2118/98623-PA (2009).

[8] D. Rosseau, L. Hadi, and L. Nabzar, SPE Prod. Oper. **23**(4), 525–531, doi:10.2118/107666-PA (2008).

[9] J. N. Ryan and M. Elimelech, Colloids Surf., A **107**, 1–56 (1996).

[10] S. B. Roy and D. A. Dzombak, Colloids Surf., A **107**, 245–262 (1996).

[11] J. Bergendahl and D. Grasso, Am. Inst. Chem. Eng. J. **45**(3), 475–484 (1999).

[12] S. A. Bradford, S. R. Yates, M. Bettahar, and J. Simunek, Water Resour. Res. **38**(12), 63-1–63-12, doi:10.1029/2002WR001340 (2002).

[13] P. Chalk, N. Gooding, S. Hutten, Z. You, and P. Bedrikovetsky, Chem. Eng. Res. Des. **90**(1), 63–77 (2012).

[14] J. E. Tobiason and C. R. O'Melia, J. Am. Water Works Assoc. **80**(12), 54–64 (1988).

[15] M. Elimelech and C. R. O'Melia, Langmuir **6**(6), 1153–1163 (1990).

[16] M. Elimelech and C. R. O'Melia, Environ. Sci. Technol. **24**(10), 1528–1536 (1990).

[17] H. Yuan and G. Sin, Chem. Eng. J. **168**(2), 635–648 (2011).

[18] C. S. Melching and S. Anmangandla, J. Environ. Eng. **118**(5), 791–805 (1992).

[19] J. Xue and J. Ma, in *2012 20th International Conference on Geoinformatics (GEOINFORMATICS), Hong Kong, China* (Institute of Electrical and Electronics Engineers, New York, NY, USA, 2012), pp. 487–491.

[20] P. Reichert and P. Vanrollenghem, Water Sci. Technol. **43**(7), 329–338 (2001).

[21] M. Neumann and W. Gujer, Environ. Sci. Technol. **42**(11), 4037–4043 (2008).

[22] A. L. James and C. M. Oldenburg, Water Resour. Res. **33**(11), 2495–2508, doi:10.1029/97WR01925 (1997).

[23] C. L. Smith, J. Idaho Acad. Sci. **30**(2), 93–105 (1994).

[24] C. Tien, ChEnC **17**(1–6), 361–382 (1982).

[25] P. A. Deshpande and D. R. Shonnard, Appl. Environ. Microbiol. **66**(2), 763–768 (2000).

[26] F. A. H. Al-Abduwani, R. Farajzadeh, W. M. G. T. van den Broek, P. K. Currie, and P. L. J. Zitha, Rev. Sci. Instrum. **76**, 103704 (2005).

[27] D. C. Mays and J. R. Hunt, Environ. Sci. Technol. **39**(2), 577–584 (2005).

[28] A. O. Imdakm and M. Sahimi, Phys. Rev. A **36**(11), 5304–5309, doi:10.1103/PhysRevA.36.5304 (1987).

[29] S. D. Rege and H. S. Fogler, Chem. Eng. Sci. **42**(7), 1553–1564 (1987).

[30] A. Santos and P. Bedrikovetsky, Comput. Appl. Math. **23**(2–3), 259–284 (2004).

[31] A. A. Shapiro, P. G. Bedrikovetsky, A. Santos, and O. O. Medvedev, TPM **67**(1), 135–164, doi:10.1007/s11242-006-0029-5 (2007).

[32] A. Shapiro and P. G. Bedrikovetsky, Physica A **389**(13), 2473–2494 (2010).

[33] A. Badalyan and P. Pendleton, Langmuir **19**(19), 7919–7928 (2003).

[34] A. Badalyan and P. Pendleton, J. Colloid Interface Sci. **326**(1), 1–7 (2008).

[35] A. Badalyan, T. Carageorgos, P. Bedrikovetsky, Z. You, A. Zeinijahromi, and K. Aji, Rev. Sci. Instrum. **83**, 095106 (2012).

[36] Z. You, A. Badalyan, and P. Bedrikovetsky, Soc. Pet. Eng. J. **18**(4), 620–633, doi:10.2118/162941-PA (2013).

[37] H. Yuan, Z. You, A. Shapiro, and P. Bedrikovetsky, Chem. Eng. J. **226**, 227–237 (2013).

[38] B. N. Taylor and C. E. Kuyatt, *Guidelines for Evaluating and Expressing the Uncertainty of NIST Measurement Results*, National Institute of Standards and Technology Technical Note 1297, 1994 ed. (U.S. Government Printing Office, Washington, DC, 1994).

[39] *Quantifying Uncertainties in Analytical Measurements, EURACEM/CITAC Guide CG4*, 2nd ed., edited by S. L. R. Ellison, M. Rosslein, and M. Williams (EURACHEM, UK, 2000).

[40] Z. A. Kuznar and M. Elimelech, Colloids Surf. Physicochem. Eng. Aspects **294**(1–3), 156–162 (2007).

[41] L. D. Landau and E. M. Lifshitz, *Statistical Physics, Part 1 (Course in Theoretical Physics)* (Pergamon Press, Oxford, 1980), Vol. 5.

[42] E. J. W. Verwey and J. T. G. Overbeek, *Theory of the Stability of Lyophobic Colloids* (General Publishing Company, Toronto, Canada, 1999).

[43] J. N. Israelachvili, *Intermolecular and Surface Forces*, 3rd ed. (Academic Press, Sydney, 2011).

[44] S. H. Behrens, D. I. Christl, and R. Emmerzael, Langmuir **16**(6), 2566–2575 (2000).

[45] H. Ohshima, J. Colloid Interface Sci. **163**(2), 474–483 (1994).

[46] H. Ohshima, Sci. Technol. Adv. Mater. **10**, 063001 (2009).

[47] R. J. Hunter, *Zeta Potential in Colloid Science: Principles and Applications* (Academic Press, Sydney, 1981).

[48] W. Wagner, J. R. Cooper, A. Dittmann, J. Kijima, H.-J. Kretzschmar, A. Kruse, R. Mares, K. Oguchi, H. Sato, I. Stocker, O. Sifner, Y. Takaishi, I. Tanishita, J. Trubenbach, and T. Willkommen, J. Eng. Gas Turbines Power **122**, 150–182 (2000).

[49] H. Ohshima, J. Colloid Interface Sci. **262**, 294–297 (2003).

[50] See http://www.millipore.com/techpublications/tech1/ab1946en00 for information about Merck Millipore, application brief (assessed 25 December 2012).

[51] M. Elimelech, J. Gregory, J. Xiadong, and W. Richard, *Particle Deposition and Aggregartion: Measurement, Modelling, and Simulation* (Butterworth-Heinemann, New York, 1995).

[52] R. Buchner, G. T. Hefter, and P. M. May, J. Phys. Chem. A **103**(1), 1–9 (1999).

[53] J. R. Cooper and R. B. Dooley, *Release of the IAPWS formulation 2008 for the viscosity of ordinary water substance* (The International Association of the Properties of Water and Steam, Berlin, Germany, 2008).

[54] X. Wang and V. Alvarado, Energies **4**, 1763–1778 (2011).

[55] H. Ohshima, K. Makino, T. Kato, K. Fujimoto, T. Kondo, and H. Kawaguchi, J. Colloid Interface Sci. **159**, 512–514 (1993).

[56] A. J. de Kerchove and M. Elimelech, Langmuir **21**(14), 6462–6472 (2005).

[57] R. de Levie, *Advanced Excel for Scientific Data Analysis*, 2nd ed. (Oxford University Press, New York, 2008).

[58] H. A. Abramson, L. S. Moyler, and M. H. Gorin, *Electrophoresis of Proteins* (Reinhold, New York, 1942).

[59] D. Pedoe, Am. Math. Monthly **74**(6), 627–640 (1967).

[60] H. Castrup, in *8th Annual ITEA Instrumentation Workshop* (Park Plaza Hotel and Conference Center, Lankaster, CA, 2004), p. 7.

[61] J. Gregory, J. Colloid Interface Sci. **83**(1), 138–145 (1981).

[62] J. Gregory, J. Colloid Interface Sci. **51**(1), 44–51 (1975).

[63] E. Ruckenstein and D. C. Prieve, Am. Inst. Chem. Eng. J. **22**(2), 276–283 (1976).

[64] *Evaluation of measurement data - Guide to the expression of uncertainty in measurement*, JCGM 100:2008 (Joint Committee for Guides in Metrology, France, 2008).

[65] S. Mekid and D. Vaja, Measurement **41**, 600–609 (2008).

[66] S.-Y. Jeong, L. R. Morss, and W. L. Ebert, *Scientific Basis for Nuclear Waste Management XXVI*, Materials Research Society 2001 Fall Meeting, November 26–30, 2001.

[67] R. L. Burden and J. D. Faires, *Numerical Analysis*, 8th ed. (Brooks Cole, New York, 2004).

5.2 Critical Analysis of Uncertainties during Particle Filtration

Badalyan A., Carageorgos T., Bedrikovetsky P., You Z., Zeinijahromi A., **Aji K.**

Review of Scientific Instruments, 2012, 83, 095106/1-9

Critical analysis of uncertainties during particle filtration

Alexander Badalyan, Themis Carageorgos, Pavel Bedrikovetsky, Zhenjiang You, Abbas Zeinijahromi, and
Keyiseer Aji

Citation: Review of Scientific Instruments **83**, 095106 (2012); doi: 10.1063/1.4749844
View online: http://dx.doi.org/10.1063/1.4749844
View Table of Contents: http://scitation.aip.org/content/aip/journal/rsi/83/9?ver=pdfcov
Published by the AIP Publishing

REVIEW OF SCIENTIFIC INSTRUMENTS **83**, 095106 (2012)

Critical analysis of uncertainties during particle filtration

Alexander Badalyan,[a] Themis Carageorgos, Pavel Bedrikovetsky, Zhenjiang You, Abbas Zeinijahromi, and Keyiseer Aji
Australian School of Petroleum, University of Adelaide, Adelaide, South Australia 5005, Australia

(Received 30 April 2012; accepted 19 August 2012; published online 11 September 2012)

Using the law of propagation of uncertainties we show how equipment- and measurement-related uncertainties contribute to the overall combined standard uncertainties (CSU) in filter permeability and in modelling the results for polystyrene latex microspheres filtration through a borosilicate glass filter at various injection velocities. Standard uncertainties in dynamic viscosity and volumetric flowrate of microspheres suspension have the greatest influence on the overall CSU in filter permeability which excellently agrees with results obtained from Monte Carlo simulations. Two model parameters "maximum critical retention concentration" and "minimum injection velocity" and their uncertainties were calculated by fitting two quadratic mathematical models to the experimental data using a weighted least squares approximation. Uncertainty in the internal cake porosity has the highest impact on modelling uncertainties in critical retention concentration. The model with the internal cake porosity reproduces experimental "critical retention concentration vs velocity"-data better than the second model which contains the total electrostatic force whose value and uncertainty have not been reliably calculated due to the lack of experimental dielectric data. © *2012 American Institute of Physics*. [http://dx.doi.org/10.1063/1.4749844]

I. INTRODUCTION

Experimental[1,2] and theoretical[3] approaches for description of deep bed filtration successfully coexist and complement each other leading to improvement in process design in petroleum and geothermal water processes, in environmental processes and other areas dealing with particles migration. Microparticles attachment due to electrostatic attraction to the surface of a porous medium can be studied using colloidal suspension flow through an engineered porous medium. The chemistry and hydrodynamics of the colloidal suspension, surface chemistry of colloids and porous media, and particle and pore sizes are important parameters in the particle attachment process. Attachment of particles onto a porous medium is accompanied by reduction in its permeability due to the deposit of colloidal particles that decrease the cross-sectional area available for suspension flow. The colloids deposition process can be monitored by measuring the permeability decline. This deposition can be reliably determined if experimental uncertainty in the permeability of a porous medium is known. Despite its importance, the uncertainties in experimental permeability data during coreflood tests are not routinely implemented in laboratory investigations and not much attention has been given in the literature.

Nevertheless, Kwon *et al.*[4–6] graphically determined permeability of shale specimens to NaCl solutions with standard deviation of 1%–3% excluding any errors in the evaluation of pressure drop across the shale specimen, dynamic viscosity, and compressibility of NaCl solutions. Applying the law of propagation of uncertainties and Monte Carlo simulation to Darcy equation, Dong[7] identified uncertainties in viscosity and pressure as the major sources of uncertainty in permeability. Mazumder and Wolf[8] applied an error analysis to Darcy equation and experimental data of sub- and supercritical CO_2 flow through coal samples. Uncertainty in pressure gradient along the coal specimen was the major contributor to the overall uncertainty in permeability of around 20%.

Good reproducibility of permeability measurements is important for comparison of experimental data from intra- and inter-laboratory tests.[9] Brighenti and Macini indicated that "a standardization of permeability measurement procedure is necessary, in order to ensure reliable comparisons amongst different sets of data."[10] Such standardization is difficult to achieve due to: unavailability of "certified permeability standards from recognised standard institutions,"[11] and the limited information about experimental uncertainties for permeability and particle concentration data.

Theoretical models for different particle capture mechanisms have been developed and represent the respective experimental data with various degrees of agreement.[12–15] However, according to Al-Abduwani *et al.*,[16] validation of such models via different experimental methods is limited. Additionally, unavailability of uncertainty analyses for models describing suspension transport in porous media and limited information about uncertainties for the respective experimental data makes validation of such models difficult.

In the present work, a detailed and systematic analysis of experimental and modelling uncertainties associated with permeability measurements during colloidal particle attachment to an engineered porous medium is done. Particle attachment during colloidal suspension injection at different velocities was monitored via real-time measurements of the porous medium permeability and post-experimental colloids mass balance. The law of propagation of uncertainties was applied for calculation of uncertainties in parameters of Darcy equation. Parameters having the greatest effect on uncertainties in permeability and modelling results were identified, and recommendations for reducing modelling uncertainties

---

[a] Author to whom correspondence should be addressed. Electronic mail: alexander.badalyan@adelaide.edu.au.

TABLE I. Chemical composition of a borosilicate glass filter.

Compound	SiO_2	B_2O_3	Na_2O_3	Al_2O_3	CaO	Cl	MgO	Fe_2O_3
%, w/w	80.60	12.60	4.20	2.20	0.10	0.10	0.05	0.04

were presented. Recommendations from NIST[17] and EURACHEM[18] uncertainty guidelines were used in this paper.

II. MATERIALS

A. Borosilicate glass filter

A borosilicate sintered glass filter (ROBU®, Glasfilter-Geraete GmbH, Hattert, Germany), with pore sizes varying within 10–16 μm (from now on called filter) was used as porous medium. Chemical composition of this filter according to the manufacturer is given in Table I. The filter porosity was determined as 43% by the Archimedes method.

B. Colloidal latex particles

Polystyrene latex microspheres crafted by surface carboxyl groups (Polysciences, Inc., Warrington, PA) were used for the preparation of colloidal suspension. According to the manufacturer, these microspheres have a mean diameter of $d_{c,\,mean} = 1.019 \pm 0.032\ \mu$m which translates to the mean jamming ratio of $j = \frac{d_{c,mean}}{d_{pore,mean}} = 0.08$.

The colloidal suspension was prepared by adding the microspheres to a 0.1 M NaCl aqueous solution at *p*H 3. In these conditions there is almost no self-agglomeration, bridging or size exclusion capture.[19,20]

III. EXPERIMENTAL SECTION

A. Experimental setup

A schematic diagram of the setup for filter permeability measurements is shown in Fig. 1. The filter 1 is held inside a rubber sleeve 2 located in a high-pressure core holder 3. An overburden pressure is established by pumping MilliQ water through a manual valve 4 (Swagelok®), and measured by a Bourdon tube pressure gauge 5 (Swagelok). The colloidal suspension was pumped through the filter by a high-performance liquid chromatography (HPLC) pump 6 (Scientific Systems, Inc., Lab Alliance, PA) via a manual valve 7 (Swagelok). A back-pressure regulator 8 (Swagelok) maintains the pore pressure at the desired level.

The pore pressure is measured by a PA 33X gauge pressure transmitter 9 (KELLER AG fur Druckmesstechnik, Winterthur, Switzerland). Differential pressure across the filter is measured by four differential pressure transducers 10-13 (DPTs) (Validyne Engineering, CA) with different measuring ranges. Manual valves 14-17 connect a respective DPT to a flow-through system. Each DPT is connected to a respective readout/signal conditioner. Output signals from readouts/signal conditioners (0 to 10 Vdc) and PA 33X (0–5 Vdc) enter the analog input channels of the ADAM-4019+ analog-to-digital data acquisition module 18 (Advantech®, Taipei, Taiwan), which via the ADAM-5060 RS-232/RS-485/RS-422 signal converter 19 (Advantech, Taipei, Taiwan) is incorporated into a real-time data acquisition and monitoring system based on stand-alone personal computer 20. Custom build data acquisition software based on Advantech ADAMView 4.25 application builder calculates and records differential pressures in real time. Dynamic data exchange server delivers all experimental data (temperature, pressure, differential pressure, and time) into Microsoft Excel incorporating all corresponding calculations and graphs.

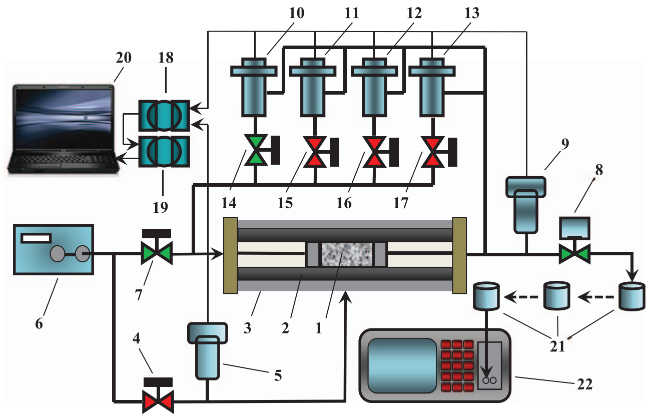

FIG. 1. Schematic of a real-time data acquisition and monitoring system for liquid permeability of porous media. ("Green" colour denotes open valves, "red" colour denotes closed valves.) (1) Filter; (2) rubber sleeve; (3) high-pressure core holder; (4, 7, 14-17) manual valves; (5) Bourdon tube pressure gauge; (6) HPLC pump; (8) back-pressure regulator; (9) PA 33X gauge pressure transmitter; (10-13) Validyne differential pressure transducers; (18) ADAM-4019+ data acquisition module; (19) ADAM-5060 RS-232/RS-485/RS-422 signal converter; (20) personal computer; (21) beakers; (22) PAMAS S4031 GO portable particle counter.

Particle deposition in the filter was studied at following velocities: 1.32×10^{-3}, and (7.92, 3.96, 2.64, and 1.32) $\times 10^{-4}$ m/s. Continuous monitoring of the filter permeability in real-time provided information about attachment of colloidal particles: stabilisation of monotonically reduced permeability within experimental uncertainty in filter permeability (3.09%) assumed the end of particle attachment process for the chosen flowrate. As an example, the decrease of filter permeability with particle deposition at velocity of 1.32 $\times 10^{-4}$ m/s is shown in Fig. 2 (vertical bars indicate the CSU in permeability).

The effluent stream was collected in plastic beakers 21 (Figure 1), and particle concentrations in the inlet and outlet streams were determined by PAMAS S4031 GO portable particle counter 22 (PAMAS GmbH, Salzuflen, Germany). The difference between these concentrations determines the volumetric concentration of the attached particles. Later, this concentration was converted to dimensionless (reduced by the volume of the filter) volumetric concentration or critical retention concentration. The following relationship was experimentally established (Fig. 3):

$$\sigma_{cr} = \sigma_{cr}(U), \tag{1}$$

where $\sigma_{cr}(U)$ is critical retention concentration of attached particles; and U is velocity, m/s. Particle deposition at 1.32 $\times 10^{-3}$ and 7.92 $\times 10^{-4}$ m/s resulted in negligibly low values of critical retained concentrations and their CSUs which are

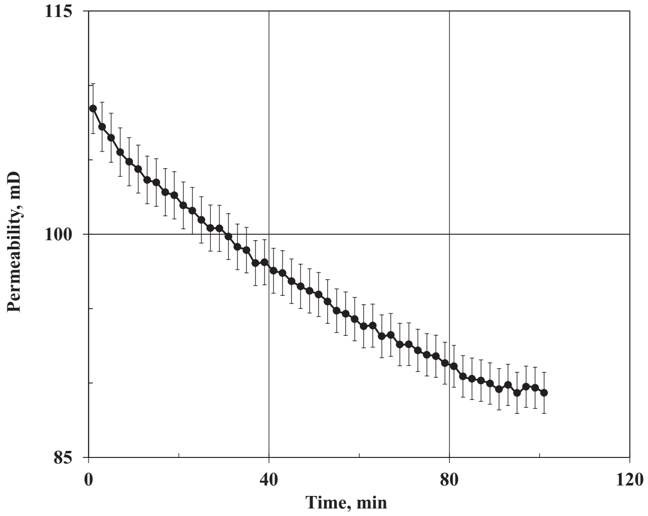

FIG. 2. Variation of glass filter permeability during colloid deposition at 1.32 × 10^{-4} m/s.

not included in all consecutive calculations and, therefore, not shown in Fig. 3.

B. Metrological characteristics of instrumentation

Manufacturer-supplied metrological characteristics of instruments used in the setup are the primary source of equipment-related uncertainties used for calculation of measurement-related uncertainties in parameters of Darcy equation, particle concentrations, and modelling results (see Table II).

Output signal from type-T thermocouple (not shown in Fig. 1) together with those from readouts/signal conditioners and PA 33 X are fed into ADAM-4019+. Taking into account the accuracy and 16-bit resolution of ADAM-4019+ and NIST[17,21] recommendations, CSUs in temperature, differential pressure, and absolute pressure of suspension were calculated (see Table III).

TABLE II. Metrological characteristics of instrumentation.

Instrument	Measuring range	Accuracy
HPLC pump	0–100 ml/min	2.0% FS
Type-T thermocouple	N/A	1.0 K
ADAM 4019+	0-5; 10 Vdc	0.1%
Valydine DPT	0-(8.62 × 10^3; 8.62 × 10^4; 8.62 × 10^5; 8.62 × 10^6) Pa	0.25% FS
PA 33X	0.1-30 MPa	0.1 FS

Note: FS means full scale.

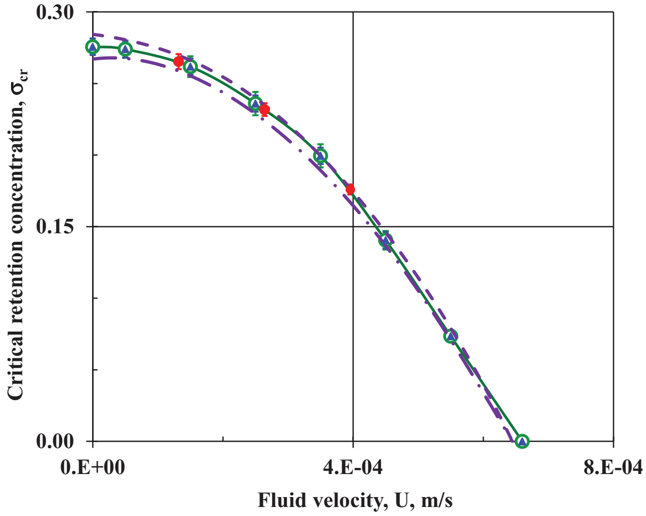

FIG. 3. Comparison of experimental data and modelled results for critical retention particle concentration. ● experimental data; ▲ quadratic function model fitting using OLSM; ○ quadratic function model fitting using WLSM; – - – lower uncertainty limit for Eq. (14); – – upper uncertainty limit for Eq. (14).

The manufacturer calibrated PAMAS using NIST traceable particles without stating its accuracy which is necessary for the evaluation of uncertainties in inlet and outlet particle concentrations. We evaluated the PAMAS repeatability by measuring number of particles across various particle size distributions for the investigated particle size. Ten consecutive measurements of particle numbers resulted in a standard deviation of $u(N_{particle}^{PAMAS}) = 4402$ or 1.75% for a narrow particle diameter range from 0.904 to 1.126 μm. Since PAMAS delivers number of particles within the particle size distribution range, the weighted mean value for particle diameter was used in calculations as $d_{c,wm} = \frac{\sum_{i=1}^{i=m} d_i n_i^{av}}{\sum_{i=1}^{i=m} dn_i^{av}} = 1.014$ ± 0.068 μm. Here, $m = 6$ is the number of measured diameters of particles; d_i is "i"-th measured diameter of particles, μm; d_i^{av} is the average of 10 values of "i"-th measured diameter of particles, μm; n_i^{av} is the average number of particles with measured diameters d_i; and 0.068 μm is weighted mean standard deviation. The obtained weighted mean value for particle diameter is in a good agreement with that reported by the manufacturer. According to NIST guidelines,[17] values 4402 and 0.068 μm are adopted as the precision of the PAMAS particle counter for number of particles and diameter, respectively.

IV. SOURCES OF UNCERTAINTIES AND THEIR CONTRIBUTIONS

According to Taylor and Kuyatt,[17] the CSU of the measurement is calculated according to the law of propagation of uncertainty as follows:

$$u_c^2(y) = \sum_{i=1}^{N} \left(\frac{\partial f}{\partial x_i}\right)^2 u^2(x_i) + 2\sum_{i=1}^{N-1} \sum_{j=i+1}^{N} \frac{\partial f}{\partial x_i} \frac{\partial f}{\partial x_j} u(x_i, x_j). \tag{2}$$

When the second term in Eq. (2) is negligible it translates to

$$u_c(y) = \sqrt{\sum_{i=1}^{N} \left[\left(\frac{\partial f}{\partial x_i}\right) u(x_i)\right]^2}. \tag{3}$$

Since the reduction of filter permeability is caused by the increased amount of attached particles, the uncertainty analysis begins from calculation of uncertainties in parameters from Darcy equation and particle concentrations.

TABLE III. Summary of experimental uncertainty analysis results.

Parameter	Units	CSU	RCSU
A	m^2	6.30×10^{-7}	4.99×10^{-4}
L	m	5.00×10^{-6}	1.24×10^{-3}
R	m	2.50×10^{-6}	1.25×10^{-4}
π	N/A	5.0×10^{-5}	1.59×10^{-5}
V_f	m^3	5.05×10^{-9}	1.74×10^{-3}
$N_{particle}^{PAMAS}$	Particles	4402	1.75×10^{-2}
$d_{c,wm}^{PAMAS}$	m	6.84×10^{-8}	6.75×10^{-2}
σ_{at}	m^3	3.56×10^{-9} to 5.98×10^{-8}	7.70×10^{-2}
σ_{cr}	N/A	$(1.40$ to $2.11) \times 10^{-2}$	$(7.75$ to $7.94) \times 10^{-2}$
Δp	Pa	7.80×10^{0}	2.6×10^{-3}
p	Pa	3.0×10^{4}	8.8×10^{-3}
p_w	Pa	3.0×10^{4}	8.8×10^{-3}
Q	m^3/s	1.67×10^{-9}	2.0×10^{-2}
T_A	K	1.0	N/A
T_B	K	2.2×10^{-2}	N/A
T	K	1.0	3.4×10^{-3}
μ_P	μPa×s	5.77×10^{-3}	6.19×10^{-6}
μ_T	μPa×s	21.8	2.34×10^{-2}
μ	μPa×s	21.8	2.34×10^{-2}
k	m^2	2.55×10^{-15}	3.09×10^{-2}
U	m/s	2.64×10^{-6} to 2.64×10^{-5}	2.00×10^{-2}
ϕ	N/A	8.30×10^{-4}	1.92×10^{-3}
ϕ_c	N/A	2.65×10^{-2}	7.39
$\sigma_{cr}^{0,\,OLSM}$ or a^{OLSM}	N/A	1.57×10^{-2}	5.68×10^{-2}
b^{OLSM}	(m/s)$^{-2}$	1.58×10^{5}	2.46×10^{-1}
U_{min}^{OLSM}	m/s	9.92×10^{-5}	1.51×10^{-1}
$\sigma_{cr}^{0,\,WLSM}$ or a^{WLSM}	N/A	1.13×10^{-2}	4.11×10^{-2}
b^{WLSM}	(m/s)$^{-2}$	1.50×10^{5}	2.38×10^{-1}
U_{min}^{WLSM}	m/s	7.96×10^{-5}	1.39×10^{-1}
σ_{cr}^{model} Eqs. (13) and (15)	N/A	4.32×10^{-3} to 1.16×10^{-2}	4.23×10^{-2} to 1.03×10^{-1}
σ_{cr}^{model} Eqs. (14) and (16)	N/A	1.14×10^{-2}	4.16×10^{-2} to 1.55×10^{-1}

A. Filter length, cross-sectional area, and volume

Glass filter dimensions were measured by a calliper with an uncertainty of $u(L) = 2u(R) = 5 \times 10^{-6}$ m. Using Eq. (3), CSUs for the cross-sectional area and volume of the filter were equal to $u_c(A) = 6.28 \times 10^{-7}$ m and $u_c(V_f) = 5.31 \times 10^{-9}$ m^3, respectively.

B. Total volume of attached particles and critical retention concentration

Critical retention concentration, σ_{cr}, is calculated according to the following formula: $\sigma_{cr} = \frac{\sigma_{at}}{V_f}$, where σ_{at} - is the volumetric concentration of attached particles, m^3. Cumulative volume of particles attached to the filter is calculated as the sum of incremental volumes of particles attached at various flowrates. Since each consecutive deposited volume of colloids is added to the previous one, $u_c(\sigma_{at})$ is calculated according to the rules of propagation of uncertainties resulting in the CSU of the next cumulative volume of particles being greater than that for the previous one. As calculated, CSUs for σ_{cr} varies from 1.40×10^{-2} (corresponding to 100 ml/min) to 2.11×10^{-2} (corresponding to 10 ml/min), with relative combined standard uncertainty (RCSU), $\delta_c(\sigma_{cr})$, varying from 7.75% to 7.94% (see Table III).

C. Pressure and differential pressure measurements

Pressure of suspension passing through the glass filter without a significant error is determined as

$$p_w = p - \frac{\Delta p}{2}, \tag{4}$$

where p is the pressure measured by PA 33X, and Δp is the differential pressure across the glass filter measured by the respective DPT. Parameters in Eq. (4) correspond to those in Eq. (3) as follows: $y = p_w, x_1 = p$ and $x_2 = \Delta p$. Each variable in Eq. (4) contributes to CSU for pressure according to Eq. (3) as follows:

$$\begin{aligned} u_c\left(p_w\right) &= \sqrt{\left[\frac{\partial p_w}{\partial p} u\left(p\right)\right]^2 + \left[\frac{\partial p_w}{\partial\left(\Delta p\right)} u\left(\Delta p\right)\right]^2} \\ &= \sqrt{\left[1 \times u\left(p\right)\right]^2 + \left[-\frac{1}{2} u\left(\Delta p\right)\right]^2}. \end{aligned} \tag{5}$$

Using data from Table III, the value of CSU in pressure is calculated as $u_c(p_w) \cong u_c(p) \cong 3.0 \times 10^4$, Pa, since $u_c(p) \gg u_c(\Delta p)$. Thus, determined $u_c(p_w)$ will be used for the evaluation of uncertainty in density and dynamic viscosity of NaCl solutions.

D. Dynamic viscosity

Dynamic viscosity data for NaCl aqueous solutions were adopted from Kestin *et al.*[22] with an accuracy of ±0.5% in the temperature and pressure range of the present study. Equations for dynamic viscosity correlations for NaCl solutions[22] include dynamic viscosity data for pure water which were adopted from Cooper and Dooley.[23] Water density data needed for the evaluation of water viscosity were obtained from Wagner *et al.*[24]

Combined standard uncertainties in temperature and pressure measurements evaluated earlier in Sec. III B (see Table III) were used to calculate the effect of pressure and temperature variation on dynamic viscosity for NaCl solutions at experimental conditions of 2.00 MPa and 298.15 K. Variation of pressure within its CSU resulted in negligible viscosity variation of 5.77×10^{-3} μPa×s or 6.19×10^{-4}%. Temperature effect on dynamic viscosity is greater than that from pressure, reaching 21.8 μPa×s or 2.34%, which is adopted as uncertainty for dynamic viscosity.

E. Evaluation of uncertainty in core permeability through uncertainty propagation and Monte Carlo simulations

Darcy's equation is used for calculation of filter permeability in the following form:

$$k = k\left(Q, \mu, L, A, p_1, p_2\right) = \frac{Q\mu L}{A\left(p_1 - p_2\right)}, \tag{6}$$

where, k is permeability of the filter, in D; A is the cross-sectional area of the filter, in m^2; p_1 and p_2 are the inlet and outlet pressure of the stream, respectively, in Pa; Q is volumetric flowrate, in m^3/s; μ is dynamic viscosity of the fluid, in Pa×s; L is the length of the filter over which the fluid is experiencing the pressure drop, in m. Each parameter in Eq. (6) contributes to the CSU in permeability,

$$\begin{aligned} u_c(k) &= \sqrt{\left[\frac{\partial k}{\partial Q}u(Q)\right]^2 + \left[\frac{\partial k}{\partial \mu}u(\mu)\right]^2 + \left[\frac{\partial k}{\partial L}u(L)\right]^2 + \left[\frac{\partial k}{\partial A}u(A)\right]^2 + \left[\frac{\partial k}{\partial\left(\Delta p\right)}u(\Delta p)\right]^2} \\ &= \sqrt{\left[\frac{\mu L}{A\Delta p}u(Q)\right]^2 + \left[\frac{QL}{A\Delta p}u(\mu)\right]^2 + \left[\frac{Q\mu}{A\Delta p}u(L)\right]^2 + \left[-\frac{Q\mu L}{A^2\Delta p}u(A)\right]^2 + \left[-\frac{Q\mu L}{A\left(\Delta p\right)^2}u\left(\Delta p\right)\right]^2}, \end{aligned} \tag{7}$$

where, $u(A)$, $u(\Delta p)$, $u(Q)$, $u(\mu)$, and $u(L)$ are earlier calculated CSUs in cross-sectional area of the filter, pressure drop across the core, suspension volumetric flowrate, water dynamic viscosity, and the length of the filter, respectively. Substituting these CSUs into Eq. (7) we obtain the following value of permeability with its CSU equal to $k = (8.844 \pm 0.274) \times 10^{-14}$ m^2 (89.61 ± 2.77 mD) and RCSU of $\delta(k)$ 3.09%.

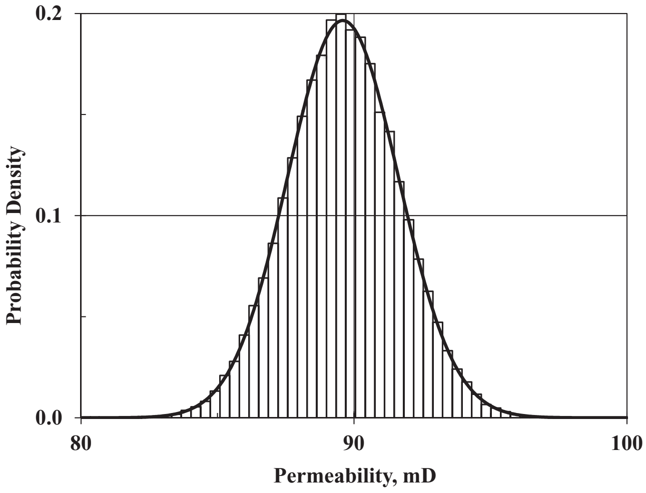

FIG. 4. Monte Carlo simulation results for permeability for an arbitrarily chosen experimental point.

A local sensitivity analysis of Eq. (6), where each parameter was varied one at a time within its CSU, identified two major contributors to CSU in permeability: dynamic viscosity (2.34%) and volumetric flowrate of suspension (2.0%). Reduction of CSU in permeability can be achieved by an increase in the accuracy of temperature measurement and by using a more accurate HPLC pump.

Uncertainty in filter permeability was also evaluated via Monte Carlo simulations using @RISK analysis software (Palisade Corporation, ITHAKA, NY) applied to Eq. (6) with the parameters and their CSUs evaluated earlier (see Table III). Results of this simulations (100 000 iterations) corresponding to the last experimental permeability point from Figure 2 are presented in the form of a histogram in Figure 4 and summarised in Table IV. LogNormal distribution showed the best fit to output results with relative

TABLE IV. Input and output results for Monte Carlo simulations for filter permeability.

Parameter	Monte Carlo simulations results	
	Output results	Log normal distribution results
k_{min}, mD	81.19	N/A
k_{max}, mD	98.92	N/A
k_{mean}, mD	89.62	89.61
σ_k, mD	2.72	2.72

standard deviation of $\delta(k) = \frac{\sigma^{LogNorm}(k)}{k^{LogNorm}_{mean}} \times 100\% = \frac{2.72\ \text{mD}}{89.61\ \text{mD}} \times 100\% \approx 3.04\%$, which excellently agrees with earlier calculated CSU in permeability (3.09%). Time consuming nature of Monte Carlo simulations makes impossible to use this method for real-time permeability variation monitoring.

V. UNCERTAINTIES FOR THEORETICAL MODELS FOR PARTICLE DEPOSITION

A. Evaluation of uncertainty for extrapolated results

A detailed analysis of physical processes governing particle attachment/detachment in porous media at various flowrates was carried out by Bedrikovetsky *et al.*[25,26] resulting in the mathematical model for the critical retention concentration as a function of velocity,

$$\sigma_{cr}(U) = \sigma_0 \left[1 - \left(\frac{U}{U_{min}} \right)^2 \right], \tag{8}$$

where $\sigma_{cr}(U)$ is the critical retention concentration of colloidal particles; σ_0 is the maximum retention concentration of colloidal particles at zero velocity; U is the velocity, m/s; and U_{min} is the minimum velocity for which no particles can be held on the grain surface by electrostatic and gravity forces, m/s. Equation (8) is used for the determination of σ_0 and U_{min} from the experimental data via extrapolation of the critical retention concentration curve to $U = 0$ and $\sigma_{cr} = 0$.

The model (8) was fitted to the experimental "σ_{cr} vs U"-data corresponding to velocities of (3.96, 2.64, and 1.32) × 10^{-4} m/s. Uncertainty in U was calculated according to Eq. (3) using uncertainties in flowrate and cross-sectional area of the filter. Uncertainty in the critical retention concentration of the attached particles, $u_c(\sigma_{cr})$, was calculated in Sec. IV B. A different approach should be applied for the evaluation of σ^0_{cr}, $u(\sigma^0_{cr})$, U_{min} and $u(U_{min})$, since parameters σ_0 and U_{min} cannot be measured directly. Instead, they should be determined by the intersection of the $\sigma_{cr}(U)$-curve with σ_{cr}-axis via its extrapolation to $U = 0$, and with U-axis via its extrapolation to $\sigma^0_{cr} = 0$, respectively.

Equation (8) can be re-written as follows:

$$\sigma_{cr}\,(U) = \sigma^0_{cr} \left[1 - \left(\frac{U}{U_{min}} \right)^2 \right] = \sigma^0_{cr} - \frac{\sigma^0_{cr}}{U^2_{min}} U^2 = a - bx^2, \tag{9}$$

and experimental data can be fitted by a quadratic equation using mean-least squares approximation.

Three experimental points are sufficient to fully determine $\sigma_{cr}(U)$-curve according to Eq. (9). Location of an experimental point along the $\sigma_{cr}(U)$-curve affects the location of the two intercept points, σ^0_{cr} and U_{min}, during data extrapolation. Applying an ordinary least squares method (OLSM) to the experimental data and assuming 68.27% confidence interval (which corresponds to ± one standard deviation) results in the following $\sigma^{0,OLSM}_{cr}$ and U^{OLSM}_{min} values, respectively, 2.765 × 10^{-1} and 6.565 × 10^{-4} m/s with their CSUs and RCSUs given in Table III.

During particle attachment experiment one moves to the left along the $\sigma_{cr}(U)$-curve, then each consecutive $u_c(\sigma_{cr})$-value incorporates uncertainties from all previous experimental points and movement towards the lower velocities is accompanied by an increase in $u_c(\sigma_{cr})$-values. Therefore, experimental σ_{cr}-values are of various "quality" which can be quantified by a weighting function $w_i = \frac{1}{[u_c(\sigma_{cr})]^2}$, meaning that the last experimental point on the $\sigma_{cr}(U)$-curve has the highest uncertainty and the lowest weight. As a result, the above-mentioned three-point curve method gives the lowest possible uncertainty for the last experimental point.

The closer the first experimental point is to U-axis and the last experimental point is to the σ_{cr}-axis, the more accurate U_{min} and σ_0-values can be determined by extrapolation of the parabolic curve. It is possible to determine the position of the last experimental point before the experiment. However, the location of the first experimental point is problematic since before the experiment it is not possible to predict the minimum velocity at which no particles can be attached to the filter (all particles are swept away by the flowing suspension).

According to Taylor,[27] it is appropriate to use the weighted least squares method (WLSM), which gives the most precise estimate of coefficients a and b from Eq. (9). Although some caution has been expressed towards the use of WLSM for non-precisely estimated weights,[28] in the present study, uncertainties in the volumes of the attached particles and, consequently, in the critical retention concentrations were accurately calculated within the experimental uncertainty of PAMAS. Applying the WLSM to the quadratic function (9), the following expressions and values for coefficients a, b, and model parameter U^{WLSM}_{min} are obtained with their CSUs and RCSUs listed in Table III:

$$\begin{aligned} a &= \frac{\left(\sum_{i=1}^n w_i\right)\left(\sum_{i=1}^n w_i x_i^2 y_i\right) - \left(\sum_{i=1}^n w_i x_i^2\right)\left(\sum_{i=1}^n w_i y_i\right)}{\left(\sum_{i=1}^n w_i\right)\left(\sum_{i=1}^n w_i x_i^4\right) - \left(\sum_{i=1}^n w_i x_i^2\right)^2} \\ &= \sigma^{0,WLSM}_{cr} = 2.757 \times 10^{-1} \end{aligned} \tag{10}$$

and

$$\begin{aligned} b &= \frac{\left(\sum_{i=1}^n w_i y_i\right)\left(\sum_{i=1}^n w_i x_i^4\right) - \left(\sum_{i=1}^n w_i x_i^2 y_i\right)\left(\sum_{i=1}^n w_i x_i^2\right)}{\left(\sum_{i=1}^n w_i\right)\left(\sum_{i=1}^n w_i x_i^4\right) - \left(\sum_{i=1}^n w_i x_i^2\right)^2} \\ &= 6.329 \times 10^5\ (\text{m/s})^{-2}, \end{aligned} \tag{11}$$

with $U_{min} = 6.600 \times 10^{-4}$ m/s. The uncertainty in σ_{cr}-values can be calculated via the following expression:

$$\begin{aligned} u^{WLSM}_c[(\sigma_{cr})_i] &= \sqrt{\frac{1}{n-2}\sum_{i=1}^n \left[(\sigma_{cr})_i - a - bU_i^2\right]^2} \\ &= 3.12 \times 10^{-3}, \end{aligned} \tag{12}$$

where $(\sigma_{cr})_i$ is experimental critical retention concentration of colloidal particles.

Although OLSM produced results for σ_{cr} which are in a good agreement with the experimental data, those obtained via WLSM are characterised by relatively smaller errors. Since OLSM treats data without consideration of their uncertainties (or as equally weighed), it underestimates uncertainties in the obtained results. It is, therefore, advisable to use

WLSM for the evaluation of σ_{cr}^{0} and U_{min}-values and their uncertainties.

B. Evaluation of uncertainty for particle attachment model

Equation (8) is a simple representation of the two more complex expressions for the critical retention concentration:[25]

$$\sigma_{cr}^{model}(U) = \left[1 - \left(\frac{h_c}{H}\right)^2\right](1-\phi_c)\phi, \tag{13}$$

$$\sigma_{cr}^{model}(U) = \left[1 - \left(\frac{\mu r_c^2 U}{\phi H F_e x}\right)^2\right](1-\phi_c)\phi, \tag{14}$$

where h_c is a cake thickness, which is a function of velocity, m; H is thickness of a rectangular pore channel adopted as $2r_p = 1.3 \times 10^{-5}$ m; F_e - is the total electrostatic force calculated as the sum of attractive London-van der Waals (LvdW) and electric double layer repulsive (DLR), and Born repulsive (BR) forces according to Derjaguin, Landau, Verwey, and Overbeek (DLVO) theory,[19] N; x is the ratio between the drag and electrostatic forces;[25] and ϕ_c is porosity of the cake formed on the internal surface of the borosilicate filter due to colloidal particle deposition.

Analysis of model (14) shows that when $U = 0$ m/s, then, $\sigma_{cr}^{model} = (1-\phi_c)\phi$, meaning that the critical retention concentration depends only on cake and filter porosities. Filter porosity is measured experimentally with the appropriately calculated uncertainty. The maximum value of σ_{cr}^{model}, therefore, greatly depends on adopted the ϕ_c-value. This depends on the assumption of the uniform particle packing (rhombohedral, orthorhombic or cubic, etc.). If the cake porosity is adopted as one of the uniform type of packing, then the appropriate calculations show that, it is not possible to adjust the maximum value of σ_{cr}^{model} to that obtained from extrapolation of the experimental $\sigma_{cr} = \sigma_{cr}(U)$-curve to the value of $U = 0$ m/s. To overcome such inflexibility of the model (14), the latter was adjusted to the value of $\sigma_{cr}^{max} = \sigma_{cr}^{0,\,WLSM} = 0.276 \pm 0.006$ (obtained earlier in this paper using WLSM) with ϕ_c as a tuning parameter, resulting in $\phi_c = 0.359 \pm 0.013$. The outcome of this approach is very important: the cake porosity is not adopted via assumptions, but is directly derived from the experimental $\sigma_{cr} = \sigma_{cr}(U)$-data. Therefore, the uncertainty for the cake porosity is also substantiated by the uncertainty in σ_{cr}^{max}-value derived from experimental critical retention concentrations.

Using Eqs. (3) and (13), CSU in critical retention concentration can be evaluated as follows:

$$\sigma_{cr}^{model}(U) = \sqrt{\begin{aligned}&\left[\left(\frac{2h_c}{H} - \frac{2h_c\phi_c}{H} - \frac{h_c^2}{H^2} + \frac{h_c^2\phi_c}{H^2}\right)u(\phi)\right]^2 + \left[\left(-\frac{2h_c\phi}{H} + \frac{h_c^2\phi}{H^2}\right)u(\phi_c)\right]^2\\ &+\left[\left(\frac{2\phi}{H} - \frac{2\phi\phi_c}{H} - \frac{2h_c\phi}{H^2} + \frac{2h_c\phi\phi_c}{H^2}\right)u(h_c)\right]^2\\ &+\left[\left(-\frac{2h_c\phi}{H^2} + \frac{2h_c\phi\phi_c}{H^2} + \frac{2h_c^2\phi}{H^3} + \frac{2h_c^2\phi\phi_c}{H^3}\right)u(H)\right]^2\end{aligned}}. \tag{15}$$

Having evaluated $\sigma_{cr}^{0,WLSM}$- and U_{min}^{WLSM}-values and their uncertainties, and thus, determined the entire $\sigma_{cr} = \sigma_{cr}(U)$-curve, it is now possible to determine $\sigma_{cr}^{model} = \sigma_{cr}^{model}(U)$-curve according to Eqs. (13) and (14). In order to evaluate uncertainties in the values of critical retention concentrations derived from the models (13) and (14), $u(\sigma_{cr}^{model})$, it is necessary to know uncertainties in the parameters of these models.

The only parameter in Eq. (13) which varies with velocity is the cake thickness, h_c. This parameter can be evaluated by fitting Eq. (13) to experimental data, with obtained results in Figure 5 showing a gradual increase in the internal cake thickness accompanied with an increase in critical retention particle concentration. For the colloidal particle with $d_{c,wm} = 1.014 \pm 0.068$ μm one-layer cake thickness can be evaluated with the uncertainty of $u_c(h_c^{1\,layer}) = \pm 0.068$ μm. The number of layers of deposited particles in the cake, n_l, is determined by the ratio between h_c and the mean particle diameter resulting in values varying from 0 to 13, when velocity

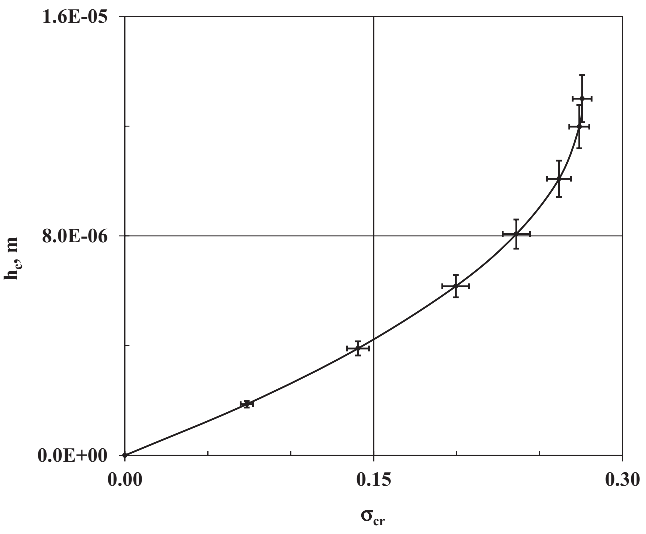

FIG. 5. Variation of cake thickness during particle deposition.

changes from 0 to 6.6 × 10^{-4} m/s. Uncertainties for the varying cake thickness are calculated according to the following formula $u_c(h_c^{n_l}) = \pm 0.068 n_l$ μm (see Table III). Uncertainty in particle radius, $u_c(r_c)$, is taken from Table III. Since the glass filter is characterised by a pore width from 10 to 16 μm with $H_{mean} = 13$ μm, then a standard deviation of 1.0 μm is adopted as $u_c(H)$. Using uncertainties for masses of dry and water-saturated filter, CSU in its porosity is equal to $u_c(\phi) = 8.30 \times 10^{-4}$.

After introducing the values of all parameters and their uncertainties into Eq. (15), we obtained $u(\sigma_{cr}^{model})$ varying from 4.23 to 10.3% when velocity changes from 0 to 6.6 × 10^{-4} m/s (see Table III). A local sensitivity analysis was performed to determine how variation of uncertainties in parameters from Eqs. (13) and (14) affects $u(\sigma_{cr}^{model})$. When we doubled uncertainties for parameters one at a time, (σ_{cr}^{model}) remained unchanged for all parameters, but for $u_c(\phi_c)$ it was doubled. Varying parameters in Eqs. (13) and (14) one at a time within their CSUs, we arrive to the conclusion that ϕ_c has the highest impact on σ_{cr}^{model} according to data presented in Table V. The procedure proposed in the present paper for the evaluation of $u_c(\phi_c)$ via experimental uncertainties in σ_{cr} resulted in the lowest possible $u_c(\phi_c)$-value for the present experimental conditions, and is, therefore, recommended for calculations.

Using Eqs. (3) and (14) it is possible to evaluate $u(\sigma_{cr}^{model})$ according to Eq. (16). Additional assumptions should be made before calculating $u(\sigma_{cr}^{model})$. The resultant electrostatic force is calculated as the derivative of the potential energy. For many parameters of the LvdW, DLR, and BR forces, it is not always possible to calculate their uncertainties. Values of Hamaker constants calculated via DLVO theory often disagree with those obtained experimentally,[29] reaching, for example, 50% for non-retarded region of ≤10 nm.[30] Direct measurements of vdW forces produced results with standard deviation ranging from 14.9% to 23.1%[31] and uncertainty of 15%.[32] In the present study, uncertainty in electrostatic force, $u_c(F_e)$ was adopted as 15%:

$$\sigma_{cr}^{model}(U) = \sqrt{\begin{aligned}&\left[\left(1-\phi_c+\frac{1-\phi\phi_c}{\phi^2}\left(\frac{\mu r_c^2 U}{HF_e x}\right)^2\right)u(\phi)\right]^2+\left[\left(-\phi+\frac{1}{\phi}\left(\frac{\mu r_c^2 U}{HF_e x}\right)^2\right)u(\phi_c)\right]^2\\&+\left[\left(\frac{2\mu(\phi_c-1)}{\phi}\left(\frac{r_c^2 U}{HF_e x}\right)^2\right)u(\mu)\right]^2+\left[\left(\frac{4r_s^3(\phi_c-1)}{\phi}\left(\frac{\mu U}{HF_e x}\right)^2\right)u(r_c)\right]^2\\&+\left[\left(\frac{2U(\phi_c-1)}{\phi}\left(\frac{\mu r_c^2}{HF_e x}\right)^2\right)u(U)\right]^2+\left[\left(\frac{2(1-\phi_c)}{\phi H^3}\left(\frac{\mu r_c^2 U}{F_e x}\right)^2\right)u(H)\right]^2\\&+\left[\left(\frac{2(1-\phi_c)}{\phi F_e^3}\left(\frac{\mu r_c^2 U}{Hx}\right)^2\right)u(F_e)\right]^2+\left[\left(\frac{2(1-\phi_c)}{\phi x^3}\left(\frac{\mu r_c^2 U}{HF_e}\right)^2\right)u(x)\right]^2\\&+\left[\left(\frac{2(1-\phi_c)}{\phi x^3}\left(\frac{\mu r_c^2 U}{HF_e}\right)^2\right)u(x)\right]^2\end{aligned}}. \qquad (16)$$

According to our calculations, h_c varies from 1.3 × 10^{-5} to 0 m when fluid velocity changes from 0 to its maximum value of 6.60 × 10^{-4} m/s, corresponding to the condition when $\sigma_{cr} = 0$ and all particles are swept away by high-velocity fluid. In this range of "particle-to-surface distances" and for the present experimental conditions, F_e calculated according to DLVO theory[25] varies from 2.72 × 10^{-21} to −9.38 × 10^{-19} N.

TABLE V. Results of sensitivity analysis for Eqs. (13) and (14).

Parameter	Variation of σ_{cr}^{model}, % Equation (13)	Equation (14)
μ	N/A	0.006
r_s	N/A	0.016
U	N/A	0.013
H	0.325	0.019
h_c	0.153	N/A
F_e	N/A	0.038
x	N/A	0.038
ϕ	0.193	0.193
ϕ_c	4.13	4.13

According to Bedrikovetsky *et al.*,[25] parameter x is the ratio between the drag and electrostatic forces, with the drag force determined according to the following formula:

$$F_d = \frac{\omega \pi r_c^2 U}{H}, \qquad (17)$$

where ω is the dimensionless empirical drag coefficient. The drag coefficient was adopted as 21 via fitting equation (14) to the experimental critical retention concentration data. Applying formula (3) to (17), we obtain that $u_c(F_d)$ varies in the range from 1.26 × 10^{-15} to 1.66 × 10^{-14} N and $u_c(x)$

from 2.73×10^6 to 1.12×10^5 for the above range of fluid velocities.

After substitution of all relevant parameters into Eq. (16) we obtained that RCSU (σ_{cr}^{model}) varies from 4.16% to 15.5% for the same range of fluid velocities (see Table III). Model (14) represents experimental $\sigma_{cr} = \sigma_{cr}(U)$-data less accurately than model (13) due to the presence in Eq. (14) of the attractive electrostatic force, whose value and uncertainty cannot be reliably established due to unavailability of dielectric data.

VI. CONCLUSIONS

Calculation of experimental uncertainties for permeability of a borosilicate filter was carried out through propagation of uncertainties for parameters in Darcy's equation and also, using Monte-Carlo simulations. Both methods provided identical values for combined standard uncertainty for permeability. The local sensitivity analysis of Darcy equation showed that the uncertainties in dynamic viscosity and volumetric flowrate of colloidal suspension have the highest impact on the overall uncertainty for filter permeability.

The uncertainty in each consecutive value of critical retention concentration incorporates uncertainties from all previous values. Therefore, the total number of experimental points for critical retention concentrations, as a function of velocity, should be limited to three points in order to reduce the uncertainty in the determination of maximum critical retention concentration. Weighing functions for the critical retention concentrations were accurately calculated through the propagation of uncertainties in the respective experimental parameters. Application of the weighted least squares method resulted in more accurate values for maximum critical retention concentration and minimum velocity.

The local sensitivity analysis of the models showed that internal cake porosity has a significant impact on the modelling results and their uncertainties. The first model, containing the internal cake thickness as one of its parameters, represented experimental critical retention concentration data better than the second model which used dynamic viscosity, particle radius, pore thickness, drag, and total electrostatic forces as model parameters. Higher deviations of the results from the second model are, probably, due to the presence of the total electrostatic force in the model's formula. The values and uncertainty for this force cannot be reliably measured and calculated, due to lack of experimental dielectric data at the current experimental conditions.

The proposed uncertainty analysis was implemented into Microsoft Excel^{TM} spreadsheet coupled with the real-time data acquisition software, such that each experimental data point is accompanied by its uncertainty, leading to timely decisions during particle attachment experiments.

Overall, the presented method for the evaluation of experimental and modelling uncertainties establishes the validity ranges for experimental permeability and particle attachment data and for the corresponding theoretical models. This makes possible intra- and inter-laboratory data comparison which is the first step towards standardizing these types of experiments.

ACKNOWLEDGMENTS

Authors thank Institute of Minerals and Energy Resources (IMER) of the University of Adelaide for financial support. Financial support from the Australian Research Council (ARC) Discovery Project 1094299, ARC Linkage Project 100100613, and Santos Pty. Ltd. is gratefully acknowledged.

[1] C. Gruesbeck and R. E. Collins, Soc. Pet. Eng. J. **22**, 847–856 (1982).
[2] N. Tufenkji and M. Elimelech, Langmuir **20**(25), 10818–10828 (2004).
[3] A. Santos and P. Bedrikovetsky, Comput. Appl. Math. **23**(2–3), 259–284 (2004).
[4] O. Kwon, A. K. Kronenberg, A. F. Gangi, and B. Johnson, J. Geophys. Res. **106**(B9), 19339–19353, doi:10.1029/2001JB000273 (2001).
[5] O. Kwon, B. E. Herbert, and A. K. Kronenberg, J. Geophys. Res. **109**, B10205, doi:10.1029/2004JB003052 (2004).
[6] O. Kwon, B. E. Herbert, and A. K. Kronenberg, J. Geophys. Res. **109**, B10206, doi:10.1029/2004JB003055 (2004).
[7] C. Dong, J. Manuf. Sci. Eng. **127**(4), 907–911 (2005).
[8] S. Mazumder and K. H. Wolf, Int. J. Coal Geol. **74**(2), 123–138 (2008).
[9] A. S. El-Dieb and R. D. Hooton, Cem. Concr. Res. **24**(5), 854–862 (1994).
[10] G. Brighenti and P. Macini, *Future Groundwater Resources at Risk* (IAHS, Helsinki, Finland, 1994), Vol. 222, pp. 409–416.
[11] American Petroleum Institute, *Recommended Practices for Core Analysis: Recommended Practice*, 2nd ed. (American Petroleum Institute Publishing Service, 1998), Vol. 40.
[12] A. C. Payatakes, R. Rajagopalan, and C. Tien, Can. J. Chem. Eng. **52**(6), 722–731 (1974).
[13] A. Santos and P. Bedrikovetsky, TPM **62**(1), 23–53 (2006).
[14] A. A. Shapiro, P. G. Bedrikovetsky, A. Santos, and O. O. Medvedev, TPM **67**(1), 135–164 (2007).
[15] P. Bedrikovetsky, TPM **75**, 335–369 (2008).
[16] F. A. H. Al-Abduwani, R. Farajzadeh, W. M. G. T. van den Broek, P. K. Currie, and P. L. J. Zitha, Rev. Sci. Instrum. **76**, 103704 (2005).
[17] B. N. Taylor and C. E. Kuyatt, "Guidelines for evaluating and expressing the uncertainty of NIST measurement results," National Institute of Standards and Technology Technical Note 1297 (U.S. Government Printing Office, Washington, DC, 1994).
[18] "Quantifying uncertainties in analytical measurements," *EURACHEM/CITAC Guide CG4*, edited by S. L. R. Ellison, M. Rosslein, and M. Williams (EURACHEM, 2000).
[19] B. Derjaguin and L. Landau, PrSS **43**(1–4), 30–59 (1993).
[20] J. Bergendahl and D. Grasso, AIChE J. **45**(3), 475–484 (1999).
[21] D. Ripple, G. W. Burns, and M. G. Scroger, "Assessment of uncertainties of thermocouple calibrations at NIST," NISTIR 5340 (National Institute of Standards and Technology, Gaithersburg, MD, 1994), p. 35.
[22] J. Kestin, H. E. Khalifa and R. J. Correia, JPCRD **10**(1), 71–87 (1981).
[23] J. R. Cooper and R. B. Dooley, The International Association for the Properties of Water and Steam (Berlin, Germany, 2008), p. 9.
[24] W. Wagner, J. R. Cooper, A. Dittmann, J. Kijima, H.-J. Kretzschmar, A. Kruse, R. Mares, K. Oguchi, H. Sato, I. Stocker, O. Sifner, Y. Takaishi, I. Tanishita, J. Trubenbach, and T. Willkommen, J. Eng. Gas Turbines Power **122**, 150–182 (2000).
[25] P. Bedrikovetsky, F. D. Siqueira, C. Furtado, and A. L. S. de Souza, TPM **86**(2), 353–383 (2011).
[26] P. Bedrikovetsky, A. Zeinijahromi, F. D. Siqueira, C. A. Furtado, and A. L. S. de Souza, TPM **91**, 173–197 (2012).
[27] J. R. Taylor, *An Introduction to Error Analysis: The Study of Uncertainties in Physical Measurements* (University Science Books, New York, 1982).
[28] R. J. Carroll and D. Ruppert, *Transformation and Weighing in Regression* (Chapman and Hall, New York, 1988).
[29] Q. Qi and G. J. Brereton, ITUFF **42**(4), 619–629 (1995).
[30] D. Chan and P. Richmond, Proc. R. Soc. London, Ser. A **353**(1673), 163–176 (1977).
[31] J. A. Kitchener and A. P. Prosser, Proc. R. Soc. London, Ser. A **242**(1230), 403–409 (1957).
[32] A. K. Mohapatra and C. S. Unnikrishnan, EL **73**(6), 839–845 (2006).

6 Summary and Conclusions

In this thesis, new experimental technology was designed to investigate particle behavior in porous media under the condition of size exclusion. The colloidal retention and permeability damage under high flow velocity have been investigated; the effects have been introduced into a modified Forchheimer equation for suspension flow under the inertial flow conditions. Experimental and modeling uncertainties at both conditions have been defined, determined and analyzed.

The experimental tests on repulsion condition between colloidal suspension and porous media carried out in the thesis yields in the straining-dominant particle capture. The particle-rock repulsion can be predicted by DLVO calculations of electrostatic forces and achieved by the correct choice of water composition, salinity, pH, the material and coating of grains (glass beads) and the particles. Creation of the significant particle-rock repulsion environment allows avoiding the particle capture by attachment; and also the expensive and cumbersome characterization of particle-rock interaction in order to model the DLVO interactions and consequent attachment. The induced particle-rock repulsion conditions leave the particle straining as a single particle retention mechanism. The tests are analogous to challenge testing of porous multi sieve membranes.

Several improvements to the laboratory set-up have been implemented in the thesis submitted: post-flow measurement of the retention profile, sieving of glass beads in the ultrasonic bath resulting in the reduced bead sieving time and more reproducible particle size distribution, and the application of a dual syringe pump system leading to the continuous pulseless colloidal suspension pumping.

The tests with different size particles allow determining pore throat size distribution for a log-normal type of distributions used in the present study. For more complex distribution functions, more studies must be performed, the method needs significantly more substantial validation. Challenge testing in real reservoir cores will be an important future stage of experimental investigation. However, the conclusion that size exclusion deep bed filtration is determined by a pore space only makes the determining of pore throat size distribution from challenge testing data a prospective method for porous media characterization.

The designed high velocity laboratory test on sequential particle injections at piece-wise increasing velocities, followed by injection of particle free water at increasing velocity, allows observing the following physics phenomena of particle attachment and detachment. Particle attachment to the surface and inter-pore filling were found to be the major mechanisms during high velocity injection in favorable attachment condition. High ionic strength and low pH of suspension together with low value of jamming ratio factor ensured particle deposition due to attachment without size exclusion (Paper 2). The particle attachment is so strong that full detaching deposited particles by increasing flow rate was impossible (paper 2). The beginning of the external cake formation was observed in paper 4. Formation of the external cake starts after the critical value of particle retained concentration was reached (Paper 4).

The designed high velocity laboratory test allows for full characterization of the colloidal flow system with particles attachment and detachment at high velocities. The maximum retention function model for high velocity flows which was calculated from the torque balance condition was validated by experimental work in paper 1. In paper 1, the problem of fines migration from the injection well was identified. It contains strained concentration dependencies for permeability, inertia coefficient, maximum concentration of retained particle and filtration coefficient.

It was found out that the modified Forchheimer equation accounting for deposit-dependent inertia coefficient can be accurately validated by experimental results (Paper 4). The test data also show that the values of the maximum retention function for high velocity flows, as calculated from the torque balance conditions on the pore scale and as obtained from laboratory measurements are in a good agreement.

The variation of the inertial coefficient is relatively low at the initial stage of particle deposition, which can be explained by the lining-type layer by layer retention without changing the geometry of porous space. The inertial coefficient increase at high retention concentration is explained by formation of the external filter cake.

The critical analysis of uncertainties during the deep bed filtration was carried out at both favorable and unfavorable conditions of attachment, corresponding to two kinds of processes studied in the thesis (paper 3 and paper 6).

The presented method for the evaluation of experimental and modelling uncertainties establishes the validity ranges for experimental permeability and particle attachment data, obtained in the thesis and for the corresponding theoretical models.

The new experimental technology of laboratory studies on size exclusion during colloidal transport, which includes the set-up and the tests methodology, is applicable at experimental porous media investigation in petroleum, chemical and environmental industries. One of important applications is determining pore size distributions from challenge testing.

Another application of the developed set-up and methodology of the particle-rock repulsion colloidal flow tests is validation of different available in the literature mathematical models of size exclusion deep bed filtration, their comparison and definition of areas of validity.

The results of the experimental study of high velocity deep bed filtration can be applied for laboratory based prediction of well index and skin factor for high rate oil and gas wells, especially under the conditions of inflow performance with fines migration.

The developed method for measurement uncertainties calculating can be applied not only for colloid suspension studies, but to a significantly wider range of experimental studies of flow in porous media.